Malaysian Construction Research Journal

Project Brief

Design

Tender

Construction

Facilities Management

PROJECT

Copyright

Contents

The contents of the published articles do not represent the views of the Editorial Committee and Construction Research Institute of Malaysia

Editorial Advisory Board

Editorial

Welcome from the Editor

The Editorial welcomes all readers to this second issue of Malaysian Construction Research Journal (MCRJ). Special thanks to all contributing authors for their technical papers. The Editorial would also like to express their acknowledgement to all reviewers for their invaluable comment and suggestion. This issue highlights seven titles which focus on topics related to Industrialised Building Systems (IBS).

In this issue, *Hamid et. al.* highlights the current state of IBS in Malaysia and its related R&D initiatives. The study addresses the current scenario of IBS adoption and identified the difficulties in its implementation. The authors also stress the important role of R&D and proposed the strategic approach to be taken on board by Construction Research Institute of Malaysia (CREAM).

Mahmood and Arizu discuss on the development of a standardised partial strength connection tables of extended end-plate connections for trapezoidal web profiled (TWP) steel sections. These tables will assist designers and improve the design of semi-continuous construction of multi-storey braced steel frames. Laboratory tests were carried out to validate the results and presented them in the standardised tables.

Ahmad Baharuddin et. al. writes on the comparative study of monolithic and precast concrete beam-to-column connection. The response of the connection subjected to incremental loading was studied. Specimens of monolithic and precast concrete beam-to-column were tested to evaluate the ultimate loading capacity, moment rotation characteristic as well as their crack response.

Mahyuddin evaluates the structural performance of ferrocement sandwich panel used in Industrialised Building Systems. Experimental investigation was carried out to assess the load-deflection characteristics, crack resistance and moment curvature of ferrocement elements that were exposed to air and salt water environment.

In his second paper, *Mahyuddin* reports on the permeability of polymer-modified cement system for structural applications. The durability enhancement of the cement system is achieved by reducing the permeability of the material through polymer modification. He had also investigated and reported the intrinsic properties, mechanical properties and the durability performance of the polymer-modified cement system.

Doh et. al. discusses the findings of their research works on the use of oil palm shell as structural topping for semi-precast concrete slab. Their works focus on the strength characteristic and flexural behaviour of concrete slab and to check its compliance to the requirement specified by the Code of Practice.

Finally, *Mohd Al Amin et. al.* investigates the response of ceramic foam core sandwich composite under flexural loading. Their study focuses on the determination of a range of sandwich properties which include shear modulus and bending stiffness through conducting a series of bending tests. They concluded that the ceramic foam core sandwich composite were comparable to those of polymeric foams core materials and has a high potential to be used as core material for sandwich structure construction.

Editorial Committee

INDUSTRIALISED BUILDING SYSTEMS (IBS) IN MALAYSIA: THE CURRENT STATE AND R&D INITIATIVES

Zuhairi Abd. Hamid[1], Kamarul Anuar Mohamad Kamar[1], Maria Zura Mohd Zain[1], Mohd Khairolden Ghani[1], Ahmad Hazim Abdul Rahim[1]

[1]*Construction Research Institute of Malaysia (CREAM), Kuala Lumpur*

Abstract

This study highlights the current scenario of IBS adoption and a number of implementation snags identified as being potential hurdles to the implementation of IBS. The facts were gathered from published documentation such as Construction Industry Master Plan 2006 – 2015 (CIMP), IBS Steering Committee's reports and minutes meetings, IBS Roadmap Mid-term Reviews and compilation of IBS Workshop's reports conducted by Construction Research Institute of Malaysia (CREAM) from 2006 to 2007.

The barriers of IBS implementation in Malaysia are categorised as follows; standardisation and quality issues, consumer acceptance, professional perception, process and supply chain, technology, training and education, finance and costing, incentive and communication related issues. The study also looks into the structured role of R&D, and recommends a new constructive focus and strategic direction of CREAM as an R&D institution to address the barriers in IBS adoption.

Keywords: *Industrialised Building Systems (IBS), Construction, Barriers, Research and Development (R&D), Shortcomings, Strategic Roles.*

INTRODUCTION

With its current level of quality, productivity, safety and excessive reliance on unskilled foreign workers, the state of the local construction industry is not in line with future development of Malaysia (CIDB, 2003a). This, together with the social problems associated with foreign workers, further aggravates the situation (Gue, 2007). As such, the Industrialised Building Systems (IBS) is a new trend introduced to promote systematic construction process and to reduce the dependency on foreign workers. Despite all the plausible advantages, early effort to promote usage of IBS as an alternative to conventional and labour intensive construction method has yet to greener a good response. CIDB (2003b) report that construction project using IBS in Malaysia only stands 15% in the year 2003. But the complete project using IBS in the year 2006 only 10% (CIDB, 2007b) less than one - third of total construction project (using at least one IBS product) in year 2006 (CIDB, 2007a) as compare to forecasting IBS project of 50 % in 2006 and 70% in year 2008 (CIDB, 2003a). Relatively, the low labour cost in Malaysia is the root cause of the problem (CIDB, 2007a). Although the members of the industry are open to the idea, a major portion of the industry stakeholders are indifferent, perhaps due to resistance towards change and insufficient information to support feasibility of change. The adoption in Malaysia is towards client-driven and the development of 'factory-like' buildings (TESCO, Giant, Carrefour etc) tends to have higher adoption of IBS than landed properties and small

commercial units (CIDB, 2007b). In this case, it has proven that it is difficult to introduce new technologies and method due to relation of such adoption with people perception. Perhaps, the industry is still lack of empirical data and research subjects on the issues of Business Process Re-engineering (BPR) and Change Management. It is considerable to the Research and Development (R&D) institutions and local universities have to provide the industry with relevant information to support the decision making process. Despite these barriers, IBS is still predicted to lead Malaysian construction industry towards nation modernisation and globalisation.

PROBLEM STATEMENTS

Prosperity and high economic growth in Malaysia have created a high demand for construction activities. As a consequence, this has attracted a huge number of foreign workers into this country to take up employment on site as unskilled labour doing manual jobs. Total foreign workers rose from 4% of total employment in year 1990 to about 10.7% in 1997 and 9% in year 2001. As at July 2004, there are about 1.3 million registered foreign workers, constituting 12% of total employment in the country (MOF, 2005). The Annual Labour Force Survey conducted by the Department of Statistics, revealed that the number of foreign workers has increased to 1.1 million in year 2000 compared to about 136,000 persons in the early 1980s. Latest immigration statistics indicate that the number of legal foreign workers in Malaysia rose to 1,359,632 workers as at July 2004 (MOF, 2005). The majority of foreign workers are from Indonesia, averaging 66.5% of total foreign workers, followed by Nepal (9.2%), Bangladesh (8.0%), India (4.5%) and Myanmar (4.2%), as shown in Table 1. In year 2001, male foreign workers accounted for 66% of total foreign workers and they dominated all major sectors, except services (MOF, 2005). As such, the contribution of foreign workers to construction industry is significant. According to Construction Industry Development Board (CIDB) Malaysia, 69% (552,000) out of total 800,000 of registered workers as at June 2007 is foreign workers (CIDB, 2007c). It was undoubtedly a shocking result for the construction observer. According to the report from the Department of Immigration Malaysia, foreign workers represent a comparative moderate percentage 44% of total workforce in construction industry (depicted in Table 2) in year 2006.

Table 1.Composition of Foreign Workers by Country of Origin (%)

Year	1998	1999	2000	2001	2002	2003	Jan–July 2004
Indonesia	53.3	65.7	69.4	68.4	64.7	63.8	66.5
Nepal	0.1	0.1	0.1	7.3	9.7	9.7	9.2
Bangladesh	37.1	27.0	24.6	17.1	9.7	8.4	8.0
India	3.6	3.2	3.0	4.0	4.6	5.6	4.5
Myanmar	1.3	0.9	0.5	1.0	3.3	4.3	4.2
Philippines	2.7	1.8	1.2	1.0	0.8	0.6	1.1
Thailand	0.7	0.5	0.4	0.4	2.4	0.9	1.0
Pakistan	1.0	0.6	0.5	0.4	0.2	0.2	0.1
Others	0.2	0.2	0.3	0.4	4.6	6.5	5.4
Total	**100.0**	**100.0**	**100.0**	**100.0**	**100.0**	**100.0**	**100.0**

Source: Department of Immigration Malaysia. (MOF, 2005)

Table 2. Percentage of Foreign Workers to Total Construction Workforce

	2003	**2004**	**2005**	**August 2006**
Local Workforce	224,877	272,053	309,528	334,704
Foriegn Workers	231,184	265,925	281,780	264,853
Total	456,061	537,978	591,308	599,557
Percentage of Foreign Workers	51%	49 %	48%	44%

Source: Department of Immigration Malaysia (MOF, 2005) and Construction Industry Development Board (CIDB) Malaysia.

Despite unskilled labour contributions, the country is in a difficult situation with a host of problems such low quality works, delays, wastages, social problems, diseases and etc. Foreign workers are usually unskilled when they first arrived in Malaysia and this impacted the productivity and the quality of the construction industry (CIDB, 2007a). To exaggerate the situation, local workforce is also reluctant to join the industry because of the issues of low wages combined with low emphasis on occupational safety and health has created an image of dirty, difficult, dangerous (3D) industry. As such, the state of the local construction industry is not in line with future development of Malaysia (CIDB, 2003a). Industrialised Building Systems (IBS) is a new trend introduced to promote systematic construction process and to reduce the dependency on foreign workers. Nevertheless, a number of implementation snags identified as being potential hurdles to the implementation over the issues of supply demand, economic volume and general readiness. Among all, cost and budget constrain along with the low labour cost (foreign) in Malaysia is the root cause of the problem (CIDB, 2007a). Despite those barriers, IBS is still predicted (or to be enforced) to lead Malaysian construction industry towards nation modernisation and globalisation.

IBS DEFINITIONS

To date there has been no one commonly-accepted or agreed definition of IBS. However, there are a few definitions by researchers who studied into this area previously were found through literature. Rahman and Omar (2006) defined IBS as a construction system that is built using pre-fabricated components. The manufacturing of the components is systematically done using machine, formworks and other forms of mechanical equipment. The components are manufactured offsite and once completed will be delivered to construction sites for assembly and erection. Parid (1997) defined IBS as a system which use industrialised production technique either in the production of component or assembly of the building or both. Lessing, *et. al.* (2005) defined IBS as an integrated manufacturing and construction process with well planned organisation for efficient management, preparation and control over resources used, activities and results supported by the used of highly developed components. Trikha (1999) defined IBS as a system in which concrete components prefabricated at site or in factory are assembly to form the structure with minimum in situ construction. IBS was also defined as a set of interrelated element that act together to enable the designated performance of the building (Warszawski, 1999). Esa and Nurudin (1998) defined IBS as continuum beginning from utilising craftsmen for every aspect of construction to a system that make use of manufacturing production in

order to minimise resource wastage and enhance value end users. Junid (1986) defined IBS as process by which components of building are conceived, planned and fabricated, transported and erected at site. The system includes balance combination between software and hardware component. The software element include system design, which is complex process of studying the requirement of the end user, market analysis and the development of standardise component (Junid, 1986). Chung and Kadir (2007) defined IBS as a mass production of building components either in factory or at site according to the specification with standard shape and dimensions and transport to the construction site to be re-arranged with certain standard to form a building.

All the above definitions emphasised on prefabrication, off-site production and mass production of building components as the main characteristic of IBS. The focal of discussion in the study synergises the key concept of IBS as defined as follows: A construction technique in which components are manufactured in a controlled environment (on or off site), transported, positioned and assembled into a structure with minimal additional site works (CIDB, 2003a).

DEVELOPMENT OF IBS IN MALAYSIA

IBS in Malaysia has begun in early 1960's when Ministry of Housing and Local Government of Malaysia visited several European countries and evaluate their housing development program (Thanoon *et. al.*, 2003). After their successful visit in 1964, the government had started first project on IBS aims to speed up the delivery time and built affordable and quality houses. About 22.7 acres of land along Jalan Pekeliling, Kuala Lumpur was dedicated to the project comprising seven blocks of 17 storeys flat there are 3000 units of low-cost flat and 40 shops lot. This project was awarded to Gammon/ Larsen Nielsen using Danish System of large panel of pre-fabricated system (CIDB, 2003b). In 1965, the second housing project initiated by the government of Malaysia, the project comprising a 6 block of 17 storeys flat and 3 blocks of 18 storeys flat at Jalan Rifle Range, Penang. The project was awarded to Hochtief/Chee Seng using French Estoit System (Din, 1984). Among the earliest housing development project using IBS was Taman Tun Sardon, Penang. IBS pre-cast component and system in the project was designed by British Research Establishment for low cost housing in tropical countries. Nonetheless, the building design was very basic and not considering the aspect of serviceability such as the need of wet toilet and bathroom (Rahman and Omar, 2006). Between 1981 and 1993, Perbadanan Kemajuan Negeri Selangor (PKNS) a state government development agency acquired pre-cast concrete technology from Praton Haus International based on Germany to build low cost house and high cost bungalow in Selangor (CIDB, 2003b). The usage of steel structure as part of IBS, first gained attention with the construction of 36-storeys Dayabumi complex that was completed in 1984 by Takenaka Corporation of Japan (CIDB, 2003b).

Today, the use of IBS as a method of construction in Malaysia is evolving. Many private companies in Malaysia have teamed up with foreign expert from Australia, Netherlands, United State and Japan to offer pre-cast solution to their project (CIDB, 2003b). In addition, more and more local manufacturers have established themselves in the market. Pre-cast, steel frame and other IBS were used as hybrid construction to build national landmark such

as Bukit Jalil Sport Complex, Lightweight Railway Train (LRT) and Petronas Twin Tower. It was reported that at least 21 of various manufactures and suppliers of IBS are actively promoting their system in Malaysia (Thanoon *et al.*, 2003). Nevertheless, the government of Malaysia still feels that the usage of IBS is still low despite the plausible potential. From the survey conducted by CIDB of Malaysia in 2003, the usage level of IBS in local construction industry stands at 15% (CIDB, 2003b). The total registered IBS contractors in Malaysia stand for 1,993 in year 2007 (Table 3 and 4) and registered IBS manufacture in Malaysia until 2007 is 138 producing 347 IBS products available in the market shown in Table 5.

Evidently that most of locally developed products are based on traditional materials such as reinforced concrete and the most innovative materials are based on imported technology (CIDB, 2007b). There is no mandatory requirement on any certification or accreditation of components, companies or installers in place. Whilst, there is no empirical data, there is some anecdotal evidence suggests that there has been sporadic dumping of sub-standard foreign products in Malaysia (CIDB, 2007b). A mechanism to ensure IBS products marked to an acceptable standard must be introduced in the manufacturing process. Testing of components, verify and certify them will limit only safe and acceptable IBS panels are erected and thus CIDB will lead this roles.

Table 3. Registered IBS Contractor (Active) in Malaysia by IBS Grade (B01, B02, B12, B15 and B19 (2007)

NO	GRADE	SPECIALISTIES	TOTAL
1	B 01	Buildings and Industrial Pre-casting Work	28
2	B 02	Buildings and Industrial Steel Structure Work	516
4	B 12	Aluminium, Glass and Steel Work	232
5	B 15	Roofing and Steel Cladding Works	108
8	B 19	Special Framework	11
		GRAND TOTAL	895

Source: Construction Industry Development Board (CIDB) Malaysia

Table 4: Registered IBS Contractor (Active) in Malaysia by CIDB Grade (2007)

GRED	NUMBERS
G7	334
G6	52
G5	83
G4	42
G3	191
G2	76
G1	71
TOTAL	**849**

Source: Construction Industry Development Board (CIDB) Malaysia

Table 5: Registered IBS Manufacturer and IBS Products available in Malaysia

NO	MATERIAL	MANUFACTURER	PRODUCT	LOCAL	FOREIGN	UNKNOWN
1	PC Panel,Frame, Box	51	245	27	3	21
2	Steel Frames/Panel Components	30	45	16	1	13
3	Systems Formwork	29	29	14	3	12
4	Timber Frames	28	28	13	2	13
	TOTAL	**138**	**347**	**70**	**9**	**59**

Source: Suruhanjaya Syarikat Malaysia (SSM) (Source : CIDB, 2007b)

IBS ROADMAP

The endorsement of IBS Roadmap 2003-2010 in Malaysia by the cabinet on 29th October 2003 expressed seriousness of the government and the urgency of IBS implementation. It is a blueprint of total industrialisation of construction industry towards achieving Open Building by the year 2010. The roadmap is a comprehensive document that divided the IBS programme into the five main focus areas that reflect the inputs needed to drive the programme, each beginning with M. They are Manpower, Materials, Management, Monetary, and Marketing (CIDB, 2003a). The inputs are then divided into its elements and the activities to be implemented for each element were then identified and included into the time span of the roadmap in order to achieve the mission within the stipulated time-frame. About 109 milestones are set to be achieved in year 2010. The content of this roadmap is focused towards achieving the industrialisation of the construction sector and the longer term objective of Open Building Systems (OBS) concept. The key elements of the roadmap are as follows:

1. To have a labour policy that gradually reduces percentage of foreign workers from the current 75% to 55% in 2005, 25% in 2007 and 15% in 2009,
2. To incorporate IBS/MC in professional courses for architects, engineers and others,
3. To incorporate syllabus on IBS/MC in architecture, engineering, building courses in local universities,
4. To enforce Modular Coordination (MC) by local authorities through Uniform Building By- Law (UBBL),
5. To develop catalogue of building components and standard plans for housing
6. To develop IBS Verification scheme,
7. To enforce utilisation of IBS for 30% of total government project (building) in 2004 and gradually increasing to 50% in 2006 and 70% in 2008,
8. To introduce buildability programme for all private building and enforcement from 2008.
9. To provide tax incentives for manufacturer of IBS components,
10. To offer green lane programme for users of standard plans (designed using standard IBS Components and MC),
11. To start vendor developing programme, training and financial aid,
12. To abolish levy for low, low-medium & medium cost houses; and to set 50% levy reduction.

One of the important milestones in the roadmap is the introduction of Modular Coordination (MC) concept. MC is a concept of coordination of dimensions and space where buildings and components are dimensioned and positioned in a basic unit or module known as 1M which is equivalent to 100 mm. The system allows standardisation in design and building components (CIDB, 2007a). It will encourage participation from manufactures and assemblers to enter the market, thus reducing the price of IBS components. In essence, MC will facilitate open industrialisation which is the prime target of the roadmaps. The proposed enforcement of using MC through Uniform Building By-Law (UBBL) would encourage the adoption through standardization and the use of IBS components. However, until the end of 2007, the UBBL have yet to be amended to include MC regulations (CIDB, 2007b).

Another important step taken by the government of Malaysia is to introduce incentives for IBS adopter. The exemption of the levy (CIDB levy - 0.125 % of total cost of the project according to Article 520) on contractors that implanted some kind of IBS in 50% of the building components was introduced effectively from 1st January 2007. In the first half of 2007, 24 residential projects qualified for the levy exemption. It is a very small percentage of total 417 residential projects during that period (CIDB, 2007b). It shows that awareness among developers and contractors on the levy exemption is still very low. IBS Centre established in 2006 at Jalan Chan Sow Lin, Cheras, Kuala Lumpur will be one-stop centre of IBS related programmes initiated by CIDB, provide the training and consultancy on IBS and showcase IBS technology through the demonstration project. The obligation to implement IBS strategies and activities from this centre serves concurrent both to improve performance and quality in construction, also to minimise the dependency of unskilled foreign labours flooding the construction market.

IBS ROADMAP MID-TERM REPORT

The IBS Centre has published IBS Roadmap Mid-term report to study the current status of IBS adoption in Malaysia on October 2007 (CIDB, 2007b). The report has highlighted the followings concerns to be addressed:

1. High rise development and 'factory-like' building tend to have higher adoption of IBS than landed properties and small commercial units,
2. Whilst there is no empirical data, there is some anecdotal evidence, suggest that there has been sporadic dumping of sub-standard foreign IBS product in IBS,
3. At presents, common practice shows manufacture of IBS components are involved only after tender stage of the value chain. IBS need to be addressed in the design stage to be successful adopted
4. There is yet any certification or accreditation of components companies and installers in place,
5. Smaller contractors view IBS as threats and not as opportunities,
6. Lack of integrated action plan to implement the IBS Roadmap,
7. It seems that most locally developed products based on traditional materials such as reinforced concrete and that most using innovative materials are based on imported technology,

8.   Until year 2007, vendor development programme have not yet been performed,
9.   Until year 2007, the certification of product and installers have yet to be implemented,
10.   The adoption of IBS in Malaysia is client driven,
11.   Only 54 out of 109 IBS Roadmap milestones have been achieved until year 2007,
12.   The contractor only use IBS as alternative option, either explicitly or through challenging time and quality requirements, demanded by clients.

THE BARRIERS TO IBS ADOPTION IN MALAYSIA

Clearly, the benefits offered by IBS are immense and plausible. Notwithstanding these achievements a number of implementation snags were identified as being potential hurdles to the implementation of the roadmap. These include the following which have been identified by IBS Steering Committee 2003-2005 (Hussein, 2007):
I.   Development of standard plans and standard component drawings for common use,
II.   Apprentice and on-the-job training in the area of IBS moulds, casts and assembly of components,
III.   IBS testing and evaluation programme,
IV.   Vendor development program,
V.   Readiness of designers and consultant practices, quality control, production of standard components in the field of IBS.

In a meeting of Malaysian IBS Steering Committee held in early 2006 the following concerns were raised (IBS Steering Committee, 2006):
I.   Poor implementation of IBS projects by government agencies,
II.   High cost of IBS components,
III.   Low standardisation of components and design solutions,
IV.   Poor IBS Knowledge Management & Human Capital Development – workers, contractors, designers, clients, etc,
V.   No centralised IBS R&D Centre,
VI.   No specialised resource centre for IBS,
VII.   No dedicated assessment and certification system for IBS products, manufacturers & installers,
VIII. Initiatives by too many parties as "coordinator".

The two main reasons for the low adoption of IBS in Malaysia as stated in Construction Industry Master Plan (CIMP 2006-2015) and being addressing in CIDB (2007a), are as follows:
I.   Lack of integration in design stage: IBS manufacturers are currently involve only after design stage. This lack of integration among relevant players in design stage has resultant in need for plan redesign and additional cost to be incurred if IBS is adopted,

II.   Poor Knowledge: Client and approving authorities have poor knowledge of IBS compared to architects and engineers. Familiarity with IBS concept and its benefits is vital to its success because IBS requires different approach in construction.

According to IBS Roadmap Mid-Term Review, there are three barriers in implementing IBS in Malaysia (CIDB, 2007b):

I.   Lack of support and understanding from construction professionals (due to lack of professionals trained in IBS) perhaps due uncoordinated and incomprehensible training awareness and syllabus,

II.   Misunderstanding and misinterpreting regulation and red-taping in getting approval from authorities,

III.   Perceive customer perception (lack of flexibility, leaky accommodation, unfamiliar materials etc.).

The barriers of IBS implementation in Malaysia can be summarised and catogorised in several themes ; standardisation and quality issues, issues in consumer perception, issues in professional perception, process and supply chain, technology, training and education, finance and costing, incentive and communication issues.

THE WAY FORWARD

Realising the implementation of IBS is still to make headway, CIDB through its research arm, Construction Research Institute of Malaysia (CREAM) has taken the initiative from the problem identified earlier and continued to conduct three series of workshops session with the industry between 2006 and 2007. After a lengthy deliberation with the stakeholders, it was concluded that the factors contributing to the delays of IBS implementation and other issues related to IBS are as follows (CREAM, 2007):

1.   IBS is not popular among design consultants,
2.   Lack of knowledge among designers,
3.   The need for mindset change through promotion and education,
4.   The stakeholders face a chicken and egg dilemma,
5.   Lack of support and slow adoption from private sector,
6.   Proprietary systems make it hard to be adopted by designers,
7.   Poor quality products available in Malaysia,
8.   Joints are not standardised making it hard to design as the design will have to be fixed to a particular manufacturer,
9.   Lack of push factor for authorities and responsible government bodies by laws and regulations,
10.   The professionals in Malaysia is lack of technical know-how e.g. structure,
11.   Volume and economy of scale,
12.   Monopoly of big boys, limiting opportunities to other contractors,
13.   Low offsite manufacturing of construction components available in the market,
14.   Require onsite specialised skills for assembly and erection of components,

15.   Lack of special equipments and machinery which hampered work. More local R&D, support services, technologies and testing labs,
16.   Mismatch between readiness of industries with IBS targets by the government,
17.   Lack of involvement from Bumiputera contractors as an erectors or manufactures,
18.   To consider IBS design for energy conservation and earthquake design,
19.   Insufficient capacity building for contractors to secure project in construction (G1-G7),
20.   Sustainability of construction industry, government to lead during downturn.

The inadequacy of corroborative scientific research undertaken to substantiate the benefit of IBS system as mentioned in Kadir (2005) and Thanoon *et. al.* (2003) require a new approach to be taken on board. As highlighted in the Construction Industry Master Plan 2003-2010 (CIMP) the role and functionality of R&D in Strategic Thrust 5: Innovate through R&D to adopt new construction method, it is pertinent to R&D to path (or lead) the way of promoting better adoption of IBS in Malaysia. The establishment of Construction Research Institute of Malaysia (CREAM) initiated by Construction Industry Development Board (CIDB) Malaysia should be seen as very significant development in the structure of R&D, which was previously at very formative stages rather organisationally ad-hoc and often confusing. CREAM can be assigned a task of managing the IBS research (CIDB, 2007a).

The R&D themes and topics for IBS identified through series of workshops organised by CREAM are aligned to the requirement of IBS Roadmap 2003-2010 (CIDB, 2003a). The initiatives in IBS though lead by CIDB, participative from contractors, consultants, universities, companies and research institutes are critical. The obligation to implement IBS serves concurrent both to improve performance and quality in construction, also to minimise the dependency of unskilled foreign labours flooding the construction market. It is a daunting task as 2010 is just around the corner. The process and mechanism to achieve the target depend on the integration and acceptance of the players towards IBS. Three years ahead will be a challenging one. A strategic approach will be the way forward. As the R&D arm for CIDB, CREAM's R&D output will geared towards industry's application and requirements.

CREAM shall take the following actions as a pre requisite to expedite the success of the roadmap implementation with respect to R&D in IBS (Hamid *et. al.*, 2007):

- A long term and strategic approach of conducting research on IBS shall be established,

- Involvement of universities, companies, organizations and research institutes right from the onset of any IBS R&D projects,

- Participation and inclusion of IBS in JKR building design, i.e. JKR IBS Design must be incorporated in its *Rekabentuk Bangunan Piawai* for government quarters, schools and government administrative offices. (CREAM will discuss this matter further with JKR on any issues related to R&D),

- Malaysian standard joints for IBS (wet or dry) must be designed and made available for use by the industry,

- CREAM initiatives to lead Centre of Research Excellence (CORE) on IBS and act as One Stop Centre for R&D are critical as this moves will consolidate the effort to centralise and able to identify issues and problems first hand from the industry,

- The formation of R&D laboratory and acts as CORE for IBS is urgent and CREAM should initiate and take the lead,

- CREAM is to apply for a double deduction status foundation to expedite participation from private entities as they will also in return be benefited in getting tax rebates when contributing research fund to the industry,

- Open Building System (OBS) must be competitive in terms of cost, performance and quality as compared to proprietary system and conventional methods in order to be sustainable in the construction market,

- Not reinventing the wheel on R&D but to focus on IBS applied research,

- Soft issues related to IBS such as marketing, social impact, involvement of Bumiputera contractors in vendor development program as highlighted in the roadmap should be taken on board right at the early stage,

- A complete comprehensive study on IBS solutions encompassing the entire value chain will ensure its success. These shall include verification, validation and certification of process on IBS components, fabricator, factory, erector and related skills of specialisation,

- A technology transfer model via knowledge management and benchmarking analogy to adapt European Union (EU), Japan and Singapore best practices in implementing IBS will add value and expedite the implementation process,

- A comprehensive study on Business Process Re-engineering, Change Management and Total Quality Management (TQM) that can be agent of chance to transform Malaysian construction industry.

A combination of integrated approach and long term strategic partnering among stakeholders tackling specific agenda on IBS 5M strategies are the way forward. A well coordinated planned R&D themes and titles discussed in previous section have to be implemented simultaneously with all players mentioned earlier in synergic and strategic way.

ACKNOWLEDGEMENT

The authors would like to acknowledge the following committees for their contribution:

1. IBS Steering Committee Session 2003-2005
2. Construction Technology and Innovation Development Sector, CIDB Malaysia
3. IBS Centre, Cheras, Kuala Lumpur
4. Participants who had attended workshop entitled:

    a) Workshop on Aligning R&D Priority Area to CIMP 2006-2015 on 26th -28th May 2006 at Guoman Port Dickson Resort, Negeri Sembilan.
    b) Workshop on Aligning R&D Themes and Titles to the Requirement of Construction Industry, 21st -22nd April 2007, Avillion Village Resort, Port Dickson, Negeri Sembilan.

REFERENCES

Construction Industry Development Board (CIDB) (2007a) *Construction Industry MasterPlan(CIMP 2006-2015).,* CIDB. Kuala Lumpur.

Construction Industry Development Board (CIDB) Malaysia (2007b) *IBS Roadmap Mid – Term Report (Final report*), 2007, IBS Centre (unpublished), Malaysia Kuala Lumpur.

Construction Industry Development Board (CIDB), Malaysia (2007c). *Malaysian Construction Outlook 2007.* CIDB*,* Kuala Lumpur.

Construction Industry Development Board (CIDB) Malaysia (2003a) *IBS Roadmap 2003-2010*, CIDB, Kuala Lumpur.

Construction Industry Development Board (CIDB) Malaysia (2003b) *IBS Survey*, CIDB, Kuala Lumpur.

Construction Research Institute of Malaysia (CREAM) (2007) *Workshop Report*, Workshop on Aligning R&D Themes and Titles to the Requirement of Construction Industry, 21st -22nd April 2007. Avillion Village Resort, Port Dickson, Negeri Sembilan. (draft report)

Chung, L. P.& Kadir, A. M. (2007) *Implementation Strategy for Industrialised Building Systems*. PhD thesis, Universiti Teknologi Malaysia (UTM), Johor Bahru.

Din, H. (1984) *Industrialised Building and Its Application in Malaysia*, Proceeding on Seminar on Prefabrication Building Construction, Kuala Lumpur.

Esa, H. and Nurudin, M.M. (1998) *Policy on Industrialised Building Systems*. Colloqium on Industrialised Construction Systems, Kuala Lumpur.

Gue, S. S. (2007) *Bridging the Gap Between R&D and Construction Industry*. Keynote address at Construction Industry Research Achievement International Conference. Putra World Trade Centre (PWTC).Kuala Lumpur.

Hamid, Z., Kamar, K. A. M, Mohd. Khairolden, G., Maria Zura, M. Z., & Ahmad Hazim, A. R. (2007) *Strategic Planning for R&D on Industrialised Building Systems (IBS) 2007-2010*. Construction Research Institute of Malaysia (CREAM), Kuala Lumpur (draft report).

Hussein, J. (2007) *Industrialised Building Systems: The Challenge and The Way Forwar*d. Keynote Address at Construction Industry Research Achievement International

Conference. Putra World Trade Centre (PWTC). Kuala Lumpur.

IBS Steering Committee (2006) *Minute meeting of IBS Steering Committee*. Construction Industry Development Board (CIDB) Malaysia. Kuala Lumpur (unpublished),

Junid, S.M.S. (1986) *Industrialised Building Systems*. Proceedings of UNESCO/ FEISEAP Regional Workshop, Universiti Putra Malysia (UPM), Serdang. Selangor.

Lessing, J., Ekholm, A., and Stehn, L. (2005) *Industrialised Housing-Definition and Categorisation of the Concept.* 13th International Group for Lean Construction. Sydney,
    Australia.

Ministry of Finance (MOF) (2005) *Economic Report Malaysia 2004-2005* (2004). Malaysia, Kuala Lumpur. (Unpublished)

Parid, W. (1997) *Global Trends in Research, Development and Construction*. Proceeding of the International Conference on Industrialised Building System (IBS 2003). Construction Industry Development Board (CIDB) Malaysia. Kuala Lumpur.

Rahman, A.B.A, Omar, W. (2006) *Issues and Challenges in the Implementation of IBS in Malaysia*. Proceeding of the 6th Asia-Pasific Structural Engineering and Construction Conference (ASPEC 2006). 5-6 September 2006. Kuala Lumpur, Malaysia

Thanoon, W.A.M., Peng, L.W., Abdul Kadir, M.R., Jaafar, M.S. and Salit, M.S. (2003) *The Experiences of Malaysia and Other Countries in Industrialised Building System in Malaysia*. Proceeding on IBS Seminar. UPM, Malaysia

Trikha, D.N. (1999) *Industrialised Building System: Prospect in Malaysia*. Proceeding of World Engineering Congress, Kuala Lumpur.

Warszawski, A. (1999) *Industrialised and Automated Building System*, Technion-Israel Institute of Technology, E & FN Spon.

STANDARDISATION OF PARTIAL STRENGTH CONNECTIONS OF EXTENDED END-PLATE CONNECTIONS FOR TRAPEZOID WEB PROFILED STEEL SECTIONS

Mahmood Md Tahir[1], Arizu Sulaiman[1]

[1]*Steel Technology Centre, Faculty of Civil Engineering,*
Universiti Teknologi Malaysia, 81310, Skudai, Johor.

Abstract:

Traditionally, connections are usually classified as pinned or rigid although the actual behaviour is known to fall between these two extreme cases. The use of partial strength or semi-rigid connections has been encouraged by codes and studies on the matter known as semi-continuous construction have proven that substantial savings in steel weight of the overall construction. The objective of this paper is to develop a series of standardised partial strength connections tables of extended end-plate connections for trapezoidal web profiled steel (TWP) sections. The range of standard connections presented in tabulated form is limited to eight tables comprised of different geometrical aspects of the connections. These tables could enhance the design of semi-continuous construction of multi-storey braced steel frames. The connections are presented in the form of standardised tables which include moment capacity and shear capacity after considering all possible failure modes. A method proposed by Steel Construction Institute (SCI) which take into account the requirements in Eurocode 3 and BS 5950:2000 Part 1 were adopted to predict the moment capacity and shear capacity in developing the tables. A series of tests have been carried out to validate the results of the standardised tables. The test results showed good agreement between theoretical and experimental values.   It can be concluded that the proposed standardised tables for TWP sections is suitable to be used in the design of semi-continuous construction.

Keywords: *Partial Strength Connection; Extended End Plate; Beam-to-Column Connection; Trapezoid Web Profiled Section; Semi-Continuous Construction*

INTRODUCTION

In the design of steel frame, connections play an important part in the determination of the types of construction. Pinned jointed connection is usually associated with simple construction and rigid jointed connection is usually associated with continuous construction. When designed as pinned jointed, the beams are assumed as simply supported and the columns are assumed to sustain axial and nominal moment only. The associated connection such as flexible end plate connection is simple and relatively easy to erect but the sizes of the beams obtained from this approach are relatively heavy and deep. On the other hand, rigidly jointed frame results in heavy columns due to the end moments transmitted through the connection. Hence, a more complicated fabrication of the connection could not be avoided.

Eurocode 3 (1992) introduces designer to use semi-rigid connection or partial strength connection which creates a balance between the two extreme approaches. This alternative semi-rigid or partial strength connection is usually associated with a connection having a moment capacity less than the moment capacity of the connected beam (Peter, *et. al.* 1996). Partial strength connection or semi-rigid connection is the term used for connection in the design of semi-continuous construction for multi-storey steel frames by Eurocode 3(1992). In semi-continuous construction design the degree of continuity between the beams and columns is greater than that in simple construction design but less than that in continuous construction design. The degree of continuity in the use of partial strength connection of beam to column can be predicted to produce an economical beam section that representing the section between pin joint and rigid joint. By adopting this approach, studies conducted on the use of partial strength connection in hot-rolled steel section have proven substantial savings in overall steel weight (Md Tahir, 1997 & Couchman. 1997). This is possible as the use of partial strength has contributed to the benefits on both the ultimate and serviceability limit states design. However, the use of partial strength connections for Trapezoid Web Profiled sections has not been established yet. To enable the use of TWP sections with partial strength connection, standardised partial strength connection tables need to be established first. Therefore, this paper intends to establish the standardised tables for partial strength connections for TWP sections based on the proposed method by SCI.

TWP SECTION AS A BUILT-UP SECTION

A trapezoid web profiled section is a built-up plate girder comprised of two flanges connected together by a thin corrugated web as shown in Figure 1 (Osman, 2001 & Hussein, 2001). The web and the flanges are welded together with different steel grade depending on the design requirements. The steel grade of the flanges is designed for S355 and the steel grade of the web is designed for S275. The steel grade of the flanges is purposely designed for S355 so that the flexural capacity of the beam can be increased. The steel grade of the web is designed for S275 so as to reduce the cost of steel material and the capacity of shear is not that critical in the design of the beam (Hussein, 2001). The use of different steel grades in the fabrication of TWP section leads to further economic contribution to steel frames design besides the use of partial strength connection. The use of thick flanges, thin web and deeper beam for TWP section compared with hot-rolled section of the same steel weight leading to heavier load capacity and greater beam span that can be achieved.
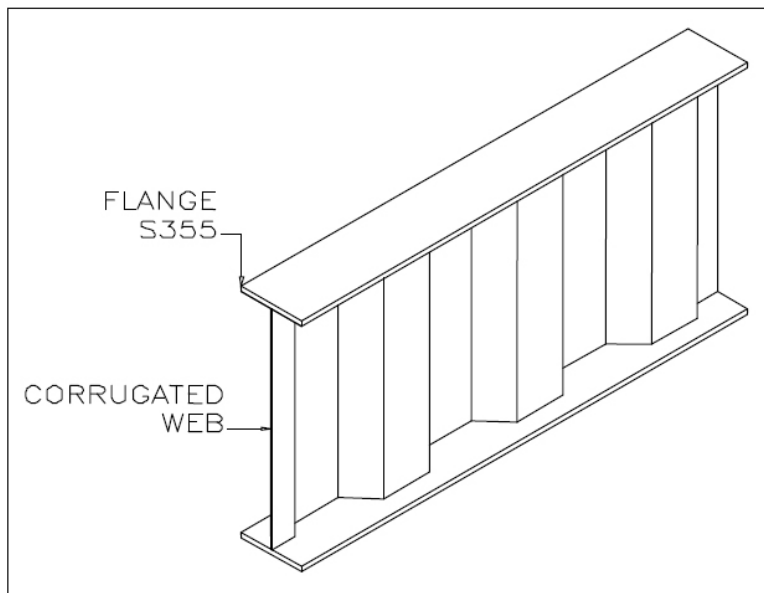
Figure 1. Configuration of Trapezoidal Web Profiled Section

Benefits of using TWP steel sections

The benefits of a TWP beam as compared to the conventional plate girder or hot rolled steel section include the following (Tan, 2004):

- Reduce the steel weight by utilizing thin web.
- Eliminate the need of stiffeners which reduced the fabrication cost.
- The use of high strength steel S355 for flanges and deep beam which lead to higher flexural capacity, wider span and less deflection.

Based on the configuration of the structure, TWP beam can offer substantial saving in the steel usage, and in some cases of up to 40% as compared to conventional rolled sections (Osman, 2001& Hussein, 2001). It is more significant when there is a need for a column free; long span structural system, such as portal frames for warehouses, girder for bridges, floor and roof beam for high-rise buildings, and portal frame for factory.

ADVANTAGES OF STANDARDIZED PARTIAL STRENGTH CONNECTIONS

In the design of braced multi-storey steel frames, the steel weight of the connections may account for less than 5% of the frame weight (Peter A, et al 1996). However, the cost of the fabrication is in the range of 30% to 50% of the total cost depending on the difficulty of the fabrication (Peter, *et. al.* 1996). The increase in the fabrication of the connections is due to the difficulty in selecting the type of connection, the grades and sizes of fittings, bolt grades

and sizes, weld types and sizes, and the geometrical aspects. Therefore, a standardized partial strength connections tables are introduced to cater for the problems arise due to so many uncertainties in the fabrication of the connections. The advantages of the partial strength approach are that it utilizes the moment resistance of connections to reduce beam depth and weight, while avoiding the use of stiffening in the joints. This practice will reduce the cost of fabrication and ease the erection of steel member in the construction of multi-storey steel frames. The potential advantages of using this approach can be listed as follows (Peter & Mike,1992)(Peter & Mike, 1993):

Lighter beams

In the design of semi-continuous braced steel frame, the required beam plastic modulus is less than those required in simple frame for the same frame. This reduction is possible as the partial strength connection reduced the design moment of the beam due to the partial restraint effect of the connection as illustrated in Figure 2 (Couchman, 1997). The design moment which a beam must resist, decreases as the moment capacity of the connection increases. As a result, a lighter beam can be selected for the design of the beam.
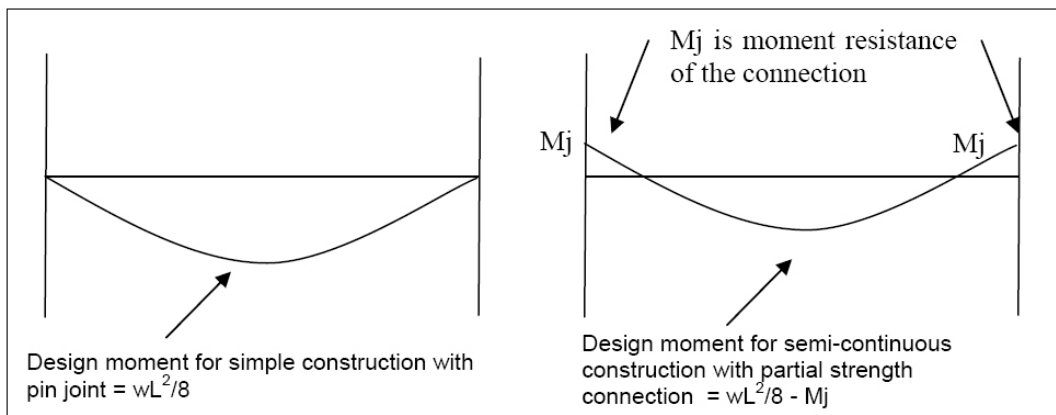
Figure 2. Design moment for beams due to different support conditions

Shallower beams

The partial restraint of the connection will also result in shallower beams. This is due to the increase in stiffness of the connection, which contributes to the decrease in deflection. The use of partial strength connection will reduce the constant coefficient β in the formulae of deflection ($\beta wL^4/384EI$) in simple construction with uniform load from β equal to 5 to β equal to 2 for internal beam and β equal to 3 for external beam (Couchman, 1997). The partial strength connection acts as restrained to the deformation of the beam due to applied load. As a result, a reduction in the deflection of the beam can be achieved which lead to the shallower beam. The relationship between connection stiffness and deflection coefficient "Beta" for uniform load on beam is shown in Figure 3.
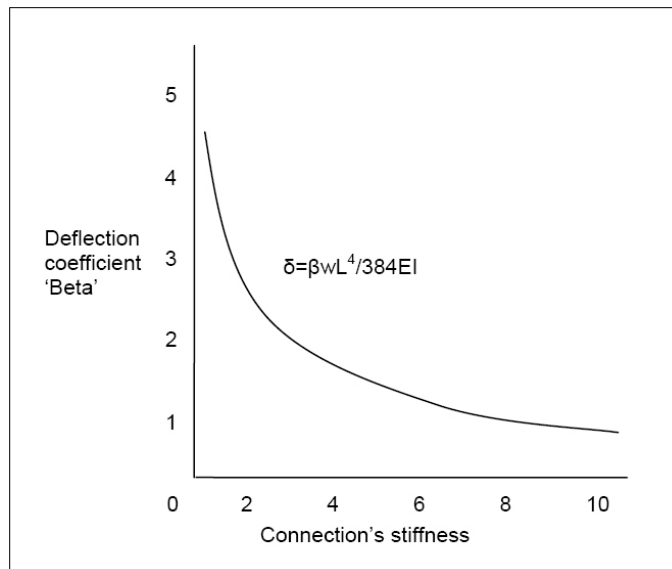
Figure 3. Deflection coefficient 'Beta' as a function of relative stiffness of connection

Greater stiffness and more robust structure

Connection stiffness means that the ends of a beam are restrained against rotation. Partial strength connection has higher capacity to restrain against rotation, shear, moment, and tying force. The rotation capacity should be in the range of 0.02 to 0.03 radians at failure for the connection to be considered as ductile and stiff enough to be categorised as partial strength (Peter, *et. al.*, 1996). The shear capacity of the connection is designed in such a way that the capacity is higher than the shear capacity of the connected beam, and the moment capacity of the connection can resist up to 50% of the moment capacity of the connected beam (M_{cx}) depending on the size and number of bolts for the proposed standard tables. The tying force of the connection is two to three times greater than the tying force required by (BS 5950:2000 Part 1) that is 75kN. Therefore, the connection can be categorized as strong, stiff, and robust connection.

Lower overall cost

Good connection should be the one which can ease the design process, the preparation of detailing, the fabrication process, and the erection works. It should also consider the most cost effective in the development of the connection. The saving in the overall cost can be achieved due to the following reasons (Peter & Mike, 1992)(Peter & Mike, 1993):

- A reduction in the number of connection types may lead to a better understanding of the cost and type of connection by all steel players such as fabricator, designer, and erector.
- A standardised connection can enhance the development of design procedures and encourage in the development of computer software.

- The use of limited standardised end-plates or fittings can improves the availability of the material leading to reduction in material cost. At the same time, it will improve the order procedures, storage problems and handling time.
- The use of standardised bolts will reduce the time of changing drills or punching holes in the shop which lead to faster erection and less error on site. The drilling and welding process can be carried out at shop as the geometrical aspects of the connection have already been set. This leads to fast and quality fabrication.

Although the advantages or benefits of using the partial strength connections are quite significant, the disadvantages of this approach should also be addressed. The disadvantage in this approach is that it may be marginally more expensive to fabricate partial-strength connection rather than simple connections. However, the benefit of overall cost saving of the partial strength connections has proven to be more than simple connections. It is reported that the savings in steel weight of using partial strength connection in multi-storey braced steel frames using British hot-rolled section was up to 12% (Md Tahir, 1997). The overall cost saving was up to 10% of the construction cost which is quite significant (Md Tahir, 1997). This is quite significant as the proposed partial strength connection is able to satisfy the requirement of the design code without implicate any problems with the safety of the structure.

PROPOSED STANDARDIZED EXTENDED END-PLATE CONNECTIONS

The use of partial strength connections for hot-rolled British sections has well established by SCI (Peter, *et. al*., 1996). A series of tests at the University of Abertay, Dundee has been successfully been carried out to verify the predicted moment and shear capacity with the experimental tests capacities (Bose, 1993). The results confirmed with the predicted values and the standardized tables for the connection have been published by SCI (Peter, *et. al.*, 1996). In partial strength connections, two types of connections are preferred: flush end plate connection and extended end plate connection. The development of standard flush end plate connections tables has been reported in another publication by the author (Md Tahir, *et. al.*, 2006). In the development of standard extended end-plate connections tables for TWP sections, only eight tables are presented in this study based on the proposed method. Although the best validation of the results presented in the tables is by comparing the predicted results with the actual experimental tests results, however, the presented standard connection tables for TWP section can still be used by adopting the same failure modes of the hot-rolled section as tested by SCI. A few tests have been carried out to support the predicted moment resistance of the connection using TWP section as a beam. Some of the results are presented later in this paper. The proposed standard connections have the following attributes, which in some cases the attributes are not exactly the same as the one described by SCI in hot-rolled section.

- The end plates are extended at the tension side only since no reversal of moments is expected as shown in Figure 4. This type of connection is recommended for braced steel frame.
- 12mm thick end plates in conjunction with the use of M20 bolts.
- 15mm thick end plates in conjunction with the use of M24 bolts.
- Strength of end plates was maintained as S275 steel.
- Width of the end plate was kept at 200mm and 250mm with the vertical height of the end-plate was kept at the beam depth plus 90mm.
- Only one row of bolts is used in the extended part of end plates.
- Full strength of flange welds with size of weld proposed at 10mm but an 8 mm weld is also adequate.
- Full strength of web welds with size of weld proposed at 8mm but a 6 mm weld is also adequate.
- The vertical and horizontal distance between the bolts was maintained at 90mm.

Figure 4, shows a typical extended end plate connection for TWP section as beam connected to British hot-rolled section as column. British section is selected for the column as it is very good in compression which is not the case for TWP section as the web of TWP is too thin to carry axial load. TWP section is proposed for the beam as the corrugated web section is very effective to cater for buckling and bearing resistance. The minimum thickness for corrugated web is 3mm for shallow beam and the maximum thickness is 6mm for deeper beam. The ratio of beam depth versus web thickness is increased to at least semi-compact even though the suggested limit is compact as described by (BS5950:2000 Part 1). The limit is increased based on the observation from previous study using Flush End Plate connections that are capable to sustain higher moment capacities (Peter, *et. al.*, 1996).
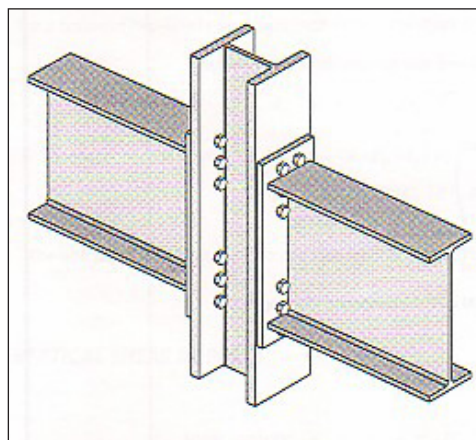

Figure 4. Typical extended end-plate connection of TWP beam section connected to British Hot-Rolled section.

DEVELOPMENT OF THE STANDARD CONNECTION TABLES

Unlike simple and rigid connections, the design of partial strength connections involves more complex and rigorous procedures. Therefore, Steel Construction Institute published a reference guide in designing moment connections, which includes sections on the standardised capacity tables for bolted end plate connections (Peter, *et. al.* 1996). The design model presented in the SCI's guide is in accordance to the procedures in Annex J of EC3, which is based on the plastic distribution of bolt forces. Traditionally, the bolt forces are taken as a triangular distribution but plastic distribution is 'accurately' representing the actual behaviour of bolt forces as shown in Figure 5 (Eurocode 3, 1992). The tension force F_{reinf} noted as the reinforcement was calculated as follows:-

$$F_{reinf} = \frac{f_y A_{reinf}}{\gamma_m}$$ where f_y is the design yield strength of reinforcement, A_{reinf} is the area of reinforcement within the effective width of the slab and γ_m is the partial safety factor for reinforcement taken as 1.05. The forces of the tension bolts are noted as F_{r1} and F_{r2} as shown in Figure. 5 are calculated by checking on the top row and working downward. This means that each of bolt rows is checked first in isolation which is then combined with the lower row to get the potential force for that particular bolt. The potential force for the bolts can be summarised as follows:-
F_{r1} = (resistance of row 1 alone)
F_{r2} = minimum of (resistance of row 2 alone or (resistance of rows 2 + 1) – F_{r1})

In the SCI's guide, the beam-to-column arrangements constitute of conventional hot rolled sections for both the beams and the columns. In this study, TWP sections are used as beams; therefore, the tables provided in the design guide for hot rolled British sections are not applicable to the TWP sections as the section properties of TWP sections are not similar.
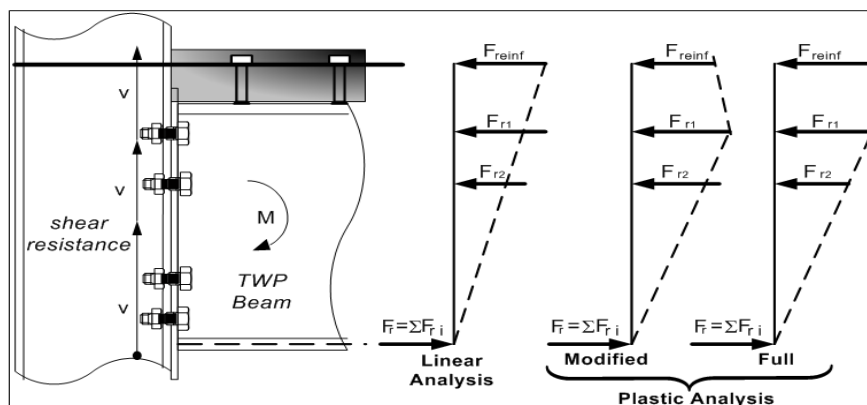

Figure 5. Forces in connection and corresponding distribution

Design philosophy of the connections

The design model adopted in this study is actually presented in Annex J of Eurocode 3: Part 1.1 (1992). For checking the details of strength on the bolts, welds, and steel section, modification to suit (BS 5950:2000 Part 1) have been done. The checking on the capacity of the connections is classified into three zones namely tension zone, compression zone, and shear zone as shown in Figure 6 (Peter, *et. al.*, 1996). The basic principles of the distribution of bolt forces need to be addressed first before details of the checking on all possible modes of failures can be discussed.
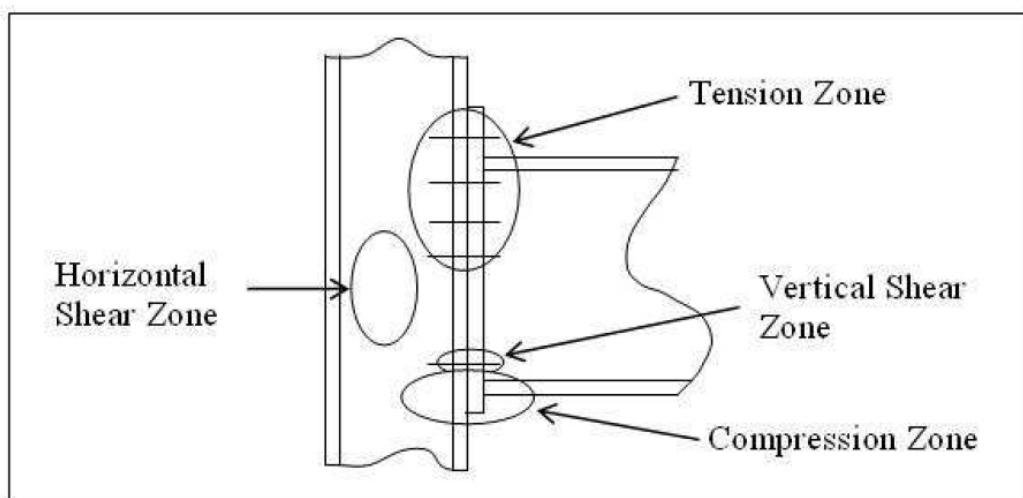

Figure 6. Critical zones that need to be checked for failure

Distribution of Bolt Forces

The moment resistance of a connection transmitted by an end plate connection is through the coupling action between the tension forces in bolts and compression force at the centre of the bottom flange. Each bolt above the neutral axis of the beam produced tension force whereas the bolts below the neutral axis are dedicated to shear resistance only. Eurocode 3(1992) suggests that the bolt forces distribution should be based on the plastic distribution instead of the traditional triangular distribution. Figure 5 shows the forces in the connection and the corresponding distributions. The forces of the bolt are based on the plastic distribution which is the actual value calculated from the critical zones in Figure. 6. The force from the top bolt row transmits to the end-plate connection as tension force which balanced up by the compression force at the bottom flange of the beam to the column. The end-plate is connected to web and both of the flanges by welding. The formation of tension at the top and compression at the bottom contributes to the development of moment resistance of the connection. Tests on the connections have showed that the centre of compression flange which bears against the column was found to be the centre of rotation of the connection (Bose, 1993). The force permitted in any bolt row is based on its potential resistance and not just the length of the lever arm.

Tension zone

The resistance at each bolt row in the tension zone may be limited due to bending of column flange, end-plate, column web, beam web, and bolt strength. Column flange or end-plate bending was checked by using Eurocode 3(1992) which converts the complex pattern of yield lines around the bolts into a simple 'equivalent tee-stub'. Details of the procedures are illustrated in SCI publication (Peter, *et. al.*, 1996).

Compression zone

The checking in the compression zone are the same procedures as mention in (BS 5950:2000 Part 1) which requires checks on web bearing and web buckling. The compression failure modes can be on the column side or on the beam side. The column side should be checked for web buckling and web bearing due to the compression force applied to the column. The use of stiffener or the effect of having other beam connected to the web of the column is not included so as to reduce the cost of fabrication and simplified the calculation. The compression on the beam side can usually be regarded as being carried entirely by the beam flange, however when large moments combine with axial load, the compression zone will spread to the web of the beam which will effect the centre of compression. Therefore, the stiffening of the web of the beam needs to be done. However, in this study the moment resistance of the connection is not considering the use of stiffener in order to reduce the cost of fabrication.

Shear zone

The column web can fails due to the shearing effect of the tension and compression force applied to the web of the column. The failure to the shearing of the web is most likely to happen before it fails due to bearing or buckling. This is possible because the thickness of the flange is more than the thickness of the web. Again in this shear zone, stiffer is not needed so as to reduce the cost of fabrication.

Welding

Fillet weld is preferred than the butt welds as the welding of beam to the end-plate is positioned at 90 degree which is suitable for fillet weld to be used. The end-plate is connected to the web of the beam by an 8 mm fillet weld, whereas a 10 mm fillet weld is suggested for connecting the end-plate to the flange. The weld is designed is such a way that the failure mode of the connection is not on the welding. This is to ensure the ductility of the connection which is necessary for partial strength connection.

Validation of the standardised connections tables

The validation of the standardised connections tables for TWP is best presented by comparing the predicted values in the table with full scale testing of the connections. Therefore, a series of full scale testing on TWP girder sections comprised of four specimens was conducted by the Steel Technology Centre, Universiti Teknologi Malaysia. Although the tests did not cover the whole ranged of the proposed connections, the comparison of the tests and the predicted values can still be established. Figure 7(a, b, c, and d) show some of the results of the experiment by plotting the moment on the connection versus the rotation of the connection. The curves show that the moment resistance of the connection was linear at initial stage followed by non-linear stage. The tests results of moment resistance, MR were determined when a "knee" formed in each of the M-F curves plotted in Figure 7(a to d). This knee technique has been used by many researchers to predict the moment resistance of the connection from the M-F curves drawn from the tests results (Tahir, 1997, Sulaiman, 2007 & Anis, 2007). The formation of 'knee' which determine the moment resistance of the connection was developed by drawing two straight lines; a straight line drawn from linear region and intersected to another straight line drawn from a non-linear region that formed almost a plateau in the M-F curves. By adopting this technique, the test values of moment resistance, MR for the overall joint for the tests were established from the point of intersection which identified as 'knee'. This technique takes into account the deformation of the connection due to the formation of elasto-plastic, a region between elastic and plastic regions.

The moment resistance of the beam should be based on the slenderness of the section and the stress block as shown in Fig. 8. This approach is applicable of web-to-depth ratio not greater than 62ε where the beam is assumed not to be susceptible to shear buckling. Otherwise, the beam should be checked for shear buckling using clause 4.4.4.2 in BS 5950:2000 Part 1. As the web of TWP sections is thin, the determination of moment resistance of the sections can be simplified by using a "flange only method" as suggested by BS 5950:2000 Part 1 for built-up section. This method assumed that the flanges fully yielded and with d/t of the thin web is more than 62ε, the contribution of the web is ignored to ease engineers in design calculation. The failure modes of end-plate of the connections are shown in Figure 9 as expected from the calculation. Details of the method of testing and the discussion of the result have been published elsewhere (Sulaiman, 2007).
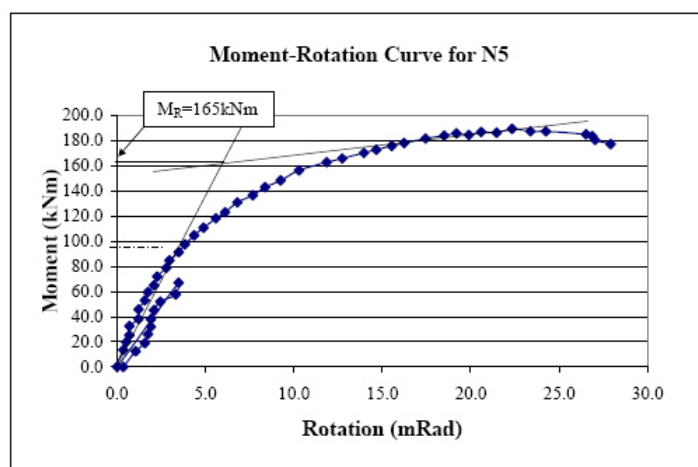
**Figure 7(a).** Moment versus rotation for specimen N5 (E2R20P1)
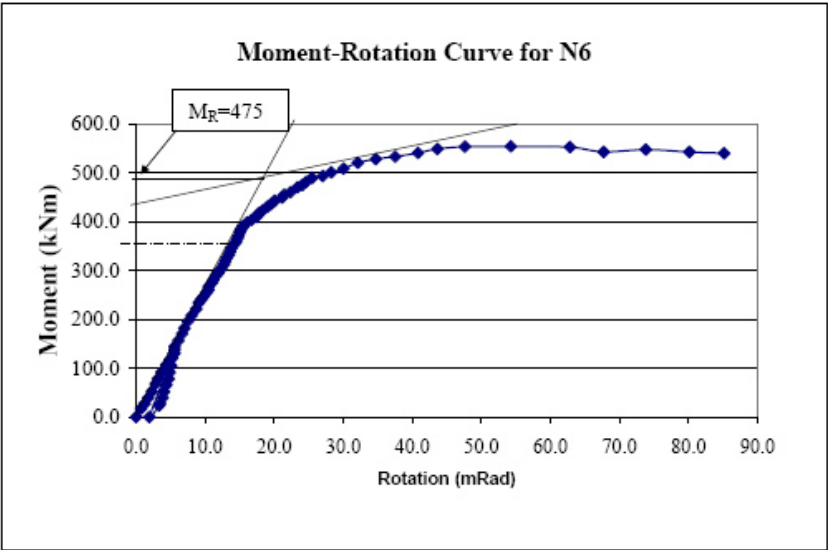
**Figure 7(b).** Moment versus rotation for specimen N6 (E2R24P2)
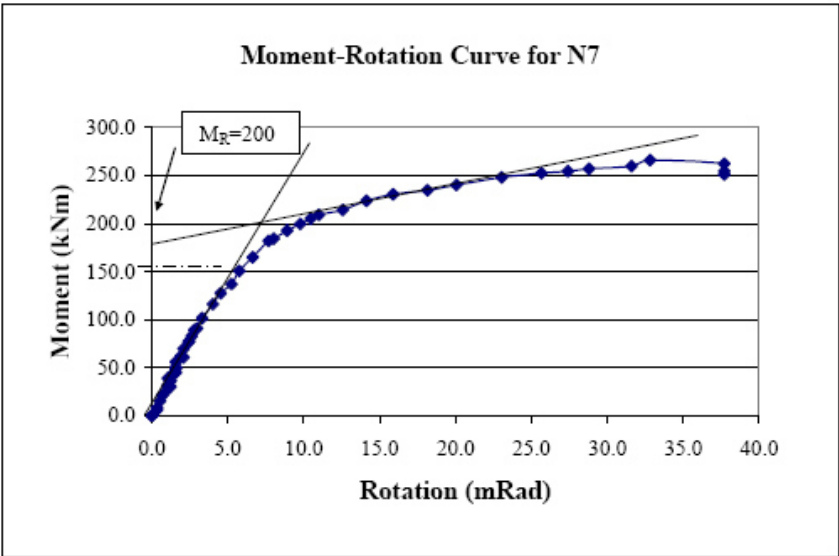
Figure 7(c). Moment versus rotation for specimen N7 (E3R20P1)
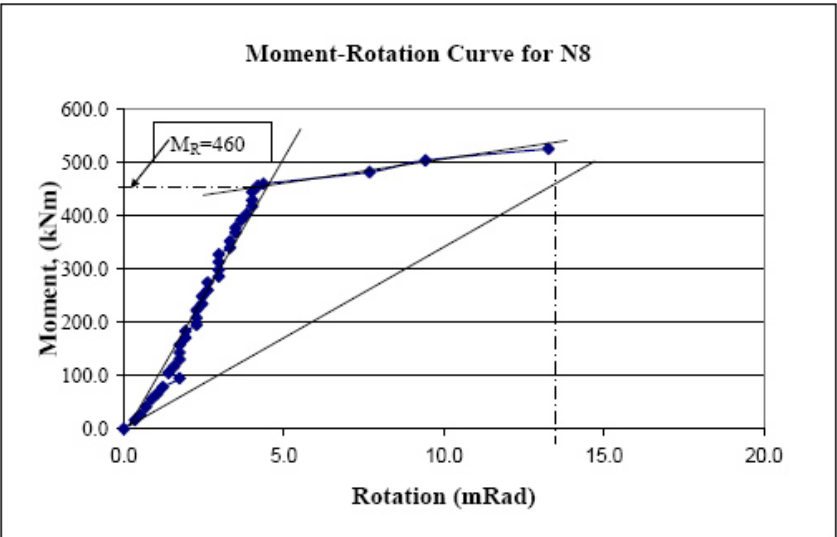
Figure 7(d). Moment versus rotation for specimen N8 (3R24P2)
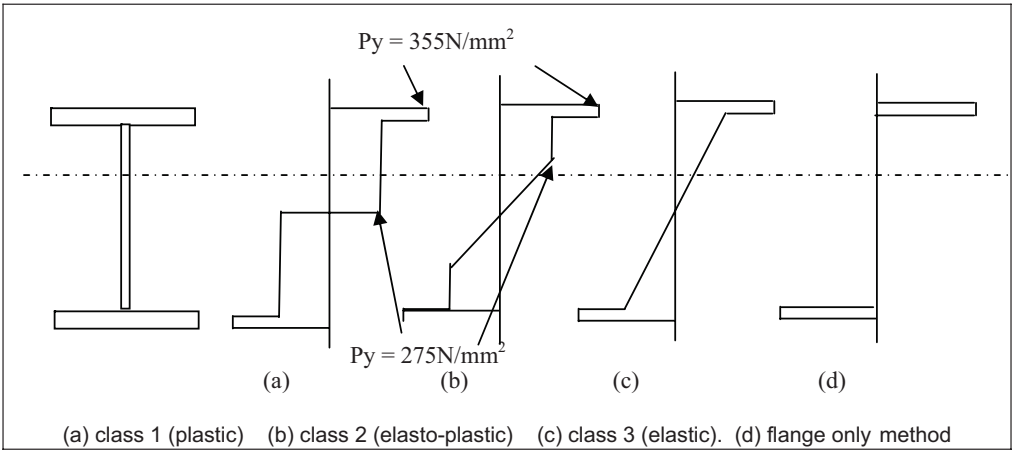

**Figure 8.** Stress block on the cross section with different design strength.
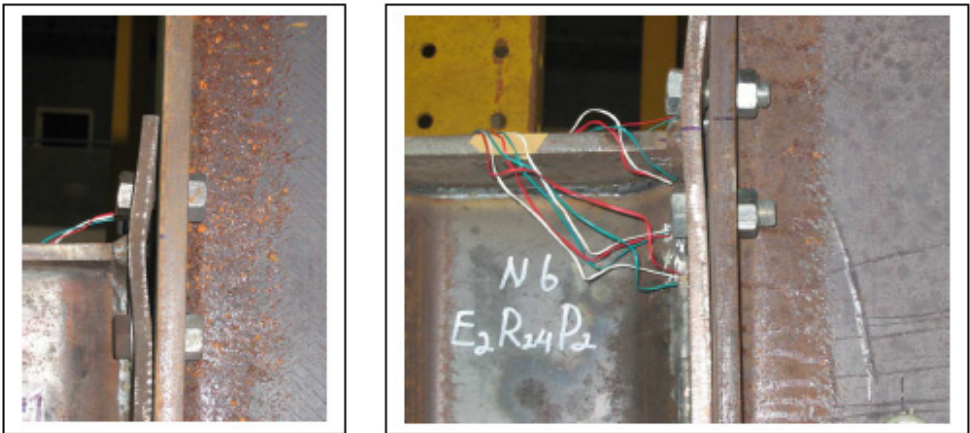
Figure 9. Failure modes of extended end-plate connection during test

Explanation on the notation used in the proposed capacity tables

Eight configurations of extended end plate connections tables have been developed as shown in Table 1. A computer programming based on spread sheet has been developed to calculate and predict the moment capacity and shear capacity of the standardised connections proposed in Table 1 based on the critical zones checks and method proposed by SCI as described earlier. The details of the capacities of the standard tables for the connections are tabulated in Table 2 to 9. The moment capacity from the proposed table is calculated from the summation of each bolt row multiply by the lever arm of the connection. The lever arm for the first tension bolt row, which is defined as 'dimension A' measured from the centre of compression capacity to the lowest row of tension, bolts. The lever arm for the second tension bolt row is measured as 'dimension A' plus the distance first tension bolt row to the second tension bolt row, in this case 90mm. All flange welds are to be fully welded with minimum fillet weld of size 10mm for flange and 8mm for web. A tick in the table indicates that the column flange and web in tensions have a greater capacity than the beam force as indicated in the beam table. If the column has a smaller capacity, the reduction of bolt force is shown in the table. A modified moment resistance that has been reduced can be determined from these lower forces. A tick in compression zone indicates that the column web has a greater compression capacity than the sum of the bolt row forces. A vertical shear capacity is the shear resistance of the bolt due to shearing, bearing to the bolt and bearing to the plate.

Table 1. Configurations of end plate connections used to generate standardised tables

Type of Connections	Row of Bolts	Type of Bolts	Size of End Plates (mm)
EEP,2BRM20,200W12TEP	2	M20 8.8	200 x 12
EEP,2BRM20,250W12TEP	2	M20 8.8	250 x 12
EEP,2BRM24,200W15EP	3	M20 8.8	200 x 12
EEP,2BRM24,250W15TEP	3	M20 8.8	250 x 12
EEP,3BRM20,200W12TEP	2	M24 8.8	200 x 15
EEP,3BRM20,250W12TEP	2	M24 8.8	250 x 15
EEP,3BRM20,200W15TEP	3	M24 8.8	200 x 15
EEP,3BRM24,250W15TEP	3	M24 8.8	250 x 15

DISCUSSION OF RESULTS

The standard tables as shown in Table 2 to 9 illustrate the geometrical configuration of the suggested connections and the capacities of the connections. The suggested size of column and beam used for the proposed connection is listed in the designated table. The moment capacity of the connection is listed base on the size of the beam. The smallest suggested size of beam (in the low capacity connection table) is taken as 350x140 (mm) whilst the largest suggested size of beam (in the high capacity connection table) is taken as 750x250 (mm). Although TWP section can be produced for up to 1600mm deep, the limited suggested size for partial strength connection is up to 750mm deep. This is to maintain the ductility of the connection that is crucial for partial strength connection. The shear capacity of the connection is based on the shear capacity of the tension bolt row and

lower bolt rows. However, the lower bolt row will carry most of the shear force. The increase in moment capacity depends on the size of bolt, the number of bolt, the size of end-plate, and the thickness of end-plate. The notation used for the designated connection such as (EEP,2BRM20,200W12TEP) meaning that the connection is an extended end-plate with two bolt rows of M20 (one row in the extended part of end plate and one row beneath the flange) grade 8.8, and an end-plate size of 200mm wide and 12mm thick. The comparison of the moment capacity of the connection based on different geometrical configuration of the connections is discussed below:

Effect of increasing the number of bolt row from two rows to three rows

Table 2, 3, 4 and 5 show the moment capacity of the connection for double bolt rows. Table 6, 7, 8 and 9 shows the moment capacity of the connection for triple bolt rows. The results of percentage increase in moment capacity for two and three bolt rows are shown in Table 10. The results showed that by increasing the number of bolt row from two to three, moment capacity of the connection is increased by an average of 30.1% for M20 bolt with 12mm thick and 200mm wide end plate, 30.8% for M20 bolt with 12mm thick and 250mm wide end plate, 32.8% for M24 bolt with 15mm thick and 200mm wide end plate, 29.4% for M24 bolt with 15mm thick and 250mm wide end plate. The combination of M24 with 15mm thick end plate has contributed to the increase in the moment capacity of the connection. The increment however is not that significant. The increase in moment capacity is very much linear to the depth of the beam. This shows that the moment capacity of the connection depends on the depth of the beam, the number and size of bolt, and the thickness of the end plate.

The vertical shear capacity of connection in Table 2 and 3 is increased from 331kN without optional shear bolt row to 515kN with shear row. The vertical shear capacity of connection in Table 4 and 5 is increased from 475kN without optional shear bolt row to 739N with shear row. The increment of the vertical shear capacity is not exactly double as the determination of the shear capacity depends on the number of row of the tension bolt too. The vertical shear capacity of the connection in Table 6 and 7 is 588kN with optional shear bolt row. The vertical shear capacity of the connection in Table 8 and 9 is 845kN with optional shear bolt row. These values are about twice the vertical shear capacities of the connections in Table 2 and 3, and Table 4 and 5 respectively without optional shear bolt row. This is because the number of bolt row at the tension zone in Table 6, 7, 8 and 9 is three rows. Panel shear capacity for all the connections is the same as the size of the columns is the same and the force of tension and compression that exert on the column web is not high enough to change the calculated values.

Table 2. Standard table for extended end-plate for 2 row M20 8.8 bolts, 200x12 end-plate (EEP,2BRM20,200W12TEP

2 ROW M20 8.8 B0LTS
200 x 12 DESIGN GRADE 43 EXTENDED END PLATE

BEAM – FLANGE S355 WEB S275

Beam Serial Size D x B x kg/m (T/t)	Dimension 'A' (mm)	Moment Capacity (kNm)
350 x 140 x 35.1 (12/3)	284	106
400 x 140 x 39.7 (12/4)	334	123
400 x 160 x 48.4 (14/4)	333	123
450 x 160 x 50.2 (14/4)	383	139
450 x 180 x 60.1 (16/4)	382	139
500 x 160 x 52.0 (14/4)	433	156
500 x 180 x 61.9 (16/4)	432	156
550 x 200 x 73.3 (16/5)	482	172
600 x 200 x 80.5 (16/6)	532	189
350 x 140 x 35.1 (12/3)	284	106

(F_{r1}) 124kN (F_{r2}) 208kN (ΣF_r) 332kN

20, 55, 90, 55 — 50, 40, 60, 90, 90, 60, 25 — Optional Shear Row

Vertical Shear Capacity
331 kN without shear row
515 kN with shear row

DESIGN GRADE S275				COLUMN	DESIGN GRADE S355			
Panel Shear Capacity (kN)	Tension Zone F_R1 (kN)	Tension Zone F_R2 (kN)	Compn. Zone	Serial Size	Compn. Zone	Tension Zone F_R1 (kN)	Tension Zone F_R2 (kN)	Panel Shear Capacity (kN)
1000	√	√	√	356 x 368 x 202	√	√	√	1302
849	√	√	√	177	√	√	√	1105
725	√	√	√	153	√	√	√	944
605	√	√	√	129	√	√	√	787
1037	√	√	√	305 x 305 x 198	√	√	√	1350
816	√	√	√	158	√	√	√	1062
703	√	√	√	305 x 305 x 137	√	√	√	915
595	√	√	√	118	√	√	√	774
503	√	√	√	97	√	√	√	649
882	√	√	√	254 x 254 x 167	√	√	√	1149
685	√	√	√	132	√	√	√	892
551	√	√	√	107	√	√	√	717
434	√	√	√	89	√	√	√	566
360	√	√	√	73	√	√	√	465
459	√	√	√	203 x 203 x 86	√	√	√	598
353	√	√	√	71	√	√	√	460
322	√	√	√	60	√	√	√	415
272	√	√	√	52	√	√	√	351
245	√	181	√	46	√	√	√	316

Tension Zone:
√   Column satifactory for bolt row tension values shown for the beam side.
xxx   Calculate reduced moment capacity using the reduced bolt row values.
Compression Zone:
√   Column capacity exceeds ΣF_r.
S (xxx)   Column requires stiffening to resist ΣF_r (value is the column web capacity).

Table 3. Standard table for extended end-plate for 2 row M20 8.8 bolts, 250x12 end-plate
(EEP,2BRM20,250W12TEP)

2 ROW M20 8.8 B0LTS
250 x 12 DESIGN GRADE 43 EXTENDED END PLATE

BEAM – FLANGE S355 WEB S275

Beam Serial Size D x B x kg/m (T/ t)	Dimension 'A' (mm)	Moment Capacity (kNm)
400 x 160 x 48.4 (14/4)	333	136
450 x 160 x 50.2 (14/4)	383	154
450 x 180 x 60.1 (16/4)	382	154
500 x 180 x 61.9 (16/4)	432	172
550 x 200 x 73.3 (16/5)	482	190
600 x 200 x 80.5 (16/6)	532	208
650 x 250 x 103.4 (18/6)	581	226

(F_{r1}) 155k
(F_{r2}) 208k
(ΣF_r) 363k

Optional Shear Row

Vertical Shear Capacity
331 kN without shear row
515 kN with shear row

DESIGN GRADE S275				COLUMN	DESIGN GRADE S355			
Panel Shear Capacity (kN)	Tension Zone		Compn. Zone	Serial Size	Compn. Zone	Tension Zone		Panel Shear Capacity (kN)
	F_{R1} (kN)	F_{R2} (kN)				F_{R1} (kN)	F_{R2} (kN)	
1000	√	√	√	356 x 368 x 202	√	√	√	1302
849	√	√	√	177	√	√	√	1105
725	√	√	√	153	√	√	√	944
605	√	√	√	129	√	√	√	787
1037	√	√	√	305 x 305 x 198	√	√	√	1350
816	√	√	√	158	√	√	√	1062
703	√	√	√	305 x 305 x 137	√	√	√	915
595	√	√	√	118	√	√	√	774
503	√	√	√	97	√	√	√	649
882	√	√	√	254 x 254 x 167	√	√	√	1149
685	√	√	√	132	√	√	√	892
551	√	√	√	107	√	√	√	717
434	√	√	√	89	√	√	√	566
360	√	√	√	73	√	√	√	465
459	√	√	√	203 x 203 x 86	√	√	√	598
353	√	√	√	71	√	√	√	460
322	√	√	√	60	√	√	√	415
272	√	√	√	52	√	√	√	351
245	√	150	√	46	√	√	√	316

Tension Zone:
√   Column satifactory for bolt row tension values shown for the beam side.
xxx   Calculate reduced moment capacity using the reduced bolt row values.
Compression Zone:
√   Column capacity exceeds ΣF_r.
S (xxx)   Column requires stiffening to resist ΣF_r (value is the column web capacity).

Effect of increasing the size of end-plate from 200mm to 250mm

Table 4 and Table 6 show the moment resistance of the connection for end-plate width of 200mm. Table 5 and Table 7 show the moment resistance of the connection for end-plate width of 250mm. The idea of comparison is to know the percentage increase due to increment of the width of the end-plate. The results of percentage increase in moment capacity for 200mm and 250mm wide of the end-plate are tabulated in Table 9. The results showed that by increasing the size of end-plate width from 200mm to 250mm, moment capacity of the connection is increased by an average of about 5.1% for M20 bolt with 12mm thick end-plate and an average of 2.7% for M24 bolt with 15mm thick end-plate. The results show that the increment of the plate size from 200 to 250mm has contributed to a marginal amount of moment capacity to the connection. For M24 bolt, the increment in moment capacity is reduced by almost half of M20 bolt. This shows that the moment capacity of the connection depends on the strength of the bolt more than the strength of the end-plate.

Effect of increasing the size of bolt from M20 with 12mm thick end-plate to M24 with 15mm thick end-plate

The need to compare the result is to know the percentage increase due to increment of the size of bolt and thickness of the end-plate. The results of percentage increase in moment capacity for M20 with 12mm thick end-plate and M24 with 15mm thick end-plate are tabulated in Table 10. The results showed that by increasing the size of bolt from M20 with 12mm thick end-plate to M24 with 15mm thick end-plate, the moment capacity of the connection is increased by an average about 48% for one bolt row and 55% for two bolt rows. The result show that the moment capacity of the connection depends on the strength of the bolt more than the strength of the end-plate.

Table 4. Standard table for extended end-plate for 2 row M24 8.8 bolts, 200x15 end-plate (EEP,2BRM24,200W15EP)

2 ROW M24 8.8 B0LTS
200 x 15 DESIGN GRADE 43 EXTENDED END PLATE

Beam Side

BEAM – FLANGE S355 WEB S275

Beam Serial Size D x B x kg/m (T/ t)	Dimension 'A' (mm)	Moment Capacity (kNm)
400 x 160 x 48.4 (14/4)	333	186
450 x 160 x 50.2 (14/4)	383	211
450 x 180 x 60.1 (16/4)	382	210
500 x 160 x 52.0 (14/4)	433	236
500 x 180 x 61.9 (16/4)	432	235
550 x 200 x 73.3 (16/5)	482	260
600 x 200 x 80.5 (16/6)	532	285

(F_{r1}) 193kN
(F_{r2}) 306kN
(ΣF_r) 499kN

Dimension A

15, 10, 8, 10, M, V, 200, 55 90 55, 50 40 60 90 90 60 25

Optional Shear Row

Vertical Shear Capacity
475 kN without shear row
739 kN with shear row

Column Side

DESIGN GRADE S275				COLUMN	DESIGN GRADE S355			
Panel Shear Capacity (kN)	Tension Zone F_R1 (kN)	F_R2 (kN)	Compn. Zone	Serial Size	Compn. Zone	Tension Zone F_R1 (kN)	F_R2 (kN)	Panel Shear Capacity (kN)
1000	√	√	√	356 x 368 x 202	√	√	√	1302
849	√	√	√	177	√	√	√	1105
725	√	√	√	153	√	√	√	944
605	√	√	√	129	√	√	√	787
1037	√	√	√	305 x 305 x 198	√	√	√	1350
816	√	√	√	158	√	√	√	1062
703	√	√	√	305 x 305 x 137	√	√	√	915
595	√	√	√	118	√	√	√	774
503	√	√	√	97	√	√	√	649
882	√	√	√	254 x 254 x 167	√	√	√	1149
685	√	√	√	132	√	√	√	892
551	√	√	√	107	√	√	√	717
434	√	√	√	89	√	√	√	566
360	√	297	S(474)	73	√	√	√	465
459	√	√	√	203 x 203 x 86	√	√	√	598
353	√	√	√	71	√	√	√	460
322	√	297	S(481)	60	√	√	√	415
272	√	203	S(395)	52	√	√	296	351
245	√	111	√	46	√	√	199	316

Tension Zone:
√   Column satifactory for bolt row tension values shown for the beam side.
xxx   Calculate reduced moment capacity using the reduced bolt row values.
Compression Zone:
√   Column capacity exceeds ΣF_r.
S (xxx)   Column requires stiffening to resist ΣF_r (value is the column web capacity).

Table 5. Standard table for extended end-plate for 2 row M24 8.8 bolts, 250x15 end-plate (EEP,2BRM24,250W15TEP)

2 ROW M24 8.8 B0LTS
250 x 15 DESIGN GRADE 43 EXTENDED END PLATE

Beam Side

BEAM – FLANGE S355
WEB S275

Beam Serial Size D x B x kg/m (T/ t)	Dimension 'A' (mm)	Moment Capacity (kNm)
450 x 180 x 60.1 (16/4)	382	234
500 x 180 x 61.9 (16/4)	432	261
550 x 200 x 73.3 (16/5)	482	288
600 x 200 x 80.5 (16/6)	532	316
650 x 250 x 103.4 (18/6)	581	343
750 x 250 x 108.7 (18/6)	681	397

(F_{r1}) 242kN
(F_{r2}) 306kN
(ΣF_r) 548kN

Vertical Shear Capacity
475 kN without shear row
739 kN with shear row

Column Side

	DESIGN GRADE S275			COLUMN	DESIGN GRADE S355			
Panel Shear Capacity (kN)	Tension Zone		Compn. Zone	Serial Size	Compn. Zone	Tension Zone		Panel Shear Capacity (kN)
	F_{R1} (kN)	F_{R2} (kN)				F_{R1} (kN)	F_{R2} (kN)	
1000	√	√	√	356 x 368 x 202	√	√	√	1302
849	√	√	√	177	√	√	√	1105
725	√	√	√	153	√	√	√	944
605	√	√	√	129	√	√	√	787
1037	√	√	√	305 x 305 x 198	√	√	√	1350
816	√	√	√	158	√	√	√	1062
703	√	√	√	137	√	√	√	915
595	√	√	√	118	√	√	√	774
503	√	√	√	305 x 305 x 97	√	√	√	649
882	√	√	√	254 x 254 x 167	√	√	√	1149
685	√	√	√	132	√	√	√	892
551	√	√	√	107	√	√	√	717
434	√	√	√	89	√	√	√	566
360	√	297	S(479)	73	√	√	√	465
459	√	√	√	203 x 203 x 86	√	√	√	598
353	√	√	√	71	√	√	√	460
322	√	276	S(486)	60	√	√	√	415
272	√	154	√	52	√	√	269	351
245	204	100	√	46	√	√	151	316

Tension Zone:
√   Column satifactory for bolt row tension values shown for the beam side.
xxx   Calculate reduced moment capacity using the reduced bolt row values.
Compression Zone:
√   Column capacity exceeds ΣF_r.
S (xxx)   Column requires stiffening to resist ΣF_r (value is the column web capacity).

Table 6. Standard table for flush end-plate for 3 row M20 8.8 bolts, 200x12 end-plate (EEP,3BRM20,200W12TEP)

3 ROW M20 8.8 B0LTS
200 x 12 DESIGN GRADE 43 EXTENDED END PLATE

Beam Side

BEAM – FLANGE S355 WEB S275

Beam Serial Size D x B x kg/m (T/ t)	Dimension 'A' (mm)	Moment Capacity (kNm)
400 x 160 x 48.4 (14/4)	243	156
450 x 160 x 50.2 (14/4)	293	180
450 x 180 x 60.1 (16/4)	292	180
500 x 180 x 61.9 (16/4)	342	203
550 x 200 x 73.3 (16/5)	392	227
600 x 200 x 80.5 (16/6)	442	251
650 x 250 x 103.4 (18/6)	491	274
750 x 250 x 108.7 (18/6)	591	321

(F_{r1}) 124kN
(F_{r2}) 208kN
(F_{r3}) 139kN
(ΣF_r) 471kN

Vertical Shear Capacity 588 kN

Column Side

Panel Shear Capacity (kN)	Tension Zone F_R1 (kN)	Tension Zone F_R2 (kN)	Tension Zone F_R3 (kN)	Compn. Zone	COLUMN Serial Size	Compn. Zone	Tension Zone F_R1 (kN)	Tension Zone F_R2 (kN)	Tension Zone F_R3 (kN)	Panel Shear Capacity (kN)
1000	√	√	√	√	356 x 368 x 202	√	√	√	√	1302
849	√	√	√	√	177	√	√	√	√	1105
725	√	√	√	√	153	√	√	√	√	944
605	√	√	√	√	129	√	√	√	√	787
1037	√	√	√	√	305 x 305 x 198	√	√	√	√	1350
816	√	√	√	√	158	√	√	√	√	1062
703	√	√	√	√	305 x 305 x 137	√	√	√	√	915
595	√	√	√	√	118	√	√	√	√	774
503	√	√	√	√	97	√	√	√	√	649
882	√	√	√	√	254 x 254 x 167	√	√	√	√	1149
685	√	√	√	√	132	√	√	√	√	892
551	√	√	√	√	107	√	√	√	√	717
434	√	√	√	√	89	√	√	√	√	566
360	√	√	√	S(465)	73	√	√	√	√	465
459	√	√	√	√	203 x 203 x 86	√	√	√	√	598
353	√	√	√	√	71	√	√	√	√	460
322	√	√	√	S(471)	60	√	√	√	√	415
272	√	√	√	S(386)	52	√	√	√	√	351
245	√	181	90	S(337)	46	S(435)	√	√	√	316

Tension Zone:
√   Column satifactory for bolt row tension values shown for the beam side.
xxx   Calculate reduced moment capacity using the reduced bolt row values.
Compression Zone:
√   Column capacity exceeds ΣF_r.
S (xxx)   Column requires stiffening to resist ΣF_r (value is the column web capacity).

Table 7. Standard table for extended end-plate for 3 row M20 8.8 bolts, 250x12 end-plate (EEP,3BRM20,250W12TEP)

3 ROW M20 8.8 B0LTS
250 x 12 DESIGN GRADE 43 EXTENDED END PLATE

Beam Side

BEAM – FLANGE S355
WEB S275

Beam Serial Size D x B x kg/m (T/ t)	Dimension 'A' (mm)	Moment Capacity (kNm)
400 x 160 x 48.4 (14/4)	243	174
450 x 160 x 50.2 (14/4)	293	200
450 x 180 x 60.1 (16/4)	292	200
500 x 180 x 61.9 (16/4)	342	225
550 x 200 x 73.3 (16/5)	392	252
600 x 200 x 80.5 (16/6)	442	278
650 x 250 x 103.4 (18/6)	491	303
750 x 250 x 108.7 (18/6)	591	355

(F_{r1}) 155kN
(F_{r2}) 208kN
(F_{r3}) 156kN
(ΣF_r) 519kN

Vertical Shear Capacity
588 kN

Column Side

DESIGN GRADE S275					COLUMN		DESIGN GRADE S355				
Panel Shear Capacity (kN)	Tension Zone			Compn. Zone	Serial Size	Compn. Zone	Tension Zone			Panel Shear Capacity (kN)
	F_{R1} (kN)	F_{R2} (kN)	F_{R3} (kN)				F_{R1} (kN)	F_{R2} (kN)	F_{R3} (kN)	
1000	√	√	√	√	356 x 368 x 202	√	√	√	√	1302
849	√	√	√	√	177	√	√	√	√	1105
725	√	√	√	√	153	√	√	√	√	944
605	√	√	√	√	129	√	√	√	√	787
1037	√	√	√	√	305 x 305 x 198	√	√	√	√	1350
816	√	√	√	√	158	√	√	√	√	1062
703	√	√	√	√	305 x 305 x 137	√	√	√	√	915
595	√	√	√	√	118	√	√	√	√	774
503	√	√	√	√	97	√	√	√	√	649
882	√	√	√	√	254 x 254 x 167	√	√	√	√	1149
685	√	√	√	√	132	√	√	√	√	892
551	√	√	√	√	107	√	√	√	√	717
434	√	√	√	√	89	√	√	√	√	566
360	√	√	√	S(465)	73	√	√	√	√	465
459	√	√	√	√	203 x 203 x 86	√	√	√	√	598
353	√	√	√	√	71	√	√	√	√	460
322	√	√	√	S(471)	60	√	√	√	√	415
272	√	√	151	S(386)	52	S(484)	√	√	√	351
245	√	150	90	S(337)	46	S(435)	√	√	147	316

Tension Zone:
√   Column satifactory for bolt row tension values shown for the beam side.
xxx   Calculate reduced moment capacity using the reduced bolt row values.
Compression Zone:
√   Column capacity exceeds ΣF_r.
S (xxx)   Column requires stiffening to resist ΣF_r (value is the column web capacity).

Table 8. Standard table for extended end-plate for 3 row M24 8.8 bolts, 200x15 end-plate (EEP,3BRM20,200W15TEP)

3 ROW M24 8.8 BOLTS
200 x 15 DESIGN GRADE 43 EXTENDED END PLATE

Beam Side

BEAM – FLANGE S355 WEB S275

Beam Serial Size D x B x kg/m (T/ t)	Dimension 'A' (mm)	Moment Capacity (kNm)
450 x 180 x 60.1 (16/4)	292	275
500 x 180 x 61.9 (16/4)	342	311
550 x 200 x 73.3 (16/5)	392	347
600 x 200 x 80.5 (16/6)	442	383
650 x 250 x 103.4 (18/6)	491	418

(F_{r1}) 193kN
(F_{r2}) 306kN
(F_{r3}) 221kN
(ΣF_r) 720kN

Vertical Shear Capacity
845 kN

Column Side

DESIGN GRADE S275					COLUMN	DESIGN GRADE S355				
Panel Shear Capacity (kN)	Tension Zone			Compn. Zone	Serial Size	Compn. Zone	Tension Zone			Panel Shear Capacity (kN)
	F_{R1} (kN)	F_{R2} (kN)	F_{R3} (kN)				F_{R1} (kN)	F_{R2} (kN)	F_{R3} (kN)	
1000	√	√	√	√	356 x 368 x 202	√	√	√	√	1302
849	√	√	√	√	177	√	√	√	√	1105
725	√	√	√	√	153	√	√	√	√	944
605	√	√	√	S(651)	129	√	√	√	√	787
1037	√	√	√	√	305 x 305 x 198	√	√	√	√	1350
816	√	√	√	√	158	√	√	√	√	1062
703	√	√	√	√	137	√	√	√	√	915
595	√	√	√	√	305 x 305 x 118	√	√	√	√	774
503	√	√	√	S(596)	97	√	√	√	√	649
882	√	√	√	√	254 x 254 x 167	√	√	√	√	1149
685	√	√	√	√	132	√	√	√	√	892
551	√	√	√	√	107	√	√	√	√	717
434	√	√	√	S(601)	89	√	√	√	√	566
360	√	297	√	S(474)	73	S(612)	√	√	√	465
459	√	√	√	√	203 x 203 x 86	√	√	√	√	598
353	√	√	√	S(555)	71	S(723)	√	√	√	460
322	√	297	183	S(481)	60	S(621)	√	√	√	415
272	√	203	118	S(395)	52	S(479)	√	√	√	351
245	√	111	90	S(345)	46	S(443)	√	199	116	316

Tension Zone:
√   Column satifactory for bolt row tension values shown for the beam side.
xxx   Calculate reduced moment capacity using the reduced bolt row values.
Compression Zone:
√   Column capacity exceeds ΣF_r.
S (xxx)   Column requires stiffening to resist ΣF_r (value is the column web capacity).

Table 9. Standard table for flush end-plate for 3 row M20 8.8 bolts, 200x12 end-plate (EEP,3BRM20,200W12TEP)

3 ROW M20 8.8 B0LTS
200 x 12 DESIGN GRADE 43 EXTENDED END PLATE

Beam Side

BEAM – FLANGE S355
WEB S275

Beam Serial Size D x B x kg/m (T/ t)	Dimension 'A' (mm)	Moment Capacity (kNm)
450 x 180 x 60.1 (16/4)	292	298
500 x 180 x 61.9 (16/4)	342	337
550 x 200 x 73.3 (16/5)	392	375
600 x 200 x 80.5 (16/6)	442	413
650 x 250 x 103.4 (18/6)	491	451
750 x 250 x 108.7 (18/6)	591	528

Diagram forces: (F_{r1}) 242kN, (F_{r2}) 306kN, (F_{r3}) 221kN, (ΣF_r) 769kN. Dim A. M, V.

Vertical Shear Capacity 845 kN

Column Side

DESIGN GRADE S275					COLUMN	DESIGN GRADE S355				
Panel Shear Capacity (kN)	Tension Zone F_{R1} (kN)	F_{R2} (kN)	F_{R3} (kN)	Compn. Zone	Serial Size	Compn. Zone	Tension Zone F_{R1} (kN)	F_{R2} (kN)	F_{R3} (kN)	Panel Shear Capacity (kN)
1000	√	√	√	√	356 x 368 x 202	√	√	√	√	1302
849	√	√	√	√	177	√	√	√	√	1105
725	√	√	√	√	153	√	√	√	√	944
605	√	√	√	S(656)	129	√	√	√	√	787
1037	√	√	√	√	305 x 305 x 198	√	√	√	√	1350
816	√	√	√	√	158	√	√	√	√	1062
703	√	√	√	√	137	√	√	√	√	915
595	√	√	√	S(749)	305 x 305 x 118	√	√	√	√	774
503	√	√	√	S(602)	97	S(777)	√	√	√	649
882	√	√	√	√	254 x 254 x 167	√	√	√	√	1149
685	√	√	√	√	132	√	√	√	√	892
551	√	√	√	S(806)	107	√	√	√	√	717
434	√	√	√	S(607)	89	S(790)	√	√	√	566
360	√	297	214	S(479)	73	S(618)	√	√	√	465
459	√	√	√	√	203 x 203 x 86	√	√	√	√	598
353	√	√	√	S(555)	71	S(730)	√	√	√	460
322	√	276	155	S(481)	60	S(627)	√	√	√	415
272	√	154	118	S(395)	52	S(515)	√	269	152	351
245	204	100	90	S(345)	46	S(451)	√	151	116	316

Tension Zone:
√   Column satifactory for bolt row tension values shown for the beam side.
xxx   Calculate reduced moment capacity using the reduced bolt row values.
Compression Zone:
√   Column capacity exceeds ΣF_r.
S (xxx)   Column requires stiffening to resist ΣF_r (value is the column web capacity).

Table 10. Percentage increase in moment capacity of the connection by increasing the number of bolt row from two to three bolt rows

Size of TWP beam	EEP,2BRM20,200W12TEP versus EEP,3BRM20,200W12TEP			EEP,2BRM20,250W12TEP versus EEP,3BRM20,250W12TEP			EEP,2BRM24,200W15TEP versus EEP,3BRM24,200W15TEP			EEP,2BRM24,250W15TEP versus EEP,3BRM24,250W15TEP		
	Two bolt rows	Three bolt rows	% increase	Two bolt rows	Three bolt rows	% increase	Two bolt rows	Three bolt rows	% increase	Two bolt rows	Three bolt rows	% increase
400 x 160 x 48.4 (14/4)	123	156	26.8%	136	174	27.9%	N/A	N/A	N/A	N/A	N/A	N/A
450 x 160 x 50.2 (14/4)	139	180	29.5%	154	200	29.9%	N/A	N/A	N/A	N/A	N/A	N/A
450 x 180 x 60.1 (16/4)	139	180	29.5%	154	200	29.9%	210	275	31.0%	234	298	27.4%
500 x 180 x 61.9 (16/4)	156	203	30.1%	172	225	30.8%	235	311	32.3%	261	337	29.1%
550 x 200 x 73.3 (16/5)	172	227	32.0%	190	252	32.6%	260	347	33.5%	288	375	30.2%
600 x 200 x 80.5 (16/6)	189	251	32.8%	208	278	33.7%	285	383	34.4%	316	413	30.7%

Table 11. Percentage increase in moment capacity of the connection by increasing the size of end-plate from 200mm to 250mm wide

Size of TWP beam	EEP,2BRM20,200W12TEP versus EEP,2BRM20,250W12TEP			EEP,2BRM24,200W15TEP versus EEP,2BRM24,250W15TEP			EEP,3BRM20,200W12TEP versus EEP,3BRM20,250W12TEP			EEP,3BRM24,200W15TEP versus EEP,3BRM24,250W15TEP		
	200mm	250mm	% increase	200mm	250mm	% increase	200mm	250mm	% increase	200mm	250mm	% increase
400 x 160 x 48.4 (14/4)	123	136	10.6	N/A	N/A	N/A	156	174	11.5	N/A	N/A	N/A
450 x 160 x 50.2 (14/4)	139	154	10.8	N/A	N/A	N/A	180	200	11.1	N/A	N/A	N/A
450 x 180 x 60.1 (16/4)	139	154	10.8	210	234	11.4	180	200	11.1	275	298	8.4
500 x 180 x 61.9 (16/4)	156	172	10.3	235	261	11.1	203	225	10.8	311	337	8.4
550 x 200 x 73.3 (16/5)	172	190	10.5	260	288	10.8	227	252	11.0	347	375	8.1
600 x 200 x 80.5 (16/6)	189	208	10.1	285	316	10.9	251	278	10.8	383	413	7.8

Table 12. Percentage increase in moment capacity of the connection by increasing the thickness of end-plate from 12mm

Size of TWP beam	EEP,2BRM20,200W12TEP versus EEP,2BRM24,200W15TEP			EEP,2BRM20,250W12TEP versus EEP,2BRM24,250W15TEP			EEP,3BRM20,200W12TEP versus EEP,3BRM24,250W15TEP			EEP,3BRM20,250W12TEP versus EEP,3BRM24,250W15TEP		
	M20/EP 12mm	M24/EP 15mm	% increase	M20/EP 12mm	M24/EP 15mm	% increase	M20/EP 12mm	M24/EP 15mm	% increase	M20/EP 12mm	M24/EP 15mm	% increase
400 x 160 x 48.4 (14/4)	123	186	51.2	N/A	N/A	N/A	N/A	N/A	N/A	N/A	N/A	N/A
450 x 160 x 50.2 (14/4)	139	211	51.8	N/A	N/A	N/A	N/A	N/A	N/A	N/A	N/A	N/A
450 x 180 x 60.1 (16/4)	139	210	51.1	154	234	51.9	180	275	52.8	200	298	49.0
500 x 180 x 61.9 (16/4)	156	235	50.6	172	261	51.7	203	311	53.2	225	337	49.8
550 x 200 x 73.3 (16/5)	172	260	51.2	190	288	51.6	227	347	52.9	252	375	48.8
600 x 200 x 80.5 (16/6)	189	285	50.8	208	316	51.9	251	383	52.6	278	413	48.6

CONCLUSIONS

This study concluded that it is possible to determine the moment capacity of extended end plate connections connected to a column flange by adopting the method proposed by SCI, even for different geometric parameters such as the TWP section. The capacities of the connection depend on the geometrical aspects of the connection such as the size of bolt, number of bolt, size of end-plate, thickness of end-plate, size of beam and size of column. For the size of column, the reduction of moment capacity is due to the effect of compression of the beam flange to the column flange without the need of stiffener. The suggested weld size for flange and web is strong enough to prevent any failure at the weld. The increment of moment capacity of the connection can be concluded as follows:

- The increase in the number of bolt row from one row to two rows has contributed to an increase in the moment capacity in the range of 50% to 59% which is quite significant.
- The increase in the size of end-plate from 200mm to 250mm has contributed to an increase in the moment capacity in the range of 2.7% to 5.1% which is not significant.
- The increase the size of bolt from M20 with 12mm thick end-plate to M24 with 15mm thick end-plate has contributed to an increase in the moment capacity in the range of 48% to 55% which is about the same as the effect of increasing the number of bolt from one to two bolt rows.
- The shear capacity of the connection depends on number of bolt used in the connection. However, the lower bolt row contributed to most of the shear capacity of the connection by an increment of 71% with the addition of optional shear bolt row.
- The proposed tables can be used in the design of semi-continuous construction in multi-storey steel frames.

The use of 'knee joint method' to predict the moment resistance connection from M-Φ curves showed good agreement with the component method suggested by Steel Construction Institute. It was concluded that the moment resistance of the connection developed in the elastic-plastic region as shown by the knee-joint method.

ACKNOWLEDGEMENT

REFERENCES

Bose, B. (1993) *Tests to verify the performance of standard ductile connections.* Dundee Institute of Technology,.

British Standards Institute BS 5950-1. (2000). *Structural Use of Steelwork in Building Part 1: Code of Practice for Design – Rolled and Welded Sections.* British Standards Institution, London.

Couchman, G. H. (1997) *Design of Semi-continuous Braced Frames,* Steel Construction Institute Publication 183, Silwood Park, Ascot, Berkshire SL5 7QN, U.K

Eurocode 3. (1992). *Design of Steel Structures: ENV 1993-1-1: Part 1.1: General Rules and Rules for Buildings.* CEN, Brussels.

Hussein, Wa' il Q. (2001). *Design Guide for Steel Plate Girder with Corrugated Webs (TWP).* Presentation in Design of Steel Structure Short Course, TWP Sdn Bhd.

Md. Tahir, M. (2003) *Design of Semi-Continuous Construction for Multi-Storey Braced Steel Frames Using TWP sections.* Steel Technology Centre, Universiti Teknologi Malaysia, Skudai, Johor, Malaysia,.

Md. Tahir, M, Sulaiman, A, Mohammad, S. and Saggaff A. (2006) Standardisation of partial strength connections of flush end-plate connections for Trapezoid Web Profiled Steel Section. *Journal of the Institute of Engineers*, Malaysia, Vol 67, No.2.

Osman, M. H. (2001). *Performance Test and Research on Trapezoid Web Profile.* Presentation in Design of Steel Structure Short Course, Universiti Teknologi Malaysia.

Peter, A. et. al. (1996). Steel Construction Institute and British Constructional Steelwork Association. *Joints in Steel Construction. Volume 1: Moment Connections.* London.

Peter, A and Mike, F. (1992) Steel Construction Institute and British Constructional Steelwork Association. *Joints in Simple Construction. Volume 1: Design Methods.* Second Edition, Silwood Park, Ascot, Berks SL 7QN, London.

Peter A and Mike, F. (1993) Steel Construction Institute and British Constructional Steelwork Association. *Joints in Simple Construction. Volume 2:Practical Applications.* First Edition, Silwood Park, Ascot, Berks SL 7QN, London.

Saggaff, A. (2007) *Behaviour of composite partial strength connections with built-up steel sections.* Ph.D Thesis, Universiti Teknologi Malaysia, Skudai, Johor, Malaysia.

Sulaiman, A. (2007) *Experimental test on steel beam with partial strength connections using trapezoid web profiled steel sections.* 1st Construction Industry Research Achievement (CIRAIC 2007), Malaysia.

Sulaiman, A. (2007), *Behaviour of Partial Strength Connections with Trapezoid Web Profiled Steel Sections.* Ph.D Thesis. Universiti Teknologi Malaysia, Skudai, Johor, Malaysia.

Tahir, M. (1995) *Structural and Economic Aspects of The Use of Semi-Rigid Joints in Steel Frames.* PhD Thesis. University of Warwick, United Kingdom.

Tan Cher Siang, Phil, M. (2004) *Buckling Analysis of Compression Member with Trapezoidal Web Profiled.* Universiti Teknologi Malaysia..

COMPARATIVE STUDY OF MONOLITHIC AND PRECAST CONCRETE BEAM-TO-COLUMN CONNECTIONS

Ahmad Baharuddin Abd. Rahman[1], Abdul Rahim Ghazali[1] and Zuhairi Abd. Hamid[2]

[1]*Faculty of Civil Engineering, Universiti Teknologi Malaysia, 81310 Skudai, Johor*
[2]*Construction Research Institute of Malaysia, Kuala Lumpur*

Abstract:

The performance of a precast concrete structure have greatly influenced by the response and characteristics of beam-to-column connections. The information on connection characteristics such as moment-rotation is very important for the analysis and design. Without proper understanding of the connection response and characteristics, it is difficult to design a safe structural system of the global precast frame. This paper discusses the connection response when subjected to incremental gravity loadings. Two specimens comprising one monolithic (CF-RC) and one precast concrete beam-to-column (CF-PC) connections were considered. The concrete strength for all specimens including the wet connection was 30 N/mm². All the two specimens were tested to failure under incremental point loads that produced hogging moments to the connections. The response of the connections was studied through the ultimate loading capacity, moment-rotation characteristic, and crack response. The results of moment-rotation characteristics of the precast connection show similar response to the monolithic connection. It was observed that the ultimate moment resistance of the precast connection was higher by about 11% as compared to the monolithic. For these reasons, the CF-PC precast connection can be categorised as a moment resisting connection under the action of gravity loads. Hence, engineers can consider similar precast connection details to obtain moment resisting connections, provided hogging moments due gravity loads are more dominant than sagging moments due to lateral loads.

Keywords : *Beam-to-column connections, precast concrete frame, rigid connection.*

INTRODUCTION

In precast construction, connections are use to assemble beams and columns to make a complete multi-storey framed building. The beam-to-column connections form the important structural component of a precast concrete structure. To satisfy the structural requirements of the overall frame, each connection must have the ability to transfer shear forces and bending moments from one precast component to another, safely.

The transfer of forces between beams and columns, and its effect to the performance of global frame, is governed by the characteristics of the connections. However, in practice, the characteristics and the response of precast connections is not well established and not fully understood to fulfil the requirements needed in design and construction. Realising the significant contributions of connections in precast concrete structures, many research works were carried out around the world.

In the United States of America, the most well known research was the PRESS projects carried out by researchers at University of Washington and University of California at San Diego; sponsored by National Science Foundation and Precast Concrete Institute. One of the successful findings was the ductile connectors developed by Englekirk (1999). The developed beam-to-column connection can be used to construct a moment resisting frame of pre-cast concrete components that could outperform comparable cast-in-place and structural steel systems (see Figure 1). This ductile connector contains a rod that yields at a well-defined strength, effectively limiting the load that can be transferred to less ductile components on the frame.
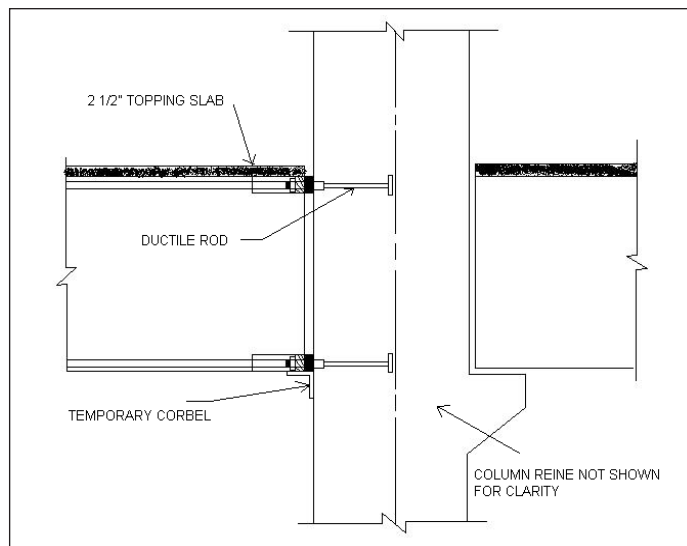
Figure 1. Ductile Connectors

In New Zealand, Restrepo *et. al.,* (1995) developed several moment resisting connections to be used with precast buildings. The trend is that the increased use of precast concrete structures has encouraged the researchers to consider innovative connections for their precast concrete structural systems because of the country's location in an active seismic zone.

In the United Kingdom, Elliot *et. al., (2003)* has conducted numerous research works on precast concrete beam-to-column connections. Knowing that most of precast connections behave semi-rigidly, he proposes that the global precast frame can be designed semi-continuously, to take advantage of the semi-rigid characteristics. This may results in more economical design, as compared to a precast structure designed with pinned connections.

In Turkey, Ertas *et. al.* investigated the performance of ductile connections, to be employed in precast concrete moment resisting frames. Several connections comprising cast-in-place, composite and bolted connections were tested and compared with the monolithic connection. The performance of each connection evaluated based on the properties of stiffness, strength, ductility and energy dissipation.

In Malaysia, research on beam-to-column connections was carried out at the Faculty of Civil Engineering, Universiti Teknologi Malaysia (UTM), with the financial support provided by Construction Industry Development Board (CIDB). Several existing and new connections were tested. The main objective of this research was to investigate the response and performance of precast concrete beam-to-column connections as part of structural components in a precast framed building. The response and the characteristics of the beam-to-column connections, as part of the cruciform subframe, was evaluated based on the ultimate loading capacity, load-deflection, moment-rotation characteristic and cracking pattern.

Moment connections are widely used in most of precast concrete buildings constructed in Malaysia (Ahmad Baharuddin Abd Rahman and Wahid Omar, 2007). The most common moment resisting precast connection is a wet connection shown in Figure 2. This connection is obtained by extending the reinforcement bars from the beam through the column and followed by casting the beam-to-column junction with wet cast-in-place concrete. This connection is normally used when a moment resisting frame is needed. However, there is no evidence to prove that this connection can provide the required moment resistance. As a result, there are different opinions among engineers regarding the performance of the precast frame when this wet connection is used. For this reason, a comparative study based on experimental results between the precast connection and monolithic was carried out.
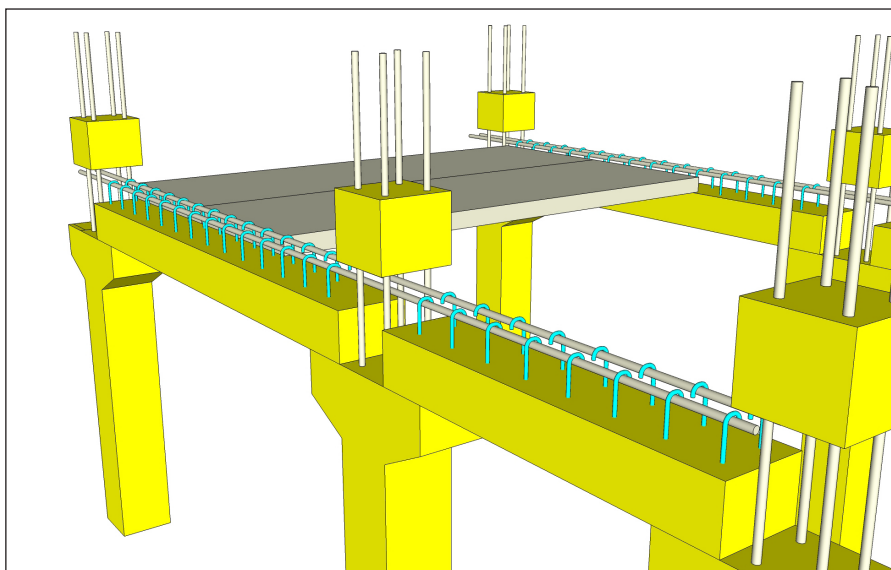
Figure 2. Beam-to-column connection using cast-in-place infill in precast concrete construction

DESCRIPTION OF MONOLITHIC AND PRECAST CONCRETE BEAM-TO-COLUMN CONNECTIONS

To model an internal connection in a multi-storey frame building, a cruciform subframe was considered (see Figure 3). In the test program, one cruciform conventional reinforced concrete denoted as CF-RC to act as the control specimen and one cruciform precast beam-to-column connection denoted as CF-PC specimen were conducted. Each cruciform subframe consisted of one column and two continuous beams.

The beams and columns for both monolithic and precast specimens were manufactured using concrete of grade 30 N/mm². The ready mixed concrete was produced using maximum coarse aggregate size of 20 mm with 60-180 mm concrete slump.

Figure 4 shows the cross-sectional details of all beams, columns and corbels for the cruciform specimens. Each beam specimen comprised 2Y16 in Grade 460 for its top (tension) and bottom (compression) steel bars respectively, and R8 mild steel bar in Grade 250 N/mm² at 125 mm spacing for the stirrups. Each column specimen comprised 4Y16 in Grade 460 for the main longitudinal bars and R8 in Grade 250 at 125 mm spacing for the stirrups. In addition, more information on the making of the monolithic and precast subframes is illustrated in Figures 5 and 6 respectively.

With reference to Figure 6(b), half-depth precast beams were installed on both sides of corbels, followed by the installation of 2Y16 top reinforcement bars, while 2Y16 of the bottom reinforcement bars were already cast in the half beam. To complete the connection between precast beam and precast column, see Figure 6(c), a second stage of concreting using wet cast in-place concrete was carried out, with the use of simple side formwork along the beam. Due to the procedures of installation, the top steel bars continue to the adjacent beam but the bottom steel bars terminated at beam end resulting in discontinuity. This steel bar discontinuity might affect the moment resistance of the connection. Therefore, it was the objective of this paper to asses the moment resistance of the connection based on experimental tests.
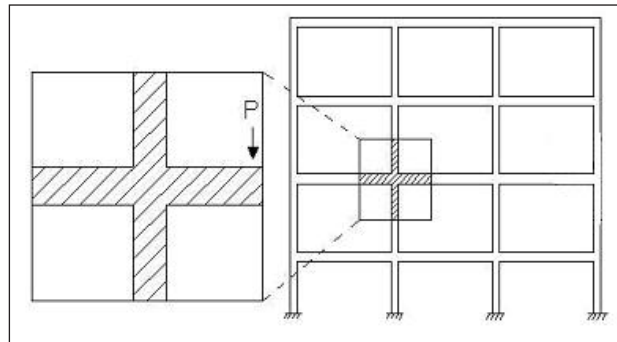

Figure 3. Cruciform subframe, CF
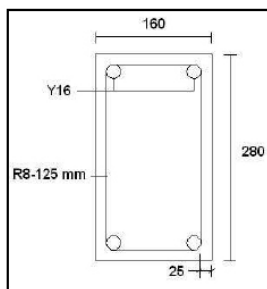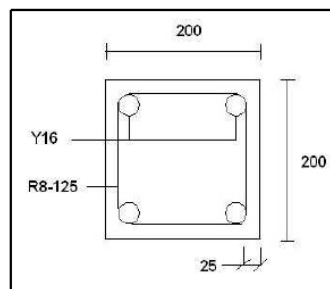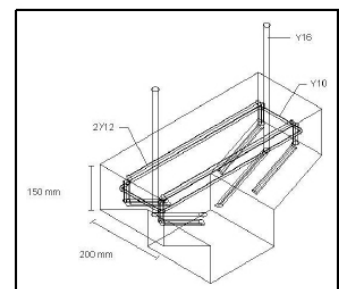
(a) Beam   (b) Column   (c) Corbel for precast specimen

Figure 4. Details of beam and column for both monolithic and precast specimens, and corbel for precast specimen
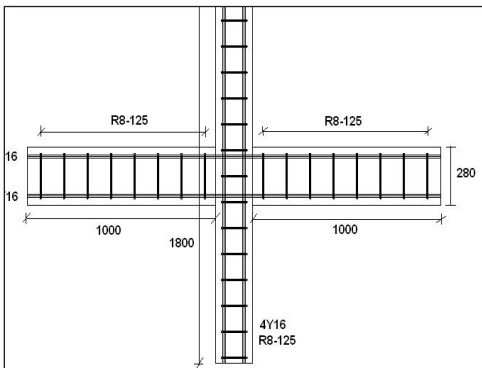
(a) Reinforcement details

(b) Monolithic specimen
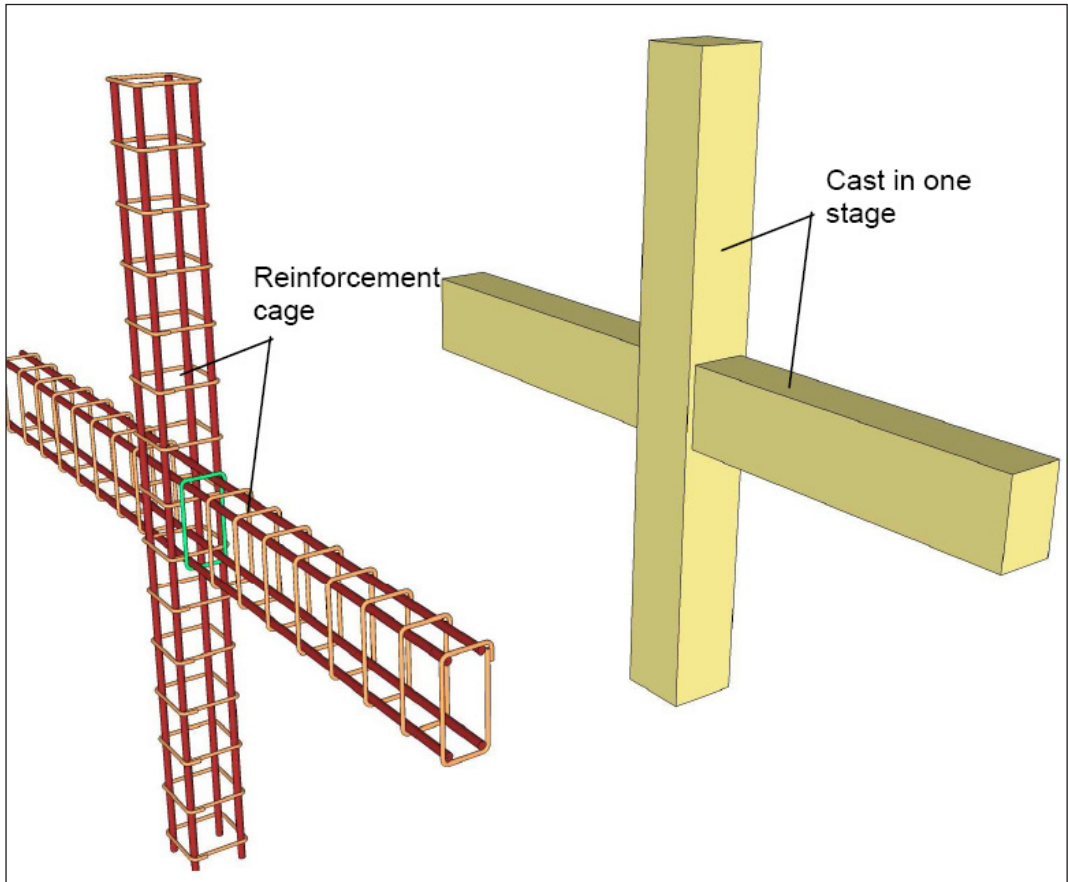
(c) Before and after concreting of monolithic connection

Figure 5. Monolithic specimen, CF-RC
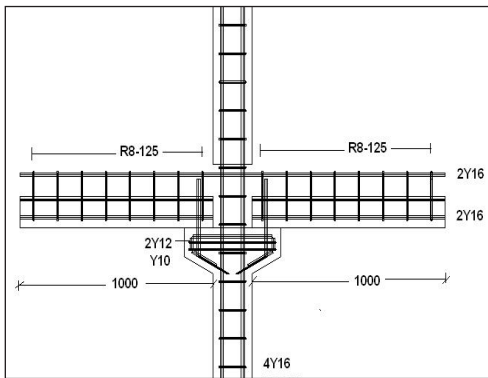
(a) Reinforcement details


(b) Precast specimens ready for wet connection
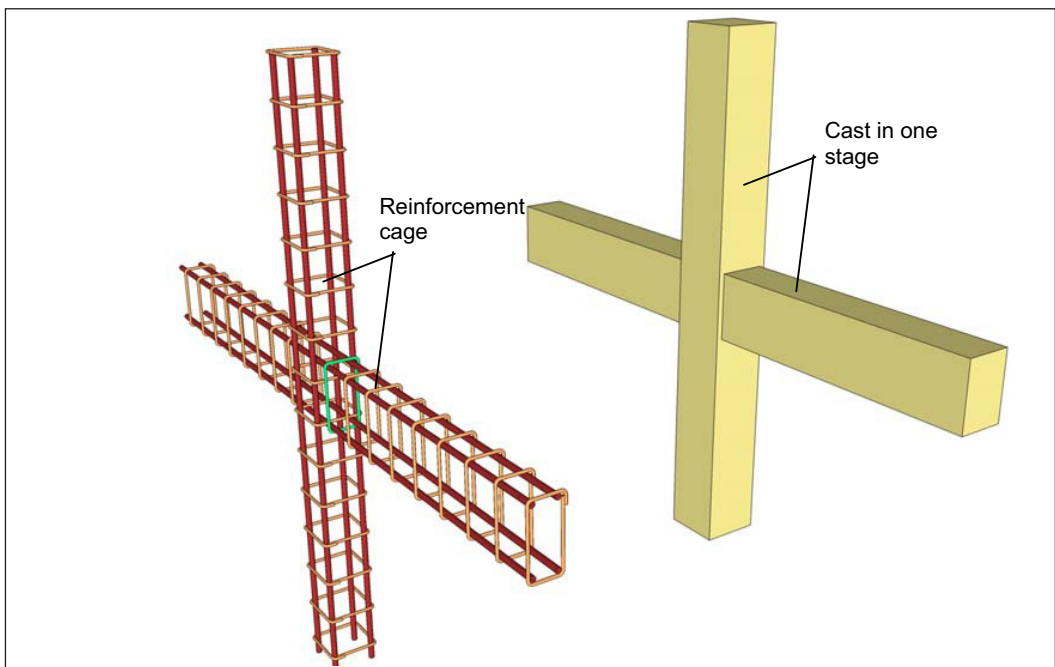
Figure 6. Precast specimen, CF-PC

EXPERIMENTAL SETUP AND PROCEDURES

Test specimens were restrained at both top and bottom ends of the column as shown in Figure 7. All the beam-to-column specimens were extensively instrumented to record their response under incremental loads. Strain gauges were installed at midspan of internal steel bars of the beam and at the extreme compression face of the concrete. Six linear variable displacement transducers (LVDT), T1 to T6, were used in the test whereby four of them were located under the beam and another two at the column.

External loads were applied by two hydraulic jacks denoted as jack 1 and jack 2 as shown in Figure 7. In addition, jack 3 was provided to act as a reaction support. In each test, an axial load, P2 was first applied at the top of the column, using jack 2. This load, which was equal to 80 percent of the design axial strength of the column, was kept constant throughout the test. Then, using jack 1, incremental vertical loads, P1 were applied to the beam end in stages to produce incremental hogging moments to the connections. The results were monitored by a high accuracy load cell with a load sensitivity of 0.1 kN. The incremental loadings, P1 were applied at 1 kN to 2 kN intervals up to the ultimate load of the beam-to-column connections.

Concrete and reinforcement strains, deflections and applied loads were recorded at every load increment using a data logger. In between load applications, visual inspection and manual marking of cracks and crack propagation were carried out. For each test, the loading was continued until failure occurred. Failure was indicated by a significant increase in beam deflection accompanied by a rapid decrease in the vertical load, P1.
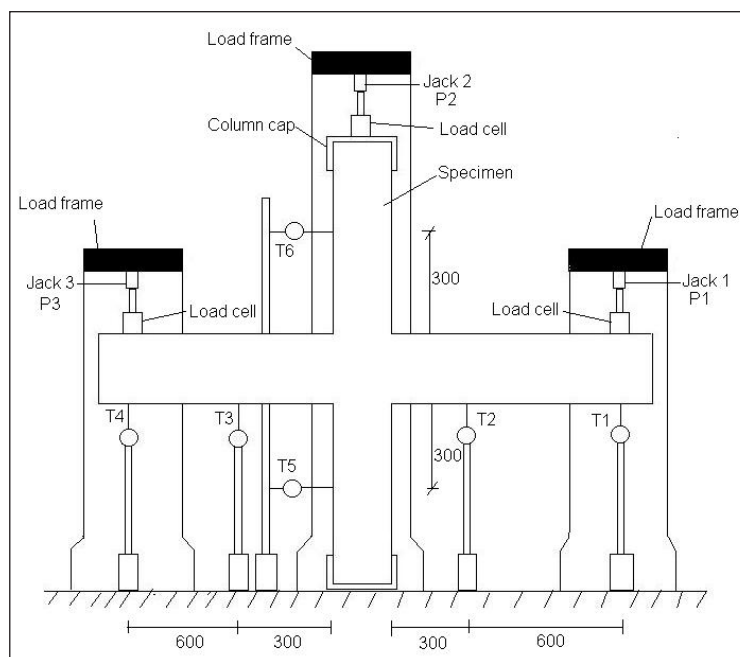

Figure 7. Schematic diagram for the setup of the beam-to-column specimens

RESULTS AND DISCUSSION

The response of beam-to-column connection, in particular the moment-rotation relationship, is very complex. Currently, there is no theoretical formulation available to predict the moment-rotation response of a reinforced or precast concrete connection. For this reason, in this paper, the moment-rotation response of each connection is compared against the theoretical moment resistance of the beam. This comparison is valid because a connection can be considered rigid if it is capable to transmit more than 90% of the beam moment resistance (Segui W. T., 2003). Also for this reason, the paper compared the response of the precast connection against the monolithic connection.

Response of Moment-Rotation

The response and characteristics of beam-to-column connections is best described by plotting the M-φ curves of the connections, describing the relationship between the applied moments and the corresponding connection rotations.

The M-φ curves of the monolithic and precast connections obtained from the tests are shown in Figure 8. The maximum moment resistance achieved by the monolithic connection, CF-RC was 52.84 kNm. While for the precast beam-to-column connection, CF-PC, the ultimate moment resistance was 59.5 kNm, about 11 % higher than the monolithic.

The ultimate moment resistance of the connections can also be compared with the design moment resistance of the beam. Taking the design strength of longitudinal steel bars equals 460N/mm^2, the design moment resistance of the beam is M = 0.95fy.A$_s$.z = 35 kNm. The results show that the ultimate moment resistance of CF-PC and CF-RC connections exceeded the design moment resistance of the beam by factors of 1.7 and 1.5 respectively. These results reflect that the strength of precast connection has outperformed the monolithic connection.

At the early stage of loadings, within the range of 0 to 5 milliradians of the connection rotation, it was seen that the characteristic of stiffness and strength of precast specimen CF-PC were close to the monolithic specimen, CF-RC. However, beyond 5 milliradians of connection rotation, the stiffness of monolithic specimen, CF-RC decreased significantly, as can be seen from the reduction of M-φ curve slope. Subsequently, the strength or moment resistance of the connection decreased accordingly. However, in the case of precast specimen, CF-PC, the stiffness continued to increase without any deterioration. It is believed, this response was due to the corbel that contributed to the increased stiffness of the precast beam-to-column connection and consequently delayed the yielding of the top steel bars. Finally, after further stages of loading, in particular at 58 kNm, the connection stiffness of CF-PC reduced drastically, and subsequently the connection rotations increased rapidly. This response occurred due to the yielding of the top steel reinforcement bars and cracking of concrete at the beam-to-column connection.
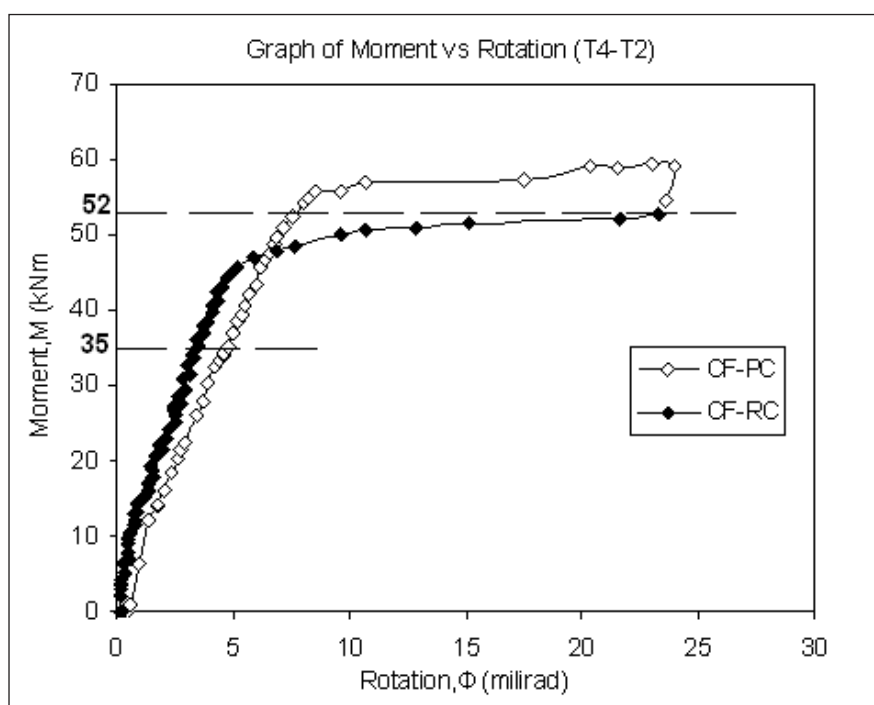
Figure 8. Moment – rotation curve

Response of Load-Deflection

The comparison of ultimate load and the corresponding deflection between monolithic and precast beam-to-column specimens is listed in Table 1. The results show that the ultimate load and the corresponding deflection of CF-RC were 57.9 kN and 42.63 mm respectively. In the case of CF-PC, the ultimate load and the corresponding deflection were 65.3 kN and 43.91 mm respectively. The results show that CF-PC outperformed CF-RC.

One of the parameters that influences beam stiffness is the fixity provided by the connections. Figure 9 shows the load-deflection behaviour of each beam with the slope of the curve representing the stiffness of the beam as influenced by the connection. It can be seen that the precast beam with cast-in-place connection, CF-PC performed satisfactorily and showed smaller deflection as compared to the monolithic beam, CF-RC. In the beginning of the test and within the range of 0 to 27 kN of the loading applied, the precast concrete specimen, CF-PC had the flexural stiffness that was similar to the monolithic specimen, CF-RC. As the incremental load reached 52 kN, the load-deflection slope of the precast specimen, CF-PC continued to increase, whereas, the load-deflection curve of the monolithic specimen, CF-RC decreased significantly to a second level of stiffness deterioration. At this load stage, the deterioration of the monolithic beam stiffness was contributed by the excessive strain of top internal steel bars, located at the middle of the connection (see Figure 10). However, the precast concrete specimen, CF-PC did not show any stiffness reduction as the monolithic specimen, CF-RC because the presence of corbel might delay the development of excessive strain in the top internal steel bars.

Table 1. Comparison of ultimate load and deflection between monolithic and precast specimens

Specimen	Ultimate Load (kN)	Deflection at Ultimate Load (mm)	Ultimate Load Difference (kN)	Percentage Difference (%)
CF-RC	57.9	42.63	-	-
CF-PC	65.3	43.91	7.4	11.3
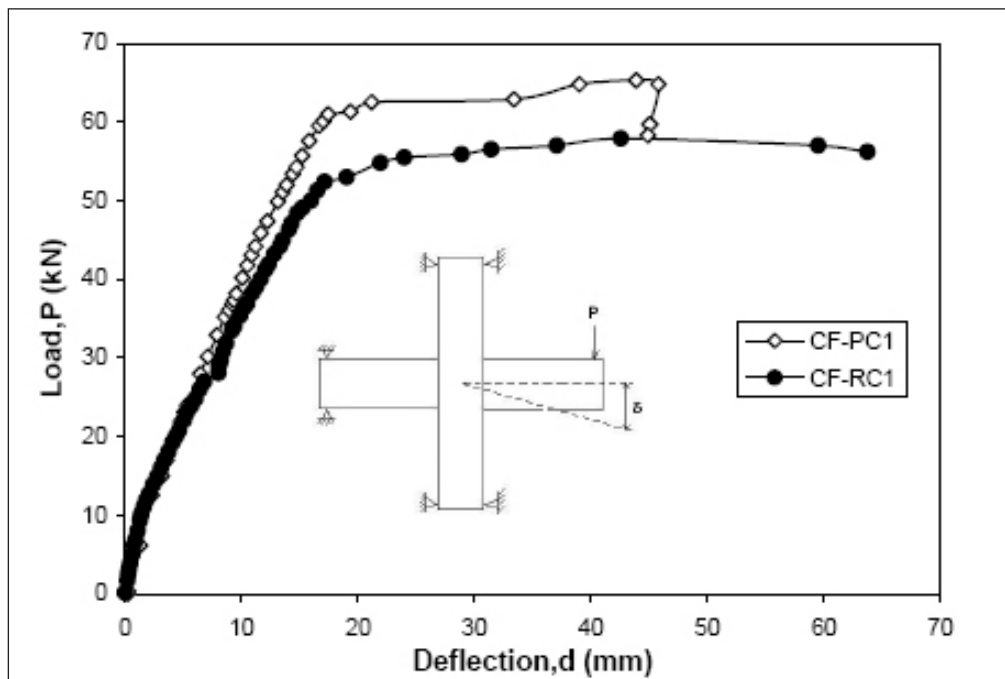
Figure 9. Load-deflection relationship
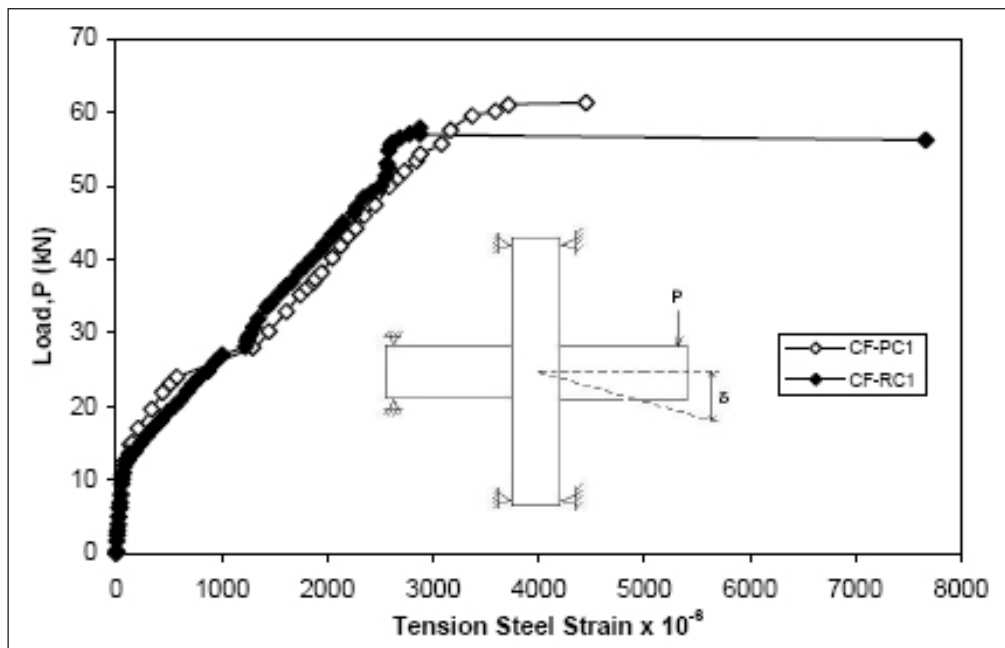
Figure 10. Load – strain at midspan of internal steel bar of the beam

Cracking Response

The illustrations of crack patterns between CF-RC and CF-PC are shown in Figure 11. The actual crack patterns of CF-RC and CF-PC at the ultimate loads are shown in Figure 12 and Figure 13 respectively.

In the case of monolithic specimen CF-RC, see Figure 11(a), the first crack developed at point 1 within the tension zone of the beam, where hogging moments were maximum. As the hogging moment increased, crack at point 1 propagated further towards the neutral axis of the beam, followed by cracks at points 2 and 3. Based on Figure 12(b), it can be seen that the first concrete hair crack in the beam of CF-RC became visible at the beam-to-column interface, when the applied load was 16 kN. The load to cause this first hair crack to the connection was about 28% of the ultimate load. At load 52 kN (see Figure 12(b)), the crack at point 1 widened, resulting in the lost of connection stiffness, as the slope of the load-deflection curve of CF-RC decreased (see Figure 9). Subsequently, the connection rotation increased rapidly with the small increased in the applied loads. When the applied loads were close to the ultimate load, concrete at point 4 started to crush due to the high compression stresses produced by the applied loads.

However, in the precast specimen (CF-PC), see Figure 11(b), the first vertical hair crack developed at location 2, that is about 75mm from the column face, when the applied load was 24 kN. The load to cause this first hair crack was about 38% of the ultimate load. As the hogging moments increased, the vertical hair crack at point 2 propagated further into the neutral axis of the beam followed by flexural crack at points 1 and 3. At load 62 kN (see Figure 13(b)), the vertical crack at point 2 widened and caused the connection to lose its stiffness as can be seen from the reduced slope of the load deflection curve of CF-PC (see Figure 9). It was seen that the vertical crack at point 2 was the most severed as compared to the cracks at points 1 and 3.
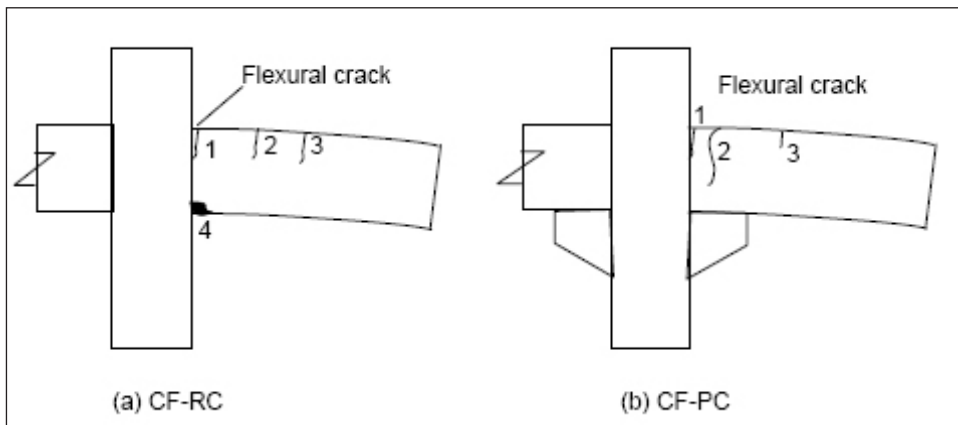

Figure 11. Comparison of crack development between CF-RC and CF-PC

(a)

(b)

Figure 12. Crack pattern of monolithic specimen CF-RC at ultimate load
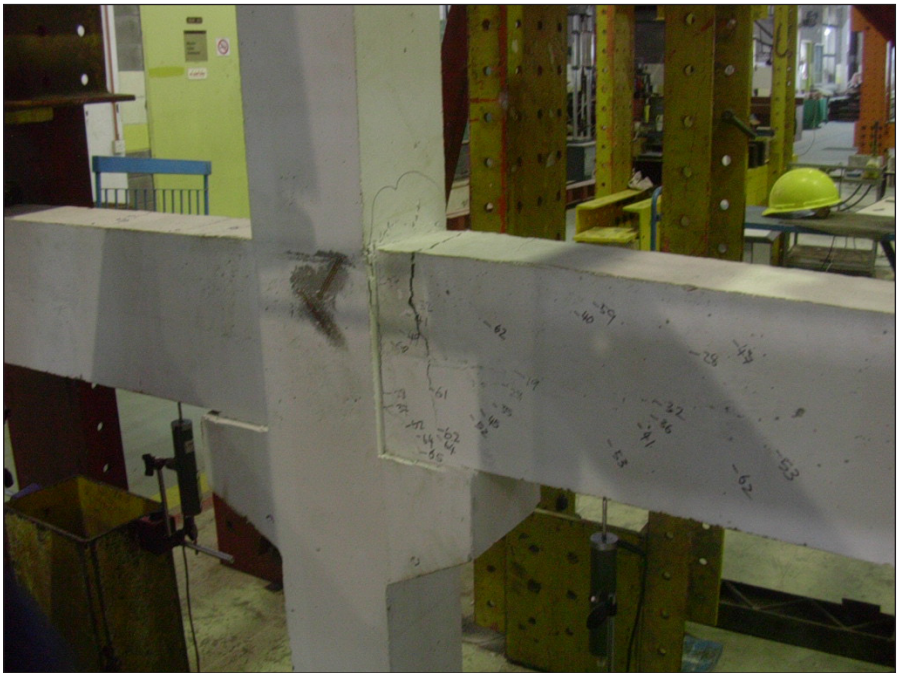
(a)

(b)

Figure 13. Crack pattern of precast specimen CF-PC at ultimate load

CONCLUSION

This paper describes the testing and the response of interior beam-to-column connections under incremental hogging moments generated from incremental beam loads. Two subframes consisted of monolithic and precast beam-to-column connections were tested to failure.

Based on the limited tests carried out, the following conclusions are drawn:

1. The response of moment-rotation, M-ϕ of the precast connection is close to the monolithic connection in terms of stiffness and strength characteristics. This shows that the CF-PC precast connection can perform effectively, similar to the conventional CF-RC reinforced concrete connection.

2. The stiffness of CF-PC precast connection, as can be seen from the M-ϕ curve slope, is similar to the monolithic connection. This means the precast connection can provide degree of restraint to the precast beam similar to the monolithic connection.

3. The deflection of the precast beam is governed by the degree of fixity or stiffness provided by the CF-PC connection.

4. The ultimate moment resistance of the precast connection is larger than the monolithic. This may be due to the corbel that delays the yielding of top steel bars and hence maintains the precast connection stiffness at higher load levels and correspondingly the precast connection strength.

5. The CF-PC precast connection behaves as a moment resisting connection under the action of gravity loads only. Hence, engineers can consider similar precast connection details to obtain moment resisting connections, provided hogging moments due gravity loads are more dominant than sagging moments due to lateral loads.

ACKNOWLEDGEMENT

REFERENCES

Ahmad Baharuddin Abd Rahman and Wahid Omar (2007) *Industrialised Building Systems in Malaysia* Construction Industry Development Board (CIDB Malaysia). 1st edition.

Elliot, K. S., Davies G. and Ferreira M. (2003) *Can precast concrete structures be designed as semi-rigid frames? Part 1 – The Experimental Evidence*. 19 August 2003. The Structural Engineer.

Ertas O., Ozden S. and Ozturan T. (2006) *Ductile Connections in Precast Concrete Moment Resisting Frames.* May-June 2006, PCI Journal.

Englekirk, R.E. (1995*) Development and Testing of A Ductile Connector for Assembling Precast Concrete Beams and Column.*, March-April 1995. PCI Journal.

Restrepo J. I., Park, R. and Buchanan, A. H. (1995) *Tests on Connections of Earthquake Resisting Precast Reinforced Concrete Perimeter Frames of Buildings*. July-August 1995. PCI Journal.

Segui W. T. (2003) LRFD Steel Design. Thomson Brooks Cole, 3rd edition.

FLEXURAL STRENGTH OF FERROCEMENT SANDWICH PANEL FOR INDUSTRIALISED BUILDING SYSTEMS

Mahyuddin Ramli

Professor, School of Housing, Building & Planning, Universiti Sains Malaysia

Abstract

The significant development and improvement of existing ferrocement material into a more durable composite is a great challenge. Experimental investigation is carried out to evaluate the structural performance of the ferrocement sandwich panel for use in the industrialized building system. This includes load-deflection characteristics, crack resistance, and moment curvature of the ferrocement elements when exposed to air and salt water environments.

INTRODUCTION

Just like many other new construction materials, ferrocement sandwich panel will be required to serve as a potential construction material for housing and industrialised building systems. The panel which is developed from modified ferrocement infills may also be used for marine applications such as ships, pontoons, buoys and many other floating structures. With the significant improvement on ferrocement material, particularly on the use of polymer latexes and other binders in mortar matrix, ferrocement has potential to become the material of construction in any environment.

Ferrocement is known for its high durability performance in corrosive environment and its successful use in this structures may be an asset to major engineering applications. The significant development and improvement of the existing ferrocement material into a higher durability and higher performance material is a great challenge. The main objective of this experimental investigation is to study and evaluate the structural performance of polymer-modified ferrocement for use in industrialized building system. This includes load-deflection characteristics, first crack strength, crack width and crack spacings of ferrocement elements exposed to air and salt water environments.

DEFINITION

Ferrocement is generally defined as a kind of composite material consisting of cement mortar and layers of reinforcing mesh or small diameter bars closely spaced. The reinforcement for ferrocement may be metallic or non-metallic meshes and are uniformly spread out throughout the entire thickness of the element.

In high performance latex-modified ferrocement, the main objectives are high strength, durability and availability. Hence, it can be best defined as a ferrocement material which has higher strength, higher durability and impermeability, and hence is cost effective. From this definition, it is clear that the material to be developed is a potential ferrocement material that will meet the construction challenges in the future.

Just like concrete, the cement and water content in the mortar matrix, basically are the governing factors in producing high strength and durable matrix. However, these alone are not quite sufficient in resisting the process of deterioration in the long term. ACI Committee 201 has given its definition for durability as its ability to resist weathering action such as cycles of wetting and drying, heating and cooling, freezing and thawing, etc. This would also include chloride penetration, corrosion of steel, alkali-silika reaction, etc. Hence, with the introduction of suitable polymer latex, a high durability performance of ferrocement composites could be achieved.

Applications

Ferrocement usually behave differently from conventional reinforced concrete in performance, strength and potential applications. The high surface area to volume ratio in a cement mortar matrix enables ferrocement to enhance its engineering properties such as tensile strength, flexural properties, impact resistance, impermeability and hence durability.

Ferrocement has been used in many applications all over the world, both in developing and developed countries. Its high strength and flexibility characteristics enable the material to gain wide acceptance in structural applications. The fabrication of low cost, durable thin shell structures for agriculture and housing applications, are the typical examples of its flexibility in construction, most of which utilizes local materials and minimum skilled labour.

The durability and watertightness of ferrocement material have attracted many boat builders to use the material extensively for commercial and pleasure crafts such as floating docks, ocean barges, floating house, pontoons, buoys, etc. The common applications of ferrocement includes:

1. Swimming pool
2. Water reticulations
3. Sluice gate
4. Water tanks
5. Landscape structures
6. Architectural elements
7. Slope protection
8. Irrigation linings

Potential applications of high performance polymer-modified ferrocement include:

1. Road surfacings
2. Airport runaways
3. Bridge decks overlays
4. Structural repairs
5. High impermeability wall linings

Experimental Programme

The objective of the experimental programme was to study and evaluate the structural characteristics of sandwich concrete panels in various environmental conditions. The test included determination of load and deflection characteristics, cracking moments, crack widths, crack spacing, and number of cracks developed in the concrete elements subjected to a static flexure.

Curing Regimes

After demoulding, all the specimens were cured in water for a period of 28 days and further subjected to the following curing regimes:
(1) continuously cured in water.
(2) continuously submerged in 5 % sodium chloride solution.
(3) continuously subjected to air curing.

Characteristics of Materials

The materials used for the manufacture of test specimens were similar to that of mortar prisms or composite slabs, and their characteristics are briefly described below.

Cement

Ordinary portland cement (OPC) complying to British Standard BS 12: 1991 or ASTM Type I cement was used in the preparation of mortar mix for ferrocement specimens.

Sand

Sand is considered as the largest proportion of component material in the mortar mix. About 60 to 70 percent of the volume of the mortar is occupied by sand. A good quality sand will have significant influence on the production of a high quality mortar and also on the proper penetration of the mesh.

Natural sand complying with the aggregate grading specified in the British Standard BS 882:1983 was used as fine aggregate for the manufacture of the ferrocement. The sand was first screened through a sieve of mesh opening 4.76 mm to ensure that only sand particles smaller than this size was used in the manufacture of ferrocement test specimens.

Mixing Water

The quality of water for the mixing of mortar has vital importance on the resulting hardened ferrocement. Impurities in water may interfere with the setting of cement and will adversely affect the strength and may also lead to corrosion of the reinforcement. Good drinking water is not likely to contain impurities that may deter the quality of mortar mixes. Hence, ordinary tap water was used as mixing water for the manufacture of ferrocement specimens.

Polymer Materials

The polymer materials used in ferrocement mixes consisted of styrene-butadiene rubber latex (SBR), polyacrylic esther (PAE) emulsion, and vinyl acetate/ethylene (VAE) copolymer powder.

Superplasticiser

Superplasticizer, **CORMIX SP6** was used in the manufacture of the unmodified control ferrocement.

Mesh Reinforcement

One of the essential components of ferrocement is wire mesh. The function of wire mesh is to support the mortar in its green state. In the hardened state its function is to absorb the tensile stresses on the structure which the mortar, on its own, would not be able to withstand. The mechanical behaviour of ferrocement is highly dependent upon the type, quantity, orientation and strength properties of the reinforcing mesh.

The type of wire mesh used for the entire ferrocement test programme consisted of a square welded mesh of 2.2 mm diameter ungalvanized copper coated wires.

Manufacture of Test Specimen

The following methods were adopted for the preparation of ferrocement test specimens used in static flexure.

Preparation of Wire Mesh

A square welded ungalvanized copper coated wire mesh was used for all reinforcement of the ferrocement specimens. The mesh consisted of wires of diameter of 2.2 mm at a spacing of 50 x 50 mm. After marking the meshes, a guillotine was used for cutting the mesh to a required dimension of 90 mm in width and 490 mm in length, giving an allowance of 5 mm around the side edges. The wire mesh used for ferrocement reinforcement was laid flat in position and was accurately spaced. Because of the limited thickness of the ferrocement specimens, the three layers of mesh were bound together without any spacer in between the layers. However, 5 mm mortar spacers were tied to the bottom of the first layer of mesh by means of stainless steel wires, to give a uniform cover of minimum 5 mm throughout the depth of specimen.

Preparation of Casting Mould

Ferrocement specimens, each measuring 500 mm long, 100 mm wide and 25 mm thick were cast horizontally in group of six in a steel mould. The mould consisted of a large base plate 900 x 700 x 15 mm thick, and had removable vertical steel plates securely fixed to the required size by means of screws. The mould was designed to accommodate 6 specimens for a single cast and for easy demoulding.

Prior to casting, the inner surface of the mould was applied with mould release oil to lubricate the surface in contact with cement mortar and to allow easy removal of ferrocement specimens after casting. Silicon grease was applied externally between the base plate and the bottom of the vertical plates to prevent grout leaks.

Design of Mortar Mixes

The design of mortar mixes were done in such proportions as to give the required design strength consistently. The proportions of the mortar mix were in the weight ratios, consisting of 1 part of cement to 3 parts of sand, with water-binder ratios varying from 0.4 for unmodified control, and 0.3 for modified ferrocements.

The mixing of the cement mortar was carried out in a horizontal pan mixer with a mixing capacity of approximately 0.02 m^3, and was different from the horizontal pan mixer (approximately 0.07 m^3) normally used for mixing larger quantity of concrete or mortar. The mortar mixer has rotating blades and a fixed bowl, whereas pan mixer has a fixed blades but a rotating pan. The mortar mixer seems to give a more uniform mix and is suitable for use in the manufacture of ferrocement test specimens. The design of mortar mixes for ferrocement is presented in Table 1.

Table 1. Design of mixes for ferro cement test specimens

Type of Mix	OPC [kg/m^3]	Polymer, by weight of cement [%]	Super-plasticiser [%]	Sand [kg/m^3]	Water-cement ratio	Slump (mm)
CON	500	0	1.0	1500	0.4	140
SBR	500	15.0	0	1500	0.3	150
PAE	500	15.0	0	1500	0.3	150
VAE	500	15.0	0	1500	0.3	150

From Table 1, the unmodified control ferrocement, CON with water-binder ratio of 0.4 requires 1% (by weight of cement) of superplasticizer to give an average slump of 140 mm. However, in the modified ferrocements, no superplastizer was added to give the required slump of 150 mm, despite of their low water binder ratio of 0.3 for all ferrocements modified with 15 % styrene-butadiene rubber latex (SBR), polyacrylic ester emulsion (PAE), and vinyl acetate-ethylene, respectively. The results also indicate that a higher slump in mortar mixes can be achieved fairly easily by the use of suitable polymers. The test result showed that styrene-butadiene rubber latex seems to be better capable of producing higher slump at a low water-binder ratio compared to that of other polymers.

Manufacture of Ferrocement Panels

In assessing the structural performance of modified ferrocement composites, a number of ferrocement panels were manufactured for use in static flexure test. The panels were designed to have a nominal size of 500 mm long, 100 mm wide and 25 mm thick, reinforced with three layers of square welded mesh of wire diameter 2.2 mm and having a volume

fraction of 0.91 %. Before casting, the layers of reinforcing weld mesh had been cut to size and placed in three layers. Precast mortar spacers 5 mm thick were attached to the bottom of the first layer of the netting to provide uniform cover throughout the bottom of the mesh. The subsequent layers were placed on top and tied firmly in position ready to receive the mortar. The cement mortar was placed in the mould to the level of top layer and vibrated using internal vibrator to give good compaction. Then the final layer of cement mortar was placed and compacted again. The top surface of mortar was finally trowelled to a smooth finish using a steel trowel. The surface of mortar was covered with polythene sheet to avoid rapid loss of water from the surface. The specimens were then left in the mould for a period of approximately 24 hours before demoulding. Once demoulded, the specimens were cured according to the curing regimes previously described.

Experimental Set-up

The test in static flexure was conducted on all ferrocement specimens using a universal testing machine. Third-point loading was used over a simply supported span of 300 mm. The method was chosen to give a constant moment in the direction of the flexural span. Initially, the specimen was first placed horizontally between the stainless steel roller supports which have a distance of 300 mm between the rollers. A horizontal steel plate fitted with stainless steel rollers at a distance of 100 mm, was placed on top of the specimen as shown in Fig 1.
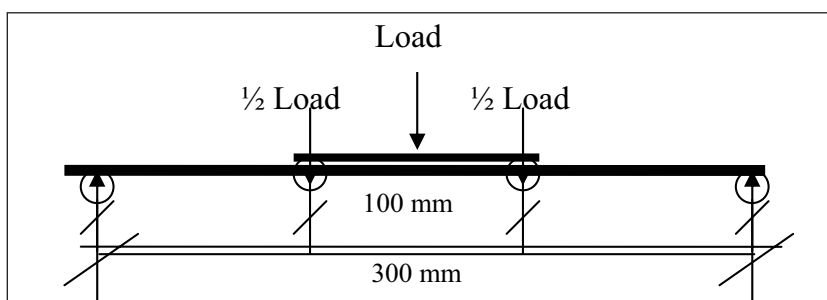

Figure 1. Loading set-up for static flexure

The static load was applied to the flexural specimen based on the reactions of the top rollers as the ram head moved upwards. The testing machine was principally ram-controlled, in which ram range can be accurately set for deflection measurement. The ram ranges available were 20, 50,100 or 200 mm. Each range is equivalent to full deflection on the x-axis of the x-y plot recorded by the machine. Deflections were measured at the loading points, based on the vertical distance recorded by the machine as the ram head moves upwards. In this test the ram range was set for 20 mm deflection, which meant that the full scale of the x-axis in the x-y plot was equivalent to 20 mm deflection of the specimens at the load points. The deflection was primarily based on the curve plotted by x-y recorder on the graph paper and was calibrated to obtain the vertical displacement of the specimen at the load points. The accuracy of the measurement was frequently checked by taking the deflection at the load points using a dial gauge. The crack width of ferrocements under static load was measured on the vertical face of the flexural span. In order to facilitate

easy identification of cracks and measurement of crack widths, the load was applied to the specimen in increments by a manually operated hydraulic jack. At each load increment, the number of cracks within the central 100 mm of the specimens was noted and the width of each crack was measured using a hand held microscope capable of measuring crack width to an accuracy of $\pm$ 0.01 mm.

Test Results and Discussions

The experimental studies on the behaviour of ferrocement in static flexure were investigated to determine its mechanical properties, such as cracking load, ultimate load, crack widths, crack spacing, deflections, etc. and comparing them with the predicted values using the test method previously described in the experimental set-up.

Mechanical Properties

The mechanical properties of mortars used for the manufacture of ferrocement specimens are presented in Tables 2 to 5. The results in Table 2 show that, although the compressive strength of the unmodified control, CON was higher than polymer-modified specimens, its flexural strength was about 15% lower than that of the modified specimens (SBR, PAE, VAE). Similarly with the Young's modulus of elasticity of mortars, in which CON showed marginally higher values than that of the polymer-modified specimens.

Table 2. Mechanical properties of mortar at 28 days

Type of Mix	Flexural strength, f_b (MPa)	Compressive strength, f_{cu} (MPa)	Young's modulus of elasticity (ACI Committee 318, 1983) $E_m = 4730\sqrt{f_{cu}} \times 10^{-3}$ (GPa)
CON	4.8	39.5	29.7
SBR	5.9	35.8	28.3
PAE	5.5	30.3	26.0
VAE	5.6	29.7	25.8

Table 3. Mechanical properties of mortar after further curing for 28 days in salt water

Type of Mix	Flexural strength, f_b (MPa)	Compressive strength, f_{cu} (MPa)	Young's modulus of elasticity (ACI Committee 318, 1983) $E_m = 4730\sqrt{f_{cu}} \times 10^{-3}$ (GPa)
CON	5.2	47.6	32.6
SBR	6.2	39.7	29.8
PAE	5.6	31.8	26.7
VAE	6.0	34.3	27.7

In Table 3, in which the specimens were subjected to continuous exposure to 5% sodium chloride solution, similar trend of strength development as in Table 2 was observed. The salt water curing seems to increase the flexural and compressive strengths of both the modified and unmodified specimens.

At 9 months of air curing, the result in Table 4 shows that the increase in flexural strength for the unmodified specimen was about 15 %, compared to that of modified specimens of about 25 %. The significant increase in flexural strength was due the prolonged air curing, which enabled a continuous formation of polymer films between cement and aggregate interphase, interconnecting and bridging the particles, thereby increasing its flexural capacity. However, the compressive strength of unmodified increased by about 35 %, compared to 20 % of that of the polymer-modified mortars. The test result showed that the compressive strength of polymer modified cement mortars was always lower than that of the unmodified cement mortars. This may be attributed to the fact that the presence of hardened polymer films, which are softer compared to the matrix of cement, filled the voids, coated and surrounded the aggregates and the cement particles, resulting in a lower compressive force.

Table 4. Mechanical properties of mortar after 9 months of air curing

Type of Mix	Flexural strength, f_b (MPa)	Compressive strength, f_{cu} (MPa)	Young's modulus of elasticity (ACI Committee 318, 1983) $E_m = 4730 \sqrt{f_{cu}} \times 10^{-3}$ (GPa)
CON	5.6	53.2	34.5
SBR	7.4	46.4	32.2
PAE	6.7	34.2	27.7
VAE	7.0	36.4	28.5

When the specimens are subjected to continuous exposure to sodium chloride solution for a period of 9 months after initial curing as shown in Table 5, surprisingly, there was an improvement in both the compressive and flexural strengths of polymer-modified cement mortars.

Table 5. Mechanical properties of mortar after 9 months of cont. exposure to salt water

Type of Mix	Flexural strength, f_b (MPa)	Compressive strength, f_{cu} (MPa)	Young's modulus of elasticity (ACI Committee 318, 1983) $E_m = 4730 \sqrt{f_{cu}} \times 10^{-3}$ (GPa)
CON	6.1	52.6	34.3
SBR	8.9	49.1	33.1
PAE	7.5	35.8	28.3
VAE	7.7	36.7	28.6

The flexural strength was found to increase by about 15 %, whereas the compressive strength increased by about 5 % compared to that for prolonged air curing. However, for the unmodified control specimen, even though the flexural strength increased by about 9%, the compressive strength decreased by about 1 %. Although the decrease is small, salt water curing does not seem favourable to the unmodified specimen. Instead, all polymer-modified cement mortars seemed to have significant benefit from prolonged salt water curing.

In summary, the compressive and flexural strengths of modified specimens were always superior than that of the unmodified specimens, proving that the polymer modification significantly improved the mechanical properties of cement mortars, and enhanced their flexural behaviour, irrespective of the curing conditions adopted.

Crack and Ultimate Load

The strength of ferrocement is commonly considered as the most valuable property. Strength always gives an overall picture of the quality of ferrocement, as strength is directly related with the properties of its hardened cement paste and reinforcement.

In this test programme, the engineer's theory of bending for tranformed uncracked section was used to estimate the first cracked load, while the ultimate load of ferro cement specimens were obtained using transformed cracked sections. Similar methods of calculation were performed on other polymer-modified test specimens, SBR, PAE, and VAE. The values obtained by the above method of calculations and their corresponding values obtained from experimental test results are summarised in Tables 6 to 9.

From Table 6, it can be seen that the predicted values of first crack load and ultimate load of specimens under static flexure were always higher than that of the experimental values. The VAE had lower first crack load than that of CON, although the ultimate load of CON was lower than that of VAE. The SBR specimen showed superior quality by exhibiting higher first crack load and ultimate load at 28 days of air curing.

The test results in Table 7 shows that, at 28 days of salt water curing, higher experimental values for first crack load were obtained for all test specimens. However, the inconsistency of the ultimate load behaviour at this stage prevents a conclusive comparison between the modified and unmodified specimens. The ultimate loads of CON and VAE specimens obtained from the experiment was lower than that of predicted values, in contrast to SBR and PAE, in which their ultimate loads obtained from experiment were consistently higher than that of predicted values. It is worth noting that the unmodified specimen, CON exhibited the lowest first crack load and ultimate load in static flexure.

Table 6. Experimental and predicted values of crack and ult. loads at 28 days curing

Type of specimen	Crack load (kN)		Ultimate load (kN)	
	Experimental	Predicted	Experimental	Predicted
CON	0.86	1.01	3.14	3.86
SBR	1.13	1.24	3.57	3.78
PAE	0.95	1.16	3.54	3.65
VAE	0.81	1.18	3.26	3.63

Table 7. Experimental and predicted values of crack and ultimate loads of specimens after 28 days of continuous exposure to salt water

Type of specimen	Crack load (kN)		Ultimate load (kN)	
	Experimental	Predicted	Experimental	Predicted
CON	1.31	1.09	3.50	3.98
SBR	1.57	1.31	3.95	3.87
PAE	1.53	1.18	3.80	3.70
VAE	1.50	1.26	3.64	3.75

Table 8. Experimental and predicted values of crack and ultimate loads after 9 months of air curing

Type of specimen	First crack load (kN)		Ultimate load (kN)	
	Experimental	Predicted	Experimental	Predicted
CON	1.02	1.18	4.55	4.04
SBR	1.32	1.56	5.02	3.96
PAE	1.29	1.41	4.37	3.76
VAE	1.20	1.48	4.68	3.80

Table 9. Experimental and predicted values of crack and ultimate loads of specimens after 9 months of continuous exposure to salt water.

Type of specimen	First crack load (kN)		Ultimate load (kN)	
	Experimental	Predicted	Experimental	Predicted
CON	1.53	1.28	4.70	4.04
SBR	2.30	1.87	6.05	4.00
PAE	2.20	1.58	5.77	3.79
VAE	1.96	1.62	5.61	3.81

Tables 8 & 9 shows experimental data and predicted values of first crack load and ultimate strength of ferrocements subjected to 9 months of air curing, and 9 months of salt water curing. The salt water curing had significantly improved flexural behaviour of ferrocement mortars by exhibiting higher experimental values of first crack load and ultimate strength of all cement mortars.

The results of crack load expressed as percentage of the ultimate loads of specimens cured for 28 days in salt water is a resemblance of the 9 months salt water curing. Similarly the results for the 28 days air curing is a typical resemblance of the 9 months air curing. The test also revealed that salt water curing proved to be of greater advantage to all specimens, by increasing the first crack strength from about 25% to 40% of the ultimate strength of specimens in flexure.

Crack Width

Cracks in ferrocement mainly result from thermal and moisture movement incompatibilities between the phases of cement paste, sand and reinforcement, repeated service loading, self load and external restraint (Singh,1994). Ferrocement specimens exhibit finer and more numerous cracks than conventional reinforced concrete. Research studies (Paul and Pama,1978) have shown that crack width in reinforced concrete structures can be reduced:

    (i)   by increasing the bond between the reinforcement and the concrete

    (ii) by increasing the distribution of the reinforcement, and

    (iii) by reducing the thickness of the cover

    All these factors can be readily achieved through ferrocement materials. Crack width is nearly zero at the interface between the steel and the mortar and increases from interface towards the surface. Hence, the smaller the distance between the interface and the surface of the structure, the smaller the crack width was appeared. The cracking behaviour of ferrocement is greatly influenced by the specific surface and volume fraction of the reinforcing mesh.

    The effect of specific surface on the first crack strength of ferrocement was also reported by Naaman and Shah (1971) and Shah and Key (1972). The stress at the first crack was observed to increase linearly with the increase in specific surface irrespective of size, type and spacing of the wire mesh. After the occurrence of first crack, the number of cracks increases with increasing load. These also indicate that the total bond forces between the steel and the mortar play an important role in influencing the cracking behaviour of ferrocement.

    On the effect of volume fraction on first crack strength, experimental investigation by Shah (1972), showed that increasing volume of reinforcement increases the stress at first crack. This increase is different for each size of wire mesh used. The average crack width is primarily a function of tensile strain in the extreme layer of mesh. It does not depend on other parameters such as clear cover of the tension reinforcement, may be because the cover is relatively small compared to the specific surface of reinforcement in ferrocement.

    The specific surface of reinforcement does not seem to have a significant influence on the cracking behaviour in flexure compared to that of in tension. Nevertheless, the specific surface should be considered if more accurate prediction of crack width is needed. Similar computations were carried out for other test specimens, SBR, PAE and VAE, and their results are presented in Table 10. The test results in Table 10 show that the average crack widths at the point near failure for the unmodified control (CON) are 0.33 mm for air curing and 0.3 mm for salt water curing, which are higher than that of the polymer-modified ferrocements. The SBR-modified ferrocement (SBR) shows the lowest average crack widths of 0.26 mm and 0.25 mm for air and salt water curing, respectively.

Table 10. Average crack width for ferrocement in static flexure

Type of Specimen	Exposure conditions (9 months)	Average crack width (mm)
CON	air	0.33
CON	salt water	0.30
SBR	air	0.26
SBR	salt water	0.25
PAE	air	0.28
PAE	salt water	0.27
VAE	air	0.31
VAE	salt water	0.29
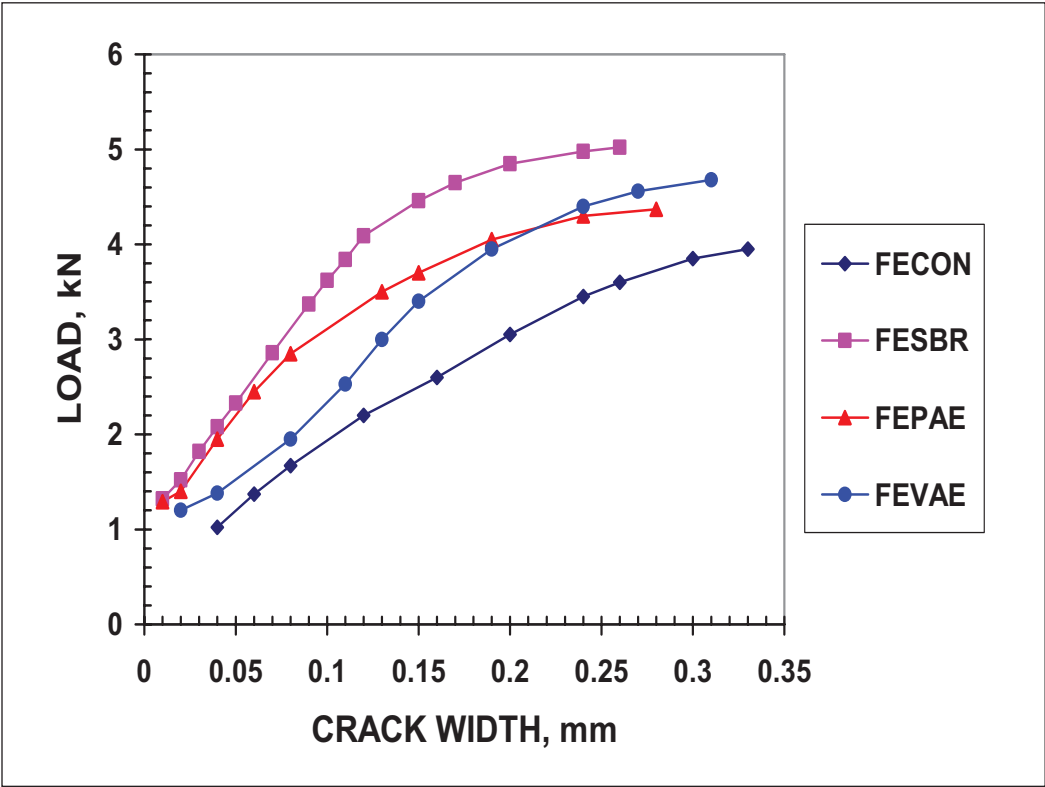
Figure 2. Crack propagation of ferrocement panel in air
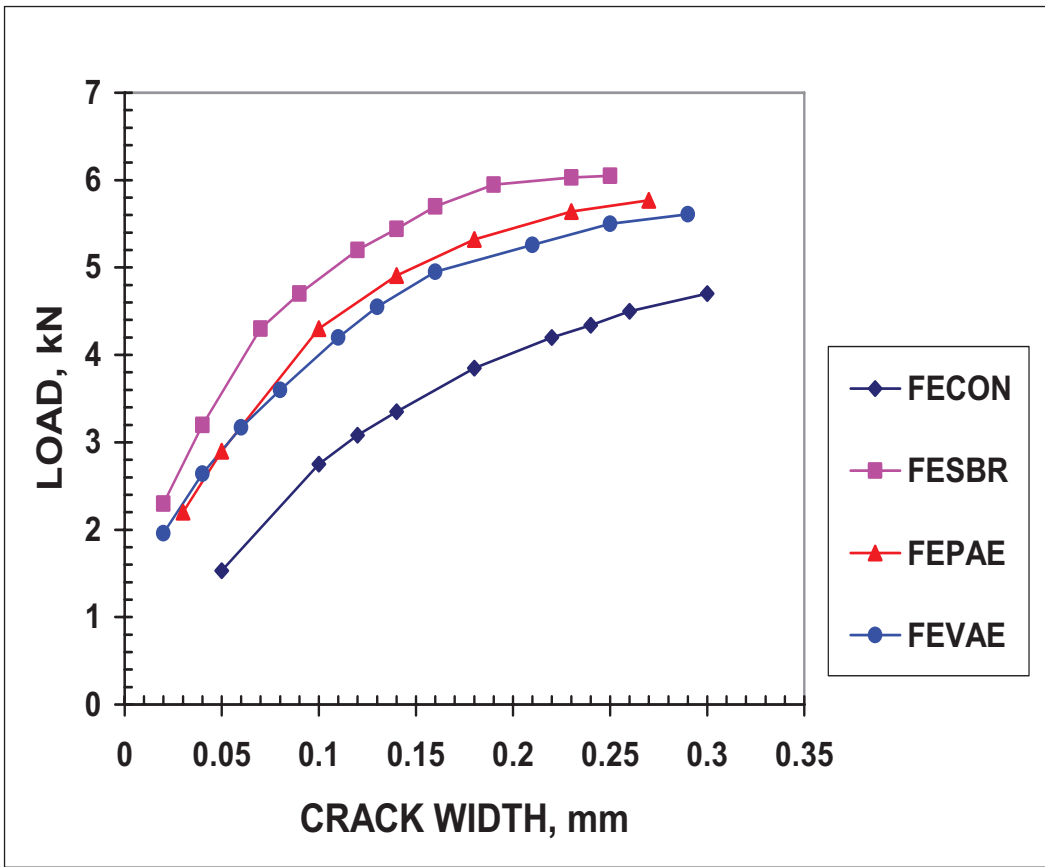
Figure 3. Crack propagation of ferrocement panel in salt water exposure

The average crack widths for PAE and VAE-modified ferrocements were 0.28 mm and 0.31mm for air-curing, and 0.27 mm and 0.29 mm for salt water-curing, respectively. All test specimens cured in salt water showed an average crack width of between 5% to 10% lower than that of in air curing. This may be due to the increase of overall stiffness of the composite during long-term exposure to salt water by salt depositing, wedging and preventing further crack propagation. The increase in average crack width with respect to static load is also presented in Figs. 2 to 3. From Fig. 2, it can be seen that the average crack width for polymer-modified specimens subjected to 9 months of air curing increased linearly with increasing static load up to about 3 kN.

Thereafter, the increase in crack width was almost fivefold, and became higher as it approached the failure load. This was different from the behaviour of the unmodified control specimen, which exhibited almost linear load-crack width relationship until near failure. The appearance of first crack varied from specimens, and it also depended on the overall stiffness of the composite. The first crack appeared at a load of about 1.3 kN for SBR and PAE, whereas for CON and VAE, the first crack appeared at a much lower load of about 1 and 1.2 kN, respectively.

Test results presented in Fig. 3 show that all polymer-modified and unmodified ferrocement in salt water exposure exhibited a higher crack and failure loads compared to that of air curing. However, the polymer-modified ferrocement seemed to exhibit superior quality when exposed to continuous salt water compared to that of the unmodified control, which showed lower cracking load for a given value of crack width. For an average crack width of 0.05 mm, the crack load in CON was about 1.5 kN, compares to 3.6 kN, 2.9 kN and 2.8 kN for SBR, PAE and VAE, respectively. A higher value of crack load was also shown by polymer-modified ferrocement in air curing. This indicated that polymer-modified ferrocement exhibited higher resistance to crack than that of the unmodified control, irrespective of the curing conditions adopted.

Crack Spacing

A relationship between the average crack spacing at crack stabilization and the specific surface of reinforcement seems to exist. The values of crack spacing obtained in the experiment are presented in Table 11.

For modified ferrocements in salt water, the average crack spacing was lower than that of the air curing. The SBR, PAE and VAE had a crack spacing of 35 mm, 37 mm and 40.5 mm, compared to that for air curing of 53 mm, 40 mm, 50.5 mm, respectively. However, in the unmodified control, the crack spacing for the specimen in air was 42 mm compared to that in salt water of 43.5 mm.

Table 11. Average crack spacings for ferro cement in static flexure

Type of Specimen	Exposure conditions (9 months)	Average crack spacing (Experimental) (mm)
CON	air	42.0
CON	salt water	54.5
SBR	air	53.0
SBR	salt water	35.0
PAE	air	40.0
PAE	salt water	37.0
VAE	air	50.5
VAE	salt water	40.5

Load-Deflection Characteristics

The main criteria in the design of ferrocement structures are deflection characteristics. Deflection in ferrocement is normally caused by the magnitude of loading it carries and also due to time-dependant factors such as shrinkage and creep. One of the main advantages of having mesh reinforcement in ferrocement is that the deflections due to shrinkage are significantly reduced by the presence of uniformly distributed mesh.

The relationship between the deflection and cracking behaviour of ferrocement was studied by Swamy and Al-Wash (1981), and found that an increase in the number of layers of mesh, resulted in a decrease in the deflection, average crack width and crack spacing.

The load-deflection curves of ferrocement have been reported to have three distinct stages (Balaguru, Naaman, and Shah, 1977), namely; before cracking of mortar (steepest slope), after the first cracking of mortar but before the yielding of steel and, after yielding of steel meshes when the slope becomes almost parallel to the axis of deflection.

From Fig. 4, it can be seen that the deflection curve of CON represented by 28 days air curing, showed three distinct stages exist in the specimen. There was linear load-deflection relationship up to about 1.3 kN, and thereafter, there was a drop in static load indicating the initiation of cracks in the specimen. As the static load increased the slope of curve became less steep towards its yield point. The specimen achieved its maximum load of about 4.1 kN, with its corresponding deflection of about 3.5 mm.
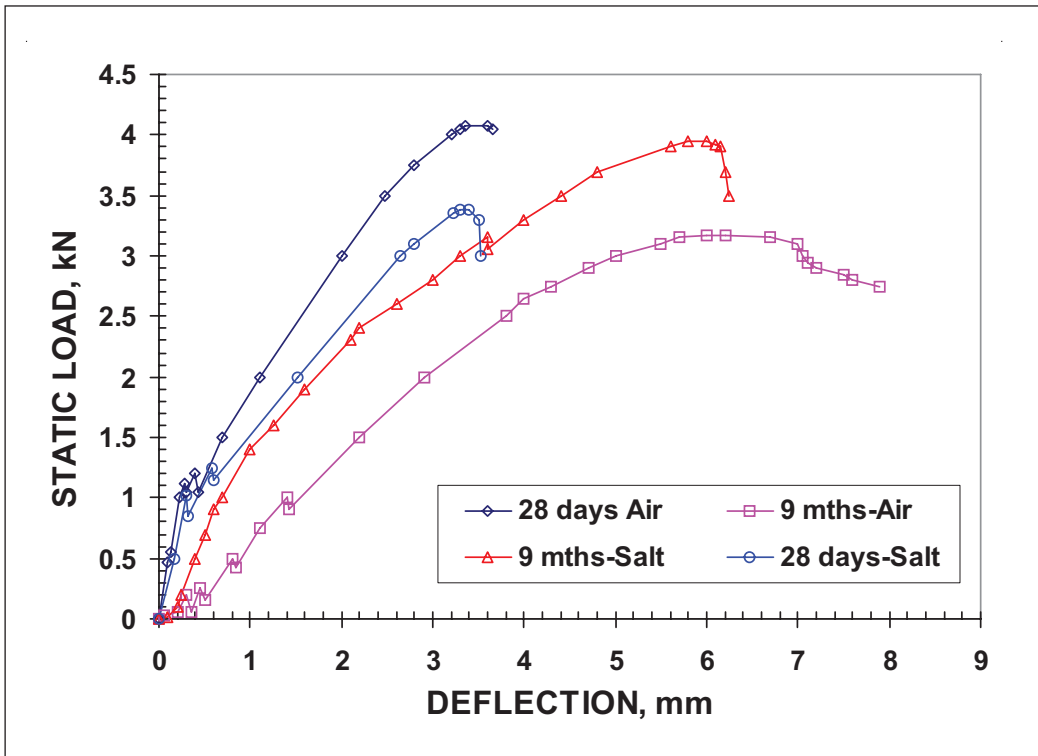

Figure 4. Load-deflection characteristics of unmodified ferrocement (CON)

Similar trend of development was also exhibited by specimens exposed to continuous salt water curing for 28 days. The first crack load occured at about 1.3 kN. The specimen achieved its maximum load before failure of about 3.3 kN at a deflection of about 3.5 mm. It seemed that air curing gave better deflection characteristics than salt water curing for the unmodified control ferrocement. However, both specimens reached their maximum deflection before failure at about 3.6 mm.

For prolonged salt water curing for a period of 9 months, there existed linear load-deflection relationship up to a static load of about 2 kN, and began to curve towards yielding and maximum load of about 3.8 kN. For this specimen, there was no indication of the occurrence of the first crack load, as that in the previous two test specimens. The specimen reached its maximum deflection before failure at about 6.2 mm. For 9 months of air curing, the linear load-deflection relationship existed up to about 1 kN, and showed greater increase in curvature with increasing static loads. The curve showed a maximum load of about 3 kN with maximum deflection before failure of about 8 mm.
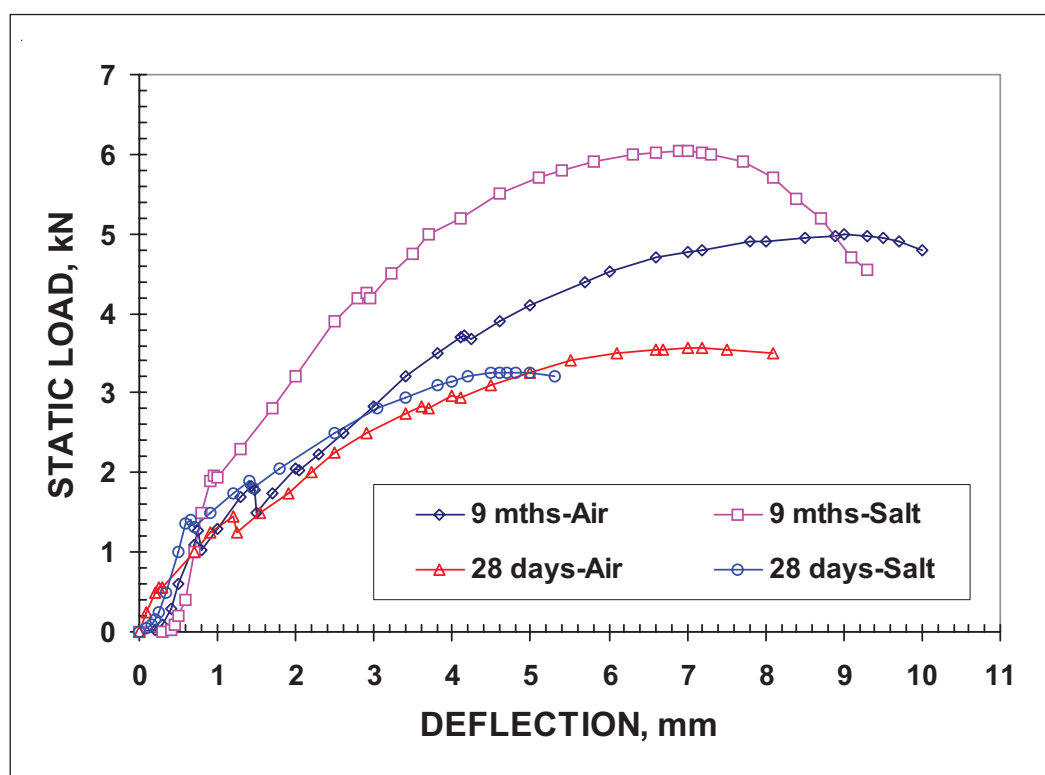
Figure 5. Load-deflection characteristics of SBR ferrocement panel

The load-deflection behaviour of SBR modified ferrocement is presented in Fig. 5. At 28 days of air curing, the first crack seemed to occur at a load of about 1 kN, thereafter, the curve deviated from linearity and gradually became almost horizontal as the applied load approached the ultimate value. The maximum load before failure was about 3.6 kN, and the corresponding maximum deflection was about 8.2 mm. At 28 days of salt water curing, linear load-deflection relationship occurred up to a static load of 1.4 kN, and thereafter, the curve began to deviate from linearity and reached its ultimate value at about 3.2 kN. The maximum deflection of this specimen before failure was about 5.4 mm.

In a continuous air curing for a period of 9 months, the gradient of the load-deflection curves were observed to be lower than that of salt water curing. For a given value of deflection after cracking, the increase in static load of specimen in salt water curing was nearly one and a half times that of air curing. The maximum load and deflection for specimen in 9 months of salt water curing were 6 kN and 9.2 mm, respectively. However, the corresponding load for 9 months of air curing was 5 kN, but its maximum deflection before failure was 10 mm, which was higher than that of the salt water curing.
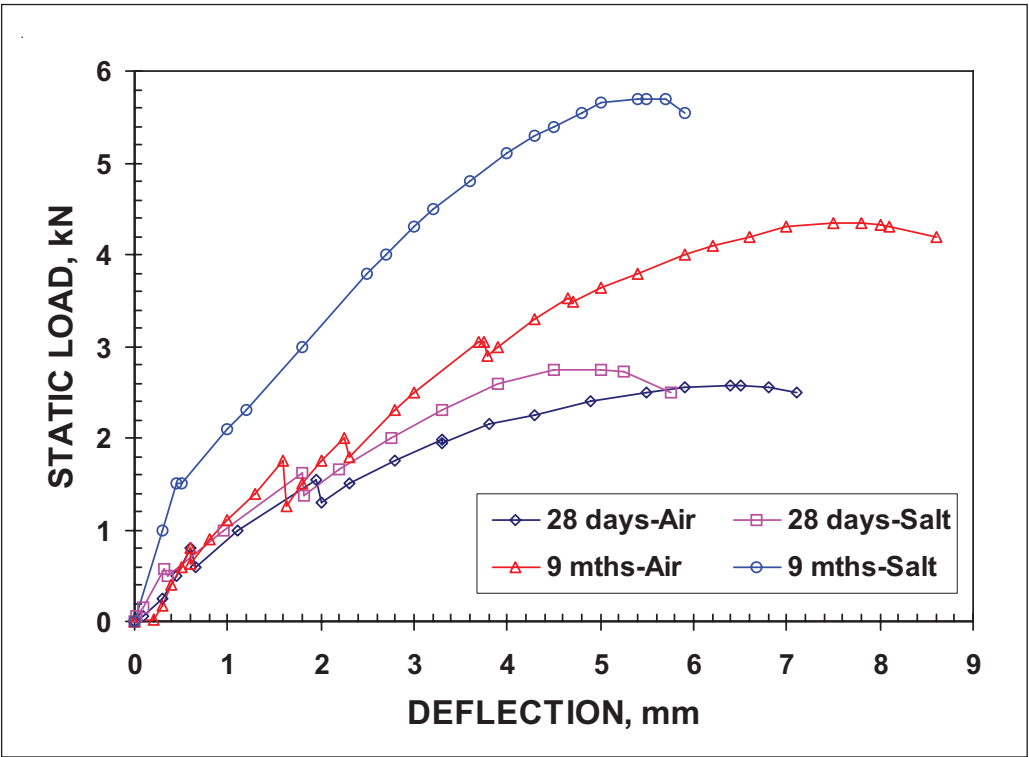
Figure 6. Load-deflection characteristics of PAE ferrocement panel
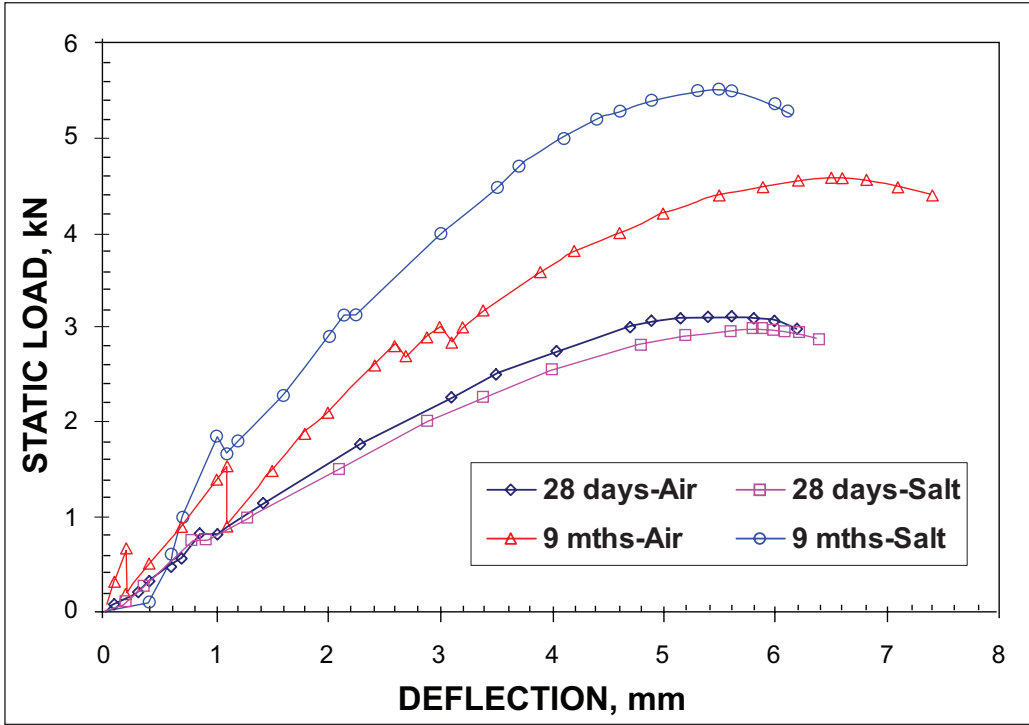
Figure 7. Load-deflection characteristics of VAE ferrocement panel

The typical load-deflection characteristics of PAE and VAE polymer-modified ferrocement are shown in Figs. 6 to 7. The specimens of PAE and VAE in salt water curing had significant improvement in the load-deflection characteristics. The ultimate load of specimen subjected to salt water exposure was always higher than that of the air curing. The maximum and ultimate loads were found to increase with the increasing age of curing. Higher deflections at failure were observed in ferrocement under prolonged air curing. The maximum deflection at failure for PAE and VAE were about 8.8 mm and 7.6 mm respectively, compared to that of salt water curing of about 6 mm each for PAE and VAE. The results also indicated that salt water curing greatly enhanced the flexural behaviour of polymer-modified ferrocement by increasing its ultimate load capacity, and by reducing its crack width, crack spacing and deflection.

CONCLUSIONS

Several conclusions can be derived from this experimental investigation and they are presented as follows:

1. Salt water increased the flexural strength, compressive strength as well as the Young's modulus of elasticity of both polymer-modified and unmodified ferrocement panels. The average flexural strength of salt water cured panels were higher than that of air cured panels by about 13% at the age of 9 months. However, the average compressive strength and its corresponding Young's modulus of elasticity of all modified ferrocement panels were only marginally higher than that of in air cured panels.

2. For both air and salt water curing, the inclusion of polymer latexes in cement mortars greatly enhanced the flexural properties of ferrocement panel. With 15% of polymer addition, the flexural strength of mortars increased by about 25% for continuous air curing, and about 32% for continuous salt water curing. The significant increase in flexural properties was due to the formation of polymer films around and in between the cement and aggregate particles, bridging and interconnecting these particles, leading to a higher flexural capacity.

3. The compressive strength of modified ferrocement showed a decrease by about 27% for a continuous air curing and about 23% for salt water curing, compared to that of the unmodified ferrocement. The lower compressive strength of modified ferrocement was due to the presence of soft polymer films in the voids and around the aggregates and cement particles, thereby reducing the magnitude of applied compressive force at failure.

4. Continuous salt water curing for a period of 9 months significantly improved the flexural behaviour of ferrocement by exhibiting higher experimental values of the crack load and ultimate strength for all specimens.

5. Lower crack widths, and higher crack loads in all modified ferrocement panels indicated that the polymer modification improved the bonding between aggregate, cement and polymer particles by the formation of polymer films, bridging and cementing them into a durable matrix and exhibiting higher resistance crack development.

6. The PAE and VAE-modified ferrocement panels in salt water showed typical load-deflection characteristics of ferrocement with polymer modification. The result showed that continuous salt water curing made significant improvement on the flexural behaviour of panels by increasing its ultimate load carrying capacity, and reducing not its crack width, crack spacing and deflection.

REFERENCES

ACI Committee 318 (1983). *Building Code Requirements for Reinforced Concrete*. American Concrete Institute. Vol.103, p132.

Balaguru, P.N., Naaman, A.E., and Shah, S.P.(1977). Analysis and behaviour of ferrocement in flexure, *Journal of Structural Division (ASCE)*. 10, 1937-1951.

Naaman, A.E., and Shah, A.P.(1971). Tensile test of ferrocement. *Journal of the American Concrete Institute*. 68(9), 693-698.

Paul, B.K., and Pama, R.P.(1978). *Ferrocement*. International Ferrocement Information Center, Asian Institute of Technology, Bangkok. p149.

Shah, S.P.(1972). Evaluation of ferrocement as a construction material. *Proc. of the Conference of New Materials in Concrete Construction*. University of Illinois at Chicago Circle.

Shah, S.P., and Key, W.H.(1972). Impact resistance of ferrocement, *Journal of the Structural Division*, *ASCE*. 98 (ST1),111-123.

Singh, G. (1994). Cracking: Its prediction and engineering significance - Keynote Lecture. *Proceedings of the Fifth International Symposium on Ferrocement*, Eds. P.J. Nedwell and R.N.Swamy, Manchester, United Kingdom. pp. 123-140.

Swamy, R.N., and Al-Wash, A.A (1981). Cracking behaviour of ferrocement in flexure, *Proc. International Symposium on Ferrocement* (eds. Shah, S.P., and Oberti, G.). A/1-A/11.

PERMEABILITY OF POLYMER-MODIFIED CEMENT SYSTEM FOR STRUCTURAL APPLICATIONS

Mahyuddin Ramli

Professor, School of Housing Building & Planning, Universiti Sains Malaysia

Abstract

The durability of cement system can always be enhanced by reducing the permeability of the material through polymer modification. Modified cement mortars are found to improve the durability of the cement matrix by reducing the permeability cement mortars. The effect of polymer modification on the permeability of cement mortar using styrene butadiene rubber latex (SBR), polyacrylic ester emulsion (PAE) and redispersable vinyl acetate ester (VAE) enhances its intrinsic properties, improves its mechanical properties and hence, its durability performance.

INTRODUCTION

Ordinary cement system offers relatively low flexural strength properties because of ease of initiation and propagation of micro cracks and also from the lack of tensile resistance of conventional cement mortars. The durability characteristics of this cement system can be greatly improved by reducing the permeability of the material through polymer modification.

Modified cement mortars are found to enhance the durability of the cement matrix and significantly reducing the depth of penetration of chloride into the mortars. As cement hydration process continues, the polymer particles coalesce to form a continuous layer of polymer film which surround the aggregates and coats the gel resulting in a less porous and a less permeable mortar matrix.

The effect of polymer modification using SBR latex, PAE emulsion and VAE powder on permeability properties of foamed ferrocement mortars enhances its intrinsic properties, improves its mechanical properties and hence, its durability. The effect of curing conditions and age of curing is also compared with the unmodified control mortars. Since the chloride penetration depends greatly on the permeability of cement paste, which in turn, directly related to the pore structure, a detail analysis is hence presented in order to establish their useful relationships.

OXYGEN PERMEABILITY

Underlying Principle

Flow rates in concrete or mortar are normally very low, resulting in laminar rather than a turbulent flow. Laminar viscous flow is dependent upon the properties of fluid (i.e. viscosity and density) as well as the characteristics of the porous medium (Dhir, *et. al*, 1989). The principle governing the permeability of a non-compressible fluid (e.g. water) can be determined according to Darcy's empirical law:

$$v = \frac{k \, A \, \Delta P}{\eta \, \ell} \tag{1}$$

Where, v is flow rate
A is cross-sectional area of specimen
ℓ is length of specimen
ΔP is fluid pressure head across specimen
η is viscosity of fluid
k is intrinsic permeability

When a compressible fluid, such as oxygen is used, having a viscosity of 2.02 x 10-5 Ns/m2 at a temperature of 20 °C, Eq (1) should be modified using the expression proposed by Grube and Lawrence (1984), which calculates the volume of fluid at the average pressure within the specimen and presented as:

$$k = \frac{2 \, P_2 \, v \, l \times 2.02 \times 10^{-16}}{A \, (P_1^2 - P_2^2)} \tag{2}$$

Where, k is intrinsic permeability (m^2)
v is the flow rate (cm^3/s)
l is thickness of specimen (m^2)
A is cross-sectional area of specimen (m^2)
P_1 is absolute applied pressure (bar), i.e.atmospheric pressure + P_2
P_2 is pressure at which the flow rate is measured, usually 1 bar.

Hence, the equation of intrinsic permeability may be written as:

$$k = \frac{4.04 \, v \, l \times 10^{-16}}{A \, (P_1^2 - 1)} \tag{3}$$

Permeability Test Apparatus

A schematic diagram of permeability cell as proposed by (Cabrera and Lynsdale, 1988) is shown in Figure 1, while Figure 2 shows the experimental set-up for measuring the permeability. The permeability cell consists of a sample holder, accurate pressure gauge, stable gas supply and flowmeter at the downstream side. The cell works on the same principle as that of the Cement and Concrete Association cell (Lawrence,1986), but the method by which the sample is confined laterally in order to ensure one-directional flow is different.

The test set-up shown in Fig.1 allows gas to flow only in the vertical direction by placing the mortar specimen (A) in a rubber cylinder (B) inside a steel ring cylinder (C), so that when a vertical force is applied through the cap of the cell (H), the rubber cylinder is forced inwards against the sample, thus preventing any leakage between the sample and rubber cylinder. The cell was checked for leak proof by using an impermeable brass cylinder as the sample and monitored at different pressure, and found to be leak proof.
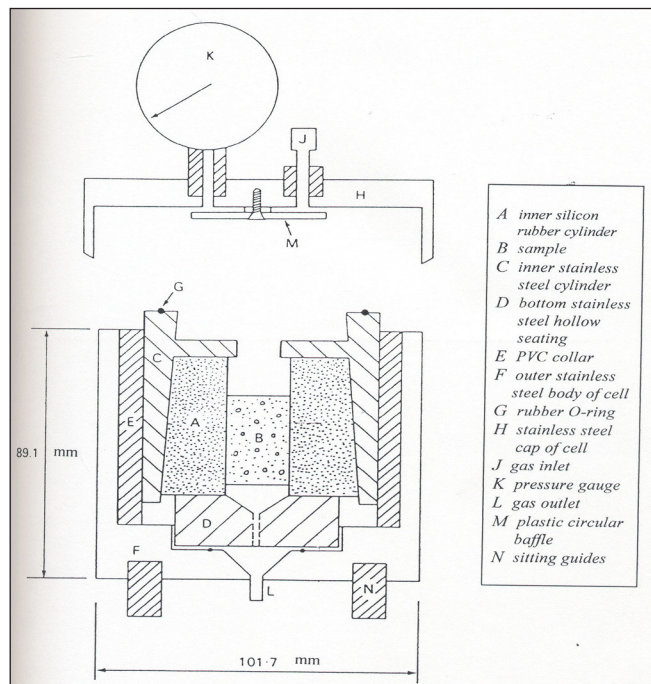
Figure 1. Schematic diagram of permeability cell apparatus
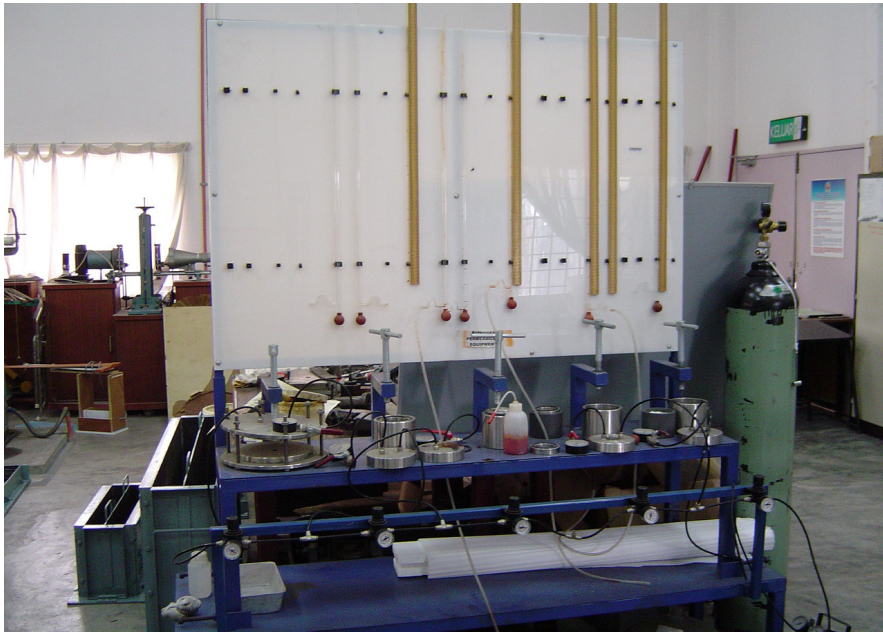
Figure 2. Permeability test set-up

EXPERIMENTAL PROGRAMME

The oxygen permeability test was conducted on the cored mortar samples at the following ages; 28, 91, 182, 364, and 546 days, to study the permeability performance of the unmodified control specimen, [CON1] and modified cement mortars, [SBR1, SBR3, PAE and VAE]. The effect of polymer modification, exposure conditions, and the age of curing was also investigated and compared, in order to establish useful relationships between intrinsic permeability and other related parameters, such as porosity, compressive strength and atmospheric carbonation.

Preparation of Samples

The samples used in the permeability test are obtained from 100 x 100 x 500 mm mortar prisms, using a 51 mm (internal diameter) diamond core drill. For each type of mix and age of curing, three prisms were cast, and subjected to three curing conditions; 7 days water curing, followed by air curing, 7 days air curing, followed by water curing and cyclic water and air curing of 7 days each. The cored samples for permeability measurement were prepared at 28, 91, 182, 364, and 546 days. A 50 mm diameter core samples were extracted from the full depth of untrowelled face of 100 mm thick mortar prism. Only central span of prism being used for core extraction to ensure consistency of results. Each core was then cut to size by removing about 10 mm thick in the top and bottom layer of the core, and cutting the remaining into two halves. The final thickness of the cores is normally between 35 - 40 mm.

Prior testing of oxygen permeability, the specimens were conditioned by drying in a ventilated oven at a temperature of 105 ± 5 °C for a period of 24 hours. On removal of samples from the oven, the samples were placed a desiccators for cooling for a minimum period of 24 hours. A total number of six samples were prepared for each mix, and the intrinsic permeability was determined from the average of six test results.

Test Procedure

The oxygen permeability of the unmodified controls and modified specimens was determined from a 50 mm diameter mortar sample as shown in Figure 3 and Figure 4. The test was carried out in a laboratory controlled temperature at 20 ± 2 °C, RH 65 ± 5 % and free from draughts. The testing procedures are described as follows:

1. The mortar samples are first determined the thickness and diameter prior to placing them into the rubber cylinder. The sample is housed in rubber cylinder inside inner stainless steel ring cylinder.
2. The stainless steel cap of cell is then fitted to the steel ring cylinder and securely tightened so that it is confined laterally and ensure that air is forced to flow in the vertical direction only.
3. The gas pressure at which the flow rate is measured is set to 1 bar. The gas is allowed to flow through the system for at least 15 minutes before the flow rates are recorded. This is important to ensure the flow of gas reaches its steady state before readings are recorded.
4. The gas flow rates are measured using a bubble flowmeter with internal diameter of 1.7 mm and 5.0 mm depending on the permeability of the samples. For each sample, five consecutive measurements are taken and their average readings represent the flow rate of the sample tested.
5. The readings obtained from the measurement are substituted in Eq (3) to determine the intrinsic permeability of the sample. For each set of reading, six mortar samples are tested and their average is taken to represent the permeability value of the specimen.
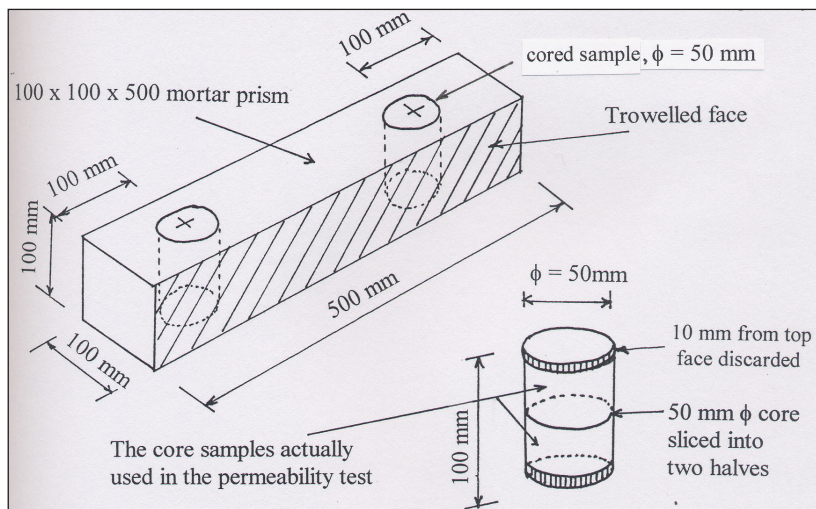
Figure 3. Extraction of core samples from a mortar prism

**Figure 4.** Core samples for permeability test

DURABILITY PROPERTIES

The intrinsic permeability relates to the internal structure of concrete or cement mortar and is independent of the properties of the migrating fluid; a sample tested with any liquid or gas should yield the same value of intrinsic permeability. Permeability also reduces with the increasing age of hydration, and is affected by the polymer modification, and curing conditions. The effects of polymer addition and curing conditions on the oxygen permeability of cement mortar were investigated. Four different types of polymer mix; namely, SBR1, SBR3, PAE and VAE were used in the permeability studies and compared with the unmodified control cement mortar, CON1. Three different curing regimes were used: 7 days in water, followed by air curing; 7 days in air, followed by water curing, and cyclic water and air curing of 7 days each.

Effect of Polymer Modification

The effect of polymer addition on the permeability characteristics of cement mortars are presented in Figure 5 and Figure 6. The results show that the permeability of all mixes decreases with the increasing age of curing. The permeability polymer-modified cement mortars are found to be very much lower than that of the unmodified controls. This is due to the partial filling micropores and voids by polymer particles as cement hydration process continues. The intrinsic permeability of SBR3 and PAE are about 0.2×10^{-16} m^2 at the age of 28 days and 0.1×10^{-16} m^2 at 18 months, compared to that of the unmodified control, CON1, which is about 1.05 and 0.4×10^{-16} m^2, respectively. However, the VAE-modified mortar, which comprise of polymer powder does not seem to perform as good as SBR latex or PAE emulsion, although their polymer loadings are the same.

The results also implied that polymer modification has greatly enhanced the permeability of cement mortar. Low permeability properties in polymer-modified cement mortars are attributed to the fact that polymer particles, being much smaller than the sand and cement particles, fill the smaller voids and eventually coalesce into a monolithic film that surrounds the aggregate and coats the cement particles (Sorousshian and Tlili,1993). The resulting matrix also prevents the formation of microcracks, thereby improving the impermeability characteristics of the mortar. The permeability of polymer-modified cement mortars is found to reduce significantly with the age of curing. This is in agreement with the result obtained by Kuhlmann and Foor (1984).
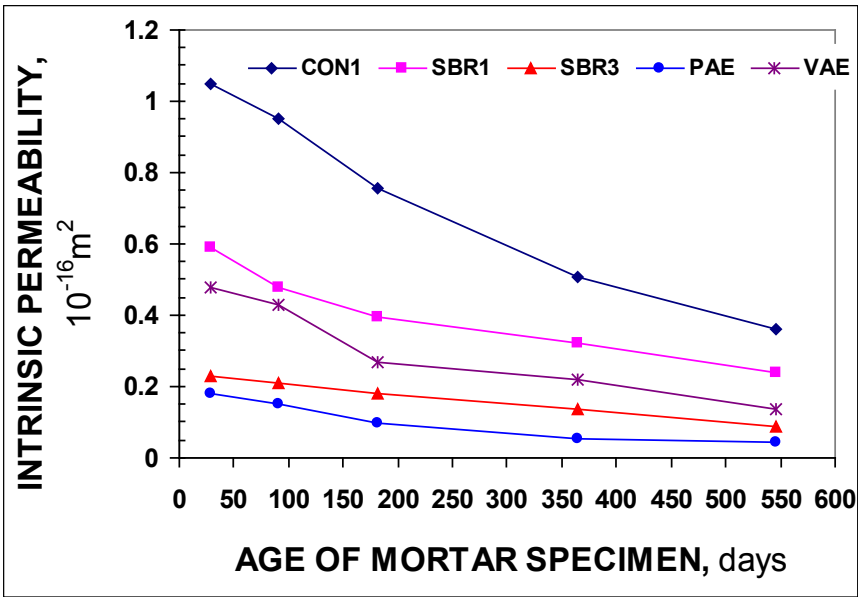
Figure 5. Intrinsic permeability of mortar specimens under prolonged air curing
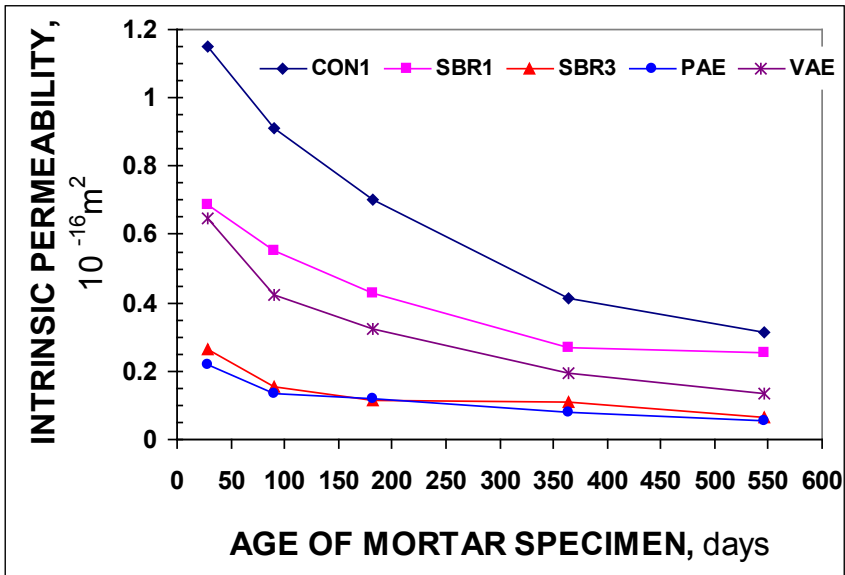
Figure 6. Intrinsic permeability of mortar specimens under prolonged water curing

Effect of Curing Conditions

The effects of curing conditions on the intrinsic permeability of all specimens at the following ages; 28 days, 6, 12, and 18 months, are carefully studied. At 28 days of curing, the difference in exposure conditions does not have a significant effect on the permeability properties of all specimens, except for SBR1 and VAE as shown in Figure 5 and Figure 6. The SBR1-modified cement mortars shows slightly lower intrinsic permeability in a 7 days initial water curing, followed by air curing, whereas VAE-modified mortar has lower permeability in both prolonged air curing, and cyclic water and air curing. All polymer-modified specimens at 28 days, show lower permeability value of between 0.2 - 0.65 x 10 $^{-16}$ m^2 compared to that of the unmodified control of about 1.1 x 10 $^{-16}$ m^2.

The permeability of cement mortars reduces with the increasing age of curing. At the age of 3 months, the intrinsic permeability shows an average reduction of about 20 % compared to that of at 28 days. However, at the age of 6 months a significant reduction in intrinsic permeability is observed in specimens (SBR3, PAE, VAE) modified with 15 % polymer solids. Cyclic water and air curing seems to be the best curing regime for all the modified cement mortars. Their intrinsic permeability values are about 50 % lower than that of the specimens at 28 days. The unmodified control seems to benefit most from prolonged water curing. Its intrinsic permeability is 0.7 x 10 $^{-16}$ m^2 compared to 1.15 x 10 $^{-16}$ m^2 at 28 days.

At the age of 12 and 18 months of curing, the polymer-modified cement mortars show little improvement in their permeability values as shown in Figure 7. Their intrinsic permeability is ranging from 0.05 to 0.10 x 10 $^{-16}$ m^2 compared to the unmodified control of about 0.4 x 10 $^{-16}$ m^2. This is attributed to the fact that, over the long period of curing, the polymer film formation slows down just like in cement hydration process. At this stage, the partial void filling also reduces, thus resulting in almost constant permeability value. However, this is not the case for unmodified cement mortars, because hydration of cement still continues so long as water becomes available.
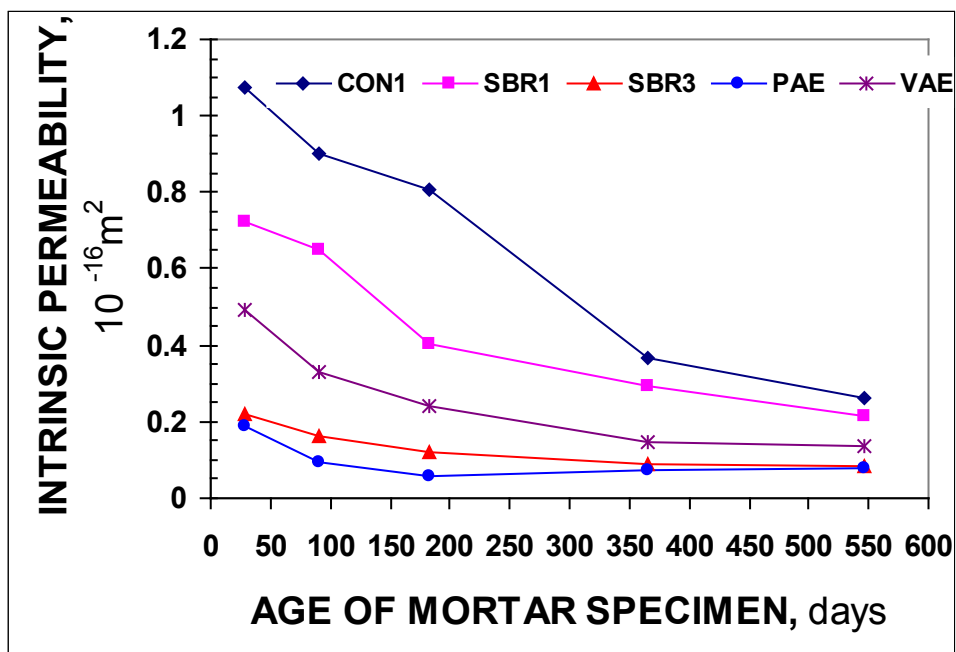

Figure 7. Intrinsic permeability of mortar specimens under cyclic water and air curing

Relationship Between Permeability and Pore Structure

The test results on oxygen permeability of polymer-modified and unmodified cement mortars subjected to various curing conditions were established. Attempt has been made to relate the pore structure and permeability properties. The relationship between the intrinsic permeability, *k*, with the mean pore radius, *r* and porosity, *p* is represented by the following expression (Beaudoin, *et. al.*, 1994):

$$k = \omega \, p \, r^{\,2} \qquad\qquad\qquad (4)$$

where   ω   is a form factor (1/8 for cylindrical pores)

Graf and Setzer (1988) identified the principle factors correlating pore size distribution with permeability. The mean pore radius determined from mercury intrusion data was taken from the maximum of the differential curve. Many authors, Nyame and Illston (1980), Diamond (1973), and Li and Roy (1986) have used pore size distribution results obtained from mercury intrusion porosimetry to define a mean pore radius (or diameter). One, derived from *dV/dP (P=* mercury intrusion pressure) versus pore radius plot was termed the 'critical pore radius', or the 'maximum continuous pore radius' (Nyame and Illston, 1980). These radii are similar but not identical to the 'threshold radius' defined by Diamond (1973). A linear relationship between log (water permeability) and mean pore radius has been reported by Li and Roy (1986). Nyame and Illston (1980) relate the pore structure and permeability using the mean pore radius (or diameter) obtained from differential mercury intrusion curve, and represented by the following expression:

$$k = 1.684 \, r_{m}^{\,3.284} \times 10^{-22} \qquad\qquad (5)$$

The correlation coefficient was 0.96, but found that, for values of r_{m} less than 100 nm, the scatter data was large.

In this study, the relationship between intrinsic permeability and pore structure parameters are investigated. The regression correlation between oxygen permeability and the mean pore diameter is presented in Figure 8, and their correlation equations are represented by the following expression:

For unmodified control, CON1,

$$k = 0.012 \, d_{m}^{\,1.1489} \times 10^{-16} \qquad (\, r = 0.929 \,) \qquad (6)$$

For SBR3-modified specimen,

$$k = 0.0098 \, d_{m}^{\,0.7987} \times 10^{-16} \qquad (\, r = 0.855 \,) \qquad (7)$$

PAE-modified mortar,

$$k = 0.0148 \, d_{m}^{\,0.5905} \times 10^{-16} \qquad (\, r = 0.518 \,) \qquad (8)$$

and VAE-modified mortar,

$$k = 0.0006\, d_m^{\,1.6195} \times 10^{-16} \qquad (\,r = 0.836\,) \qquad (9)$$

where $\quad$ k $\quad$ is the intrinsic permeability (m^2)

$\qquad\qquad$ d_m is the mean pore diameter (nm)

From Eq (6) - Eq (9), the correlation curves were derived. It can be seen Fig. 8 that although their correlation coefficients for CON1, SBR3 and VAE are fairly high, the scatter data for values of d_m less than 100 nm is large.

Figure 8 shows typical linear correlations between oxygen permeability and their corresponding value of total porosity for pore diameter less than 100 nm. For unmodified cement mortars CON1, a high correlation coefficient was observed, indicating a reasonably good relationship exists between them. For a given curing condition, the intrinsic permeability increases with the increasing value of total porosity. Similar linear relationships in polymer-modified cement mortars, (SBR3, PAE), but with a much steadier incremental rate of permeability with respect to porosity. This may be due to the partial filling of micropores and voids by smaller particles of polymer, thus enhancing the impermeability characteristics of cement mortars. In general, the relationship between permeability and pore structure may not be defined in terms of an average pore size and total porosity without taking into account the pore size distribution. Pore size distribution affects the flow pattern (Hampton and Thomas, 1993) as the flow in a given pore depends not only on the pore size being considered but also on the pore sizes around it.
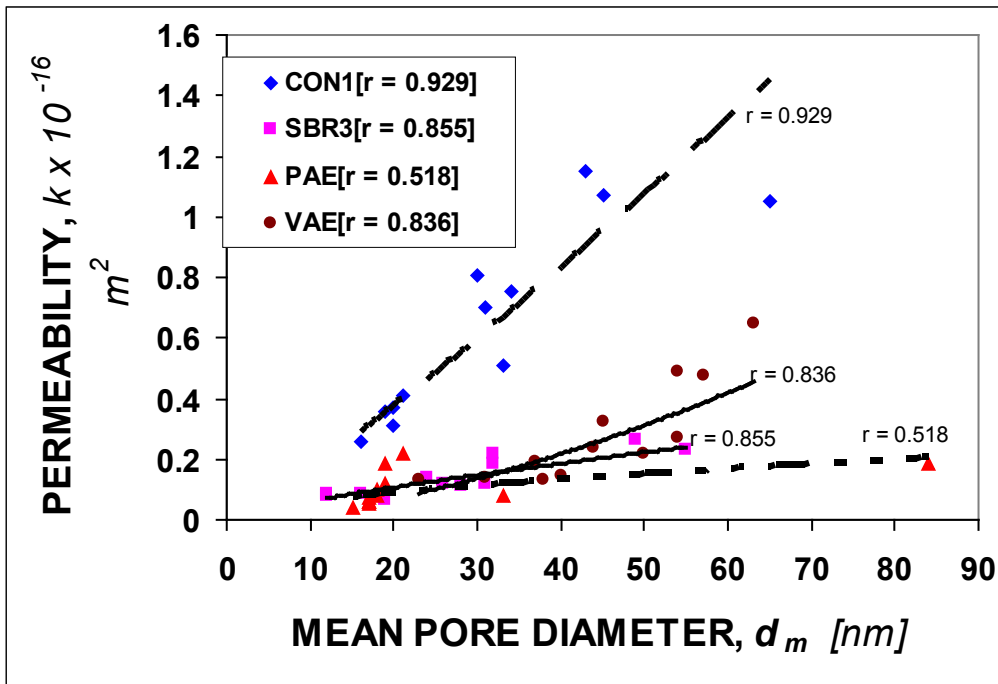
Figure 8. Regression correlation between oxygen permeability and mean pore diameter

Relationship Between Permeability and Strength

The relationship between permeability and compressive strength of cement mortars are also investigated to find their possible correlations. The regression correlations of linear form are obtained to establish the relationship between intrinsic permeability and compressive strength of all specimens at the ages of 28 days, 6, 12, and 18 months, as presented in Figure 9 and Figure 10. For a given curing condition and water-cement ratio, the intrinsic permeability decreases with increasing compressive strength, or increases with decreasing strength. It can be seen from Figure 9 that under prolonged air curing, the polymer-modified cement mortars show a higher rate of decrement indicating by steep slopes of the curve. The slopes are also dictated by the water-binder ratio of the specimens; which indicate steeper slope for low water-binder ratio and slender for higher water-binder ratio, as represented by SBR3 and PAE curves. In Figure 10, the polymer-modified mortars show less pronounced effect, since prolonged water curing is not the best curing condition for polymer materials. Similar linear relationships between compressive strength and intrinsic permeability of specimens at different water-binder ratio. The higher correlation coefficients also suggest that there has been a close relationship between oxygen permeability and the compressive strength of cement mortars. However, the results clearly demonstrate that it is misleading at this stage to suggest that strength can generally be used to predict permeability.
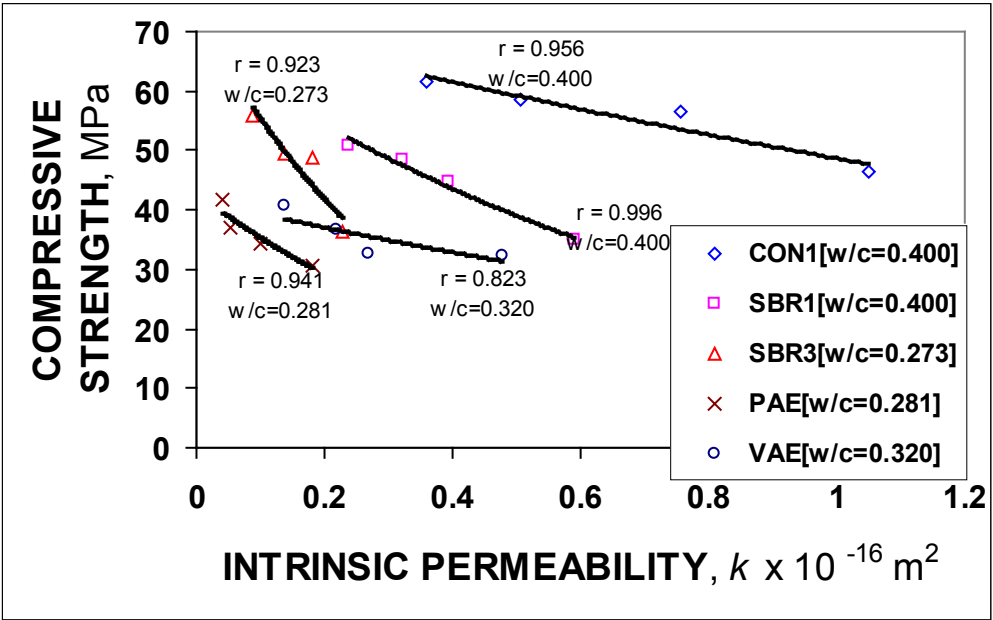
Figure 9. Relationship between compressive strength and permeability of specimens under prolonged air curing
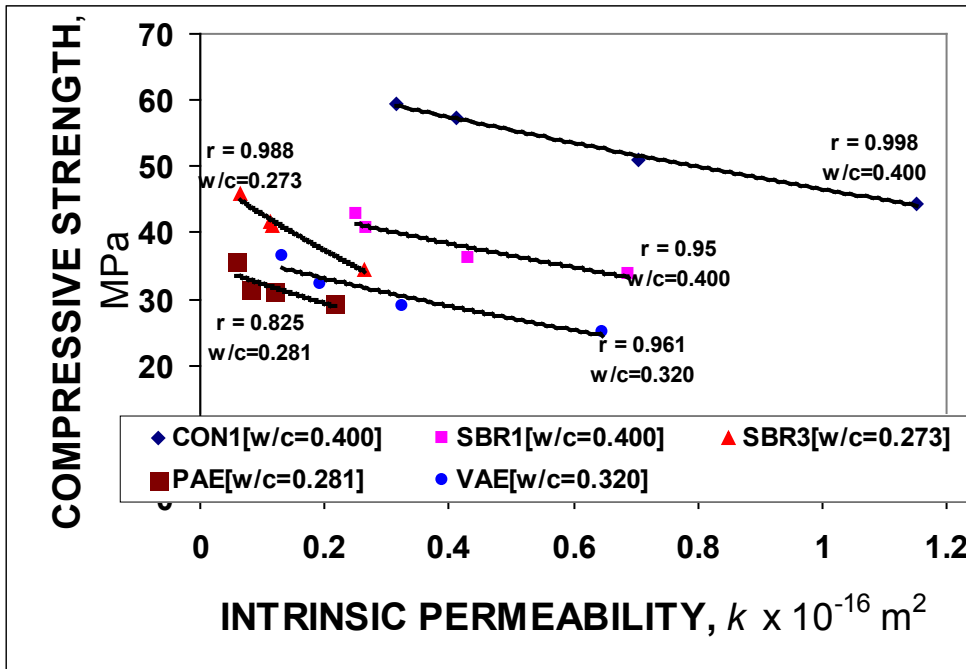
Figure 10. Relationship between compressive strength and permeability of specimens under prolonged water curing

Relationship With Water Absorption

It has been discussed earlier that water absorption of polymer-modified cement mortars reduces with increasing age of curing. This characteristic is quite similar to the behaviour exhibited by oxygen permeability. The reduction of permeability and water absorption properties is a result of polymer film formation which partially fills the micropores and voids during curing. The relationships between water absorption and oxygen permeability of polymer cement system with age of curing are discussed and their correlation results are presented in Figure 11 and Figure 12.

Figure 11 and Figure 12 show that there are linear correlations between water absorption and intrinsic permeability. The water absorption increases with the increase in permeability since both are affected by the pore structure of cement paste. The increase in water absorption in unmodified cement mortars is more pronounced compared to that of the polymer-modified specimen. This is indicated by steeper slope of regression line shown in the unmodified control. For a given value of permeability, the increase in water absorption in unmodified control is two times as high as that of the polymer-modified mortars. This may be attributed to the fact that water-binder ratio has greater influence on both permeability and water absorption, since all polymer-modified cement mortars have lower water-binder ratio of between 0.273-0.32 compared to that of the unmodified mortars of 0.4. Furthermore, the presence of polymer particles provide greater advantage to pore structure of the paste; being smaller than cement particle and sand, smaller pores can be filled and sealed as a result of the coalescence of this polymer particles. This increases the waterproofness, and the impermeability of the resulting mix. High correlation coefficients of greater than 0.95 shown by the unmodified control in all curing conditions also indicate that there is a significant linear correlation between permeability and water absorption.
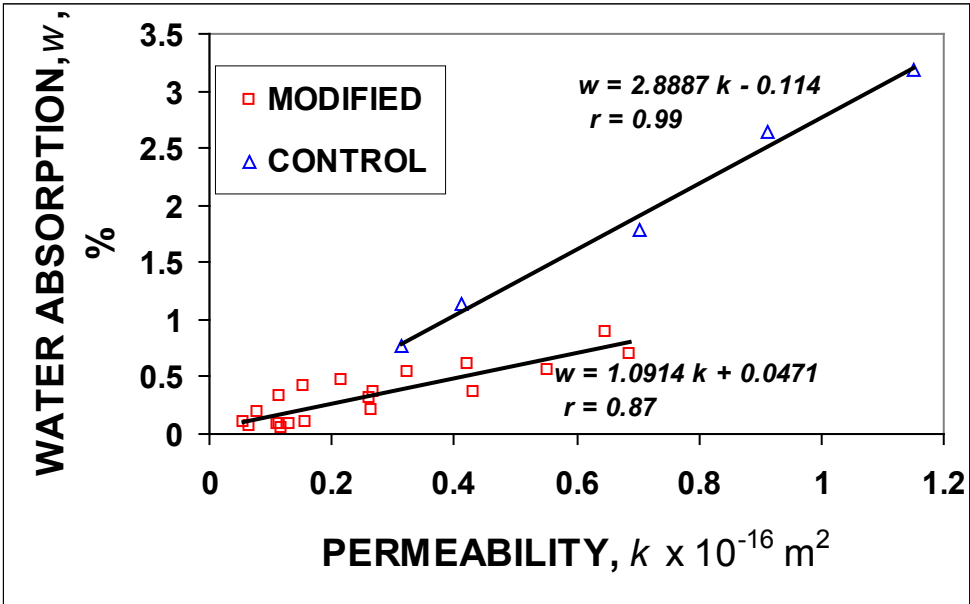
Figure 11. Relationship between water absorption and permeability under prolonged water curing
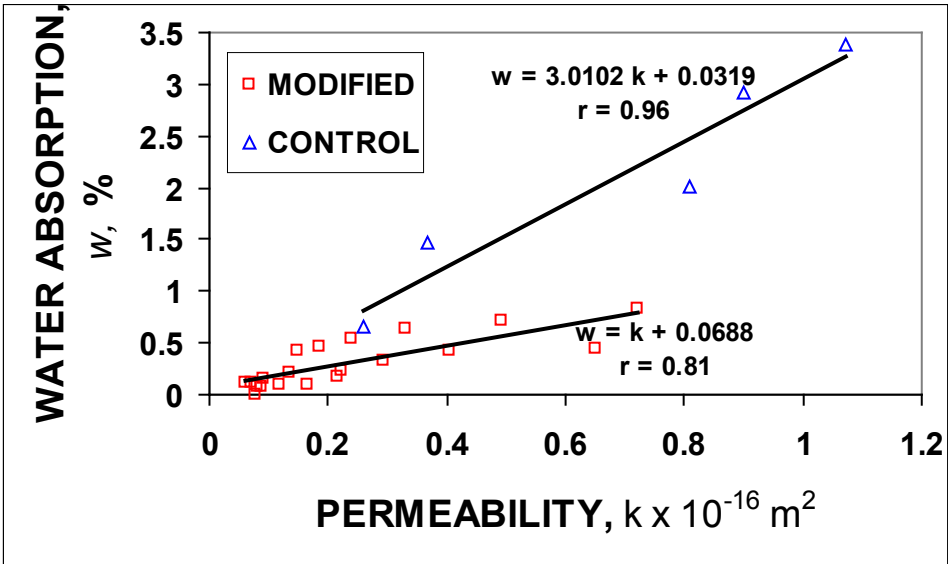

Figure 12. Relationship between water absorption and permeability under cyclic water and air curing

CONCLUSION

The main conclusions derived from the oxygen permeability test results are as follows:

1. Oxygen permeability of all mixes is found to decrease with the increasing age of curing.
2. The permeability of polymer-modified cement mortars are generally lower than that of the unmodified control mortar, due to the partial filling of micropores and voids by polymer particles as cement hydration process continues.
3. Three curing conditions applied to all test specimens do not seem to have significant effect on the permeability properties. Wet or dry curing conditions applied to specimens initially, seems to have benefited both cement hydration and polymer film formation.
5. However, the cyclic water and air curing are found to be the best curing regime for all polymer-modified cement mortars, except for unmodified cement mortar which benefit most from prolonged water curing.
6. Although the permeability of modified cement mortars decrease with increasing age of curing, they achieve the lowest permeability value when reaching the age of curing of 18 months. This may be attributed to the fact that over certain period of dry curing, most of the accessible pores and small voids in the polymer-cement system have been filled and sealed through the formation of polymer films, resulting a constant value of permeability.
7. The relationships between oxygen permeability and total porosity are found to be linearly correlated. A high correlation coefficient shown by CON1, SBR3,and PAE specimens, indicate that a reasonably good relationship exists between them.
8. For a given curing condition and water-binder ratio, the intrinsic permeability decreases with increasing compressive strength, or increases with decreasing strength.
9. In comparing relationship between permeability and water absorption, the test results show that water absorption increases with the increase in permeability since both are affected by the pore structure of the cement paste.

REFERENCES

Beaudoin, J.J., Feldman, R.F., and Tumidajski, P.J. (1994). Pore structure of hardened portland cement pastes and its influence on properties, *Advanced Cement Based Materials*. 1, 224-236.

Cabrera, J.G. and Lynsdale, C.J. (1988). A new gas permeameter for measuring the permeability of mortar and concrete. *Magazine of Concrete Research*. 40(144), 177-182.

Dhir, R.K., Hewlett, P.C., and Chan, Y.N. (1989). Near surface characteristics of concrete: intrinsic permeability, *Magazine of Concrete Research*. 41(147), 87-97.

Diamond, S. (1973). *Proceedings Conference on Pore Structure and Properties of Materials*, Prague. 1, B73-78.

Graf, H.and Setzer, M. (1988). Pore structure and permeability of cementitious materials, *Materials Research Society*. 137, 337-347.

Grube, H. and Lawrence, C.D. (1984). Permeability of concrete to oxygen, *Proceedings of*

RILEM Seminar, Durability of Concrete Structures under Normal Outdoor Exposure, University of Hanover, Institut fur Baustoffkunde und Materialprufung, p. 68-79.

Hampton, J.H.D. and Thomas, M.D.A.(1993). Modelling relationships between permeability and cement paste pore microstructures, *Cement and Concrete Research.* 23, 1317-1330.

Kuhlmann, L.A. and Foor, N.C. (1984). Chloride permeability versus air content of latex modified concrete. *Cement, Concrete, and Aggregates.* 6(1), 11-16.

Lawrence, C.D. (1986). Measurement of permeability. *Proceedings, 8th International Congress on the Chemistry of Cement,* Rio de Janeiro. 5, 29-34.

Li, S., Roy, D.M. (1986).*Cement and Concrete Research.* 16, 749-759.

Nyame, B.K. and Illston, J.M. (1980), *Proceedings 7th International Congress on Chemistry of Cement*, Paris. 3, 181-185.

Sorousshian, P. and Tlili, A.(1993). Effects of latex modification on the failure mechanism and engineering peoperties of concrete, *Polymer-Modified Hydraulic-Cement Mixtures, ASTM STP 1176*, Louis A. Kuhlmann and D. Gerry Walters, Eds, 104-119.

USE OF OIL PALM SHELL AS STRUCTURAL TOPPING FOR SEMI-PRECAST CONCRETE SLAB

Doh Shu Ing[1], V. J. Kurian[2], S.P. Narayanan[2]

[1] *School of Engineering and Information Technology, Universiti Malaysia Sabah, Locked Bag 2073, 88999 Kota Kinabalu, Sabah*
[2]*Universiti Teknologi PETRONAS, 31750 Tronoh, Perak, Malaysia.*
Email: umsdoh@yahoo.com

Abstract

Conventional coarse aggregate namely sandstone was used as coarse aggregate for the bottom layer of concrete in the semi-precast slab, while coarse aggregates such as granite, sandstone and OPS were used for the cast-in-situ top layer of concrete. The thickness of bottom and top layers were 50 mm and 75 mm respectively. Six slabs with different toppings were cast and tested. Data presented include the characteristics of deflection and cracking behaviour. The results showed that the semi-precast slab with topping of OPS concrete deflected about 30% more than similar slabs with toppings of granite concrete and sandstone concrete. The investigation also revealed that the type of topping did not affect the strength of the slab significantly. The flexural behaviour of all the three types of semi-precast slabs complied with the requirements specified by the current Codes of Practice (BS8110). Semi-precast slab with the topping of OPS concrete has an added advantage that it is lightweight, thereby reducing the cost of construction.

Keywords: *OPS, concrete, semi- precast, experimental analysis*

INTRODUCTION

Oil Palm Shell (OPS) is an agricultural waste material available abundantly in Malaysia. OPS is usually disposed by incineration or left to rot (Teo, *et.al.*, 2007). The utilisation of this waste material significantly reduces the cost of construction, and also eliminates the environmental pollution caused by it. Currently, Malaysia produces more than 4 million tonnes of OPS solid waste annually. Therefore, the use of this waste material as sustainable building material helps to preserve the natural non-renewable resources and also conserve the ecology.

OPS concrete has bright potential as it is very light compared to the conventional sandstone and granite concrete (Teo, *et.al.*, 2007, Mannan, *et. al.*, 2004 and Mannan, *et.al.* 2002). This reduces the dead load of a building and therefore reduces the cost of construction (Basri, *et. al.*, 1999). OPS concrete produced by Teo, *et. al.* (2007) has successfully achieved the 28 days compressive strength of 28.12 N/mm^2 which is greater than the minimum required strength 25 N/ mm^2 for structural residential slab. Mannan and Ganapathy (Mannan, *et. al.*, 2004) reported that the floor slab cast using OPS concrete satisfied the limit state condition for residential structure. Even though OPS aggregates are porous in nature, the resulting OPS concrete was reasonably impermeable (Teo, *et.al.*, 2007). The modulus of elasticity of OPS concrete at 28 days is relatively low (0.70-0.76×10^4 N/mm$^{2)}$ compared to the conventional concrete made of granite.

MATERIALS

Ordinary Portland Cement was used (Teo, *et.al.*, 2007). The coarse aggregates were OPS, granite and sandstone available locally in Sabah. The maximum size of coarse aggregate was 15 mm. The fine aggregates were river sand and crushed sandstone sand with fineness modulus of 1.78. The mix design for concrete using OPS, sandstone and granite aggregate is shown in Table 1.

Table 1. Mix Design of Concrete using OPS, sandstone and granite aggregate

Material	OPS Concrete	Sandstone Concrete	Granite Concrete
Cement, (kg)	450	350	350
Water, (kg)	171	151	176
Coarse Aggregate, (kg)	488	1053	1241
River Sand, (kg)	629	306	361
Crushed Sandstone Sand (kg)	0	219	257
Super plasticizer (litres)	7.50	3.88	4.20

PROPERTIES OF AGGREGATES

Sandstone and granite are inorganic while OPS is an organic material (Basri *et. al.,* 1999 & Alca, *et. al.* 1997). The properties of OPS, granite and sandstone are shown in Table 2. The table shows that the OPS aggregate is porous in nature and has low bulk density. The high value of water absorption necessitated special care in preparation of OPS to be used in concrete. The OPS was first soaked in water for 24 hours and then surface dried. The low bulk density is an advantage in producing lighter concrete (Basri *et. al.* 1999). The aggregate impact value (AIV) for OPS aggregate was only about half that for granite and sandstone and hence resulted in better capacity to absorb shock.

Table 2. Properties of Aggregates

Properties	Sandstone aggregate	OPS aggregate	Granite aggregate
Maximum Size	15 mm	15 mm	15 mm
Shell thickness	NA	0.5-3.0 mm	NA
Bulk Density	1450 kg/m^3	590 kg/m^3	1490 kg/m^3
Specific gravity (SSD)	2.58	1.17	2.63
Fineness Modulus	6.34	6.08	6.68
Los Angeles Abrasion Value	21.20	4.90 %	20.30 %
Aggregate Impact Value [3]	13.58 %	7.51 %	13.95 %
Aggregate Crushing Value [4]	21.20 %	8.00 %	19.00 %
24-hour Water Absorption	1.53 %	33.0 %	0.97 %

PROPERTIES OF CONCRETE

Six semi-precast slabs with 55 mm thick sandstone concrete for precast part were used for this study. The 75 mm thick topping was made varying the coarse aggregates used, namely granite, sandstone and OPS (two slabs for each type). The densities of these toppings were 2400 kg/m^3, 2060 kg/m^3 and 1710 kg/m^3 respectively and as the precast bottom portion 55 mm thick was made of sandstone concrete, the three types of semi-precast slabs had

equivalent densities of 2250 kg/m³, 2060 kg/m³ and 1850 kg/m³ respectively. Hence, it can be observed that the use of OPS topping resulted in a weight reduction of 23% for the whole slab, which is very close to the lightweight concrete (1800 kg/m³).

A 1500 kN compression test machine was used to test the companion concrete cubes cast along with the slabs. This test was conducted in accordance to BS 1881: Part 116:1983. Figure 1 shows the compressive strength at 3, 7 and 28 days of the concrete made of sandstone, OPS and granite coarse aggregate.
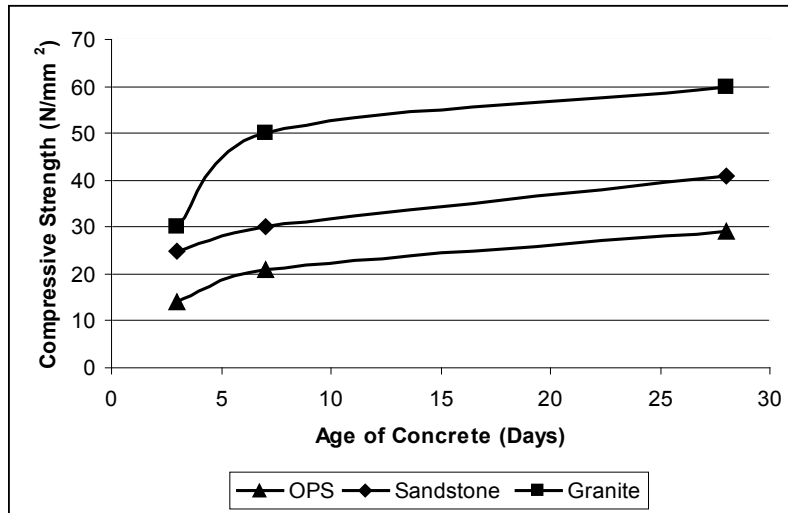
Figure 1. Compressive strength of concrete made with different aggregates at 3, 7 and 28 days

EXPERIMENTAL PROGRAMME AND SET UP

The testing programme consisted of testing six slabs having precast part made of sandstone concrete. The toppings were of concrete made of sandstone, OPS and granite coarse aggregate. Slabs were 3 m long, 1 m wide and 130 mm thick. The slabs were cast with bottom layer 55 mm thick and toppings 75 mm thick. Four Y-10 bars at bottom and two Y-10 bars at top, connected by R-6 diagonals formed two lattice girders at a spacing of 500 mm as shown in Figure 2. Steel B5 mesh was used as the bottom reinforcement. The experimental set up is shown in Figures 3 and 4. The slab was subjected to line load at one–third spans, which was increased in steps until the slab failed and observations were made at each increment of load.
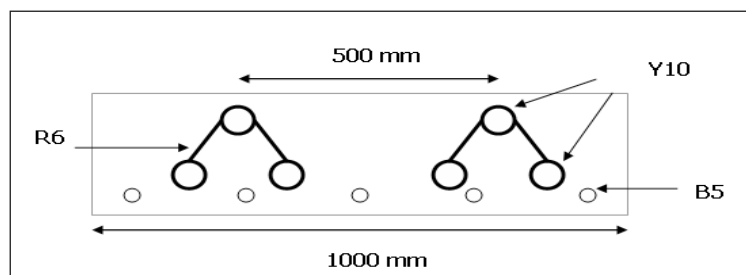
Figure 2. Arrangement of reinforcement
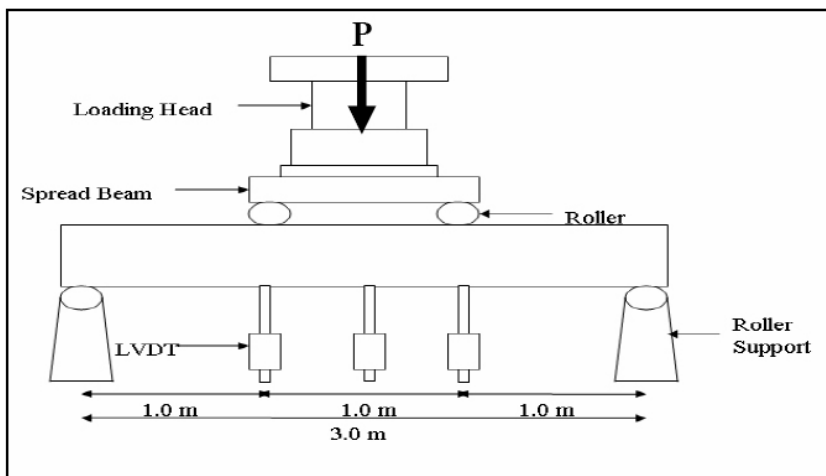
Figure 3. Experimental set up for slab test

Figure 4. Photograph of test set-up

The test for flexural behaviour of reinforced concrete beam was performed using a 1000 kN capacity, Shimadzu hydraulic actuator in the laboratory. Prior to recording, the slab was preloaded with a minimum load of 0.5 kN to allow initiation of the measuring devices. The load was applied in 2 kN increments (from 0-10 kN) and in 5 kN increments after 10 kN until the slab failed.

RESULTS AND DISCUSSIONS

MAXIMUM LOADS

The maximum loads for semi-precast slab with different concrete toppings were recorded. From the observation, the semi-precast slab with sandstone topping resisted the highest loading at approximately 65 kN. The semi-precast slabs with granite and OPS toppings resisted 64 kN and 59 kN respectively.

CRACK BEHAVIOUR

During the slab testing, at every 5 kN increment of loading, the cracks were observed using a crack magnifier. It was observed that the cracks began to form when the load reached 10-15 kN. The number of cracks occurring between the loading points and outside the loading points was recorded at every interval of loading until the slab eventually failed. After the test, the spacing of cracks was recorded. The crack behaviour of the different slabs is shown in Table 3. The slab with granite topping had the highest average crack spacing of 143 mm, while the slabs of OPS and sandstone toppings had an average crack spacing of 127 mm 126 mm respectively.

Table 3. Crack Behaviour in Different Slabs

Slab	Type of Topping	Average Crack Spacing (mm)	No. of cracks between load points	No. of cracks outside loading points	Average crack distance from the edge (mm)
S1	OPS	126.8	9	7	554.50
S2	Granite	142.5	8	7	716.00
S3	Sandstone	125.5	9	6	558.50

Figure 5 shows that the vertical cracks propagated almost to the top surface of the slab without any break or discontinuity at the interface between the precast part and the topping. This proved that there was very good composite action. When similar slabs without the lattice girders were tested, cracks were observed to develop horizontally at the interface indicating lack of composite action in the absence of lattice girders.

Figure 5. Photograph showing the propagation of cracks in the semi precast OPS slabs

DEFLECTION

The deflections of the slabs were measured using two LVDTs (100 mm range) placed at the mid span of the slab (Neville, 2005). Tshe deflections of the slab were recorded at load increments of 2 kN up to 12 kN load and at load intervals of 5 kN after that. The load versus deflection at mid span of the semi-precast slabs with different types of topping is shown in Figure 6. It can be observed that the slab with OPS topping had the maximum deflection at all load values at mid span of the slab. This is because of the low value of the modulus of elasticity for OPS concrete.
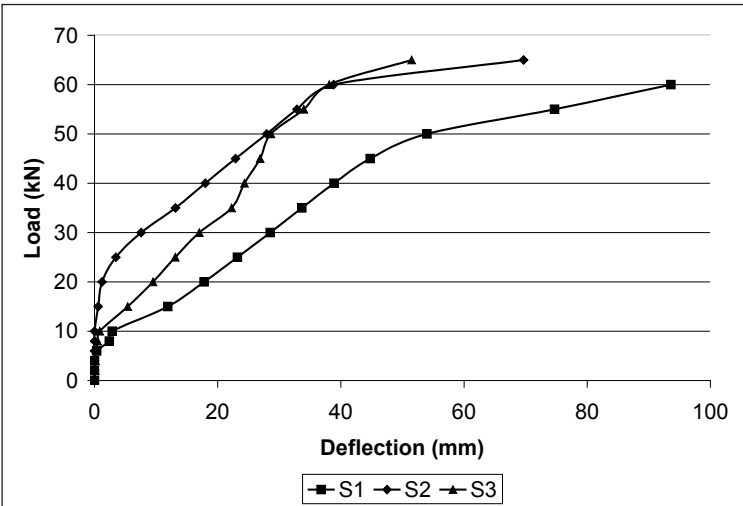
Figure 6. Load vs deflection at midspan for different types of topping

STRAIN DISTRIBUTION

Strain gauges were fixed on the slabs at mid span at 20 mm, 32.5 mm, 97.5 mm and 110 mm from the bottom from the slab. From these strain gauge readings, the strain distribution along the depth of the slab at the mid span is plotted as shown in Figures 7 to 9. The strain distribution confirms the composite behaviour of the slab. In other words, the top layer and the bottom layer are integrating as one full composite section. From the figures, it can be observed that the distance of the neutral axis from the top of the slab was about 47 mm for OPS topping, about 45 mm for granite topping and about 50 mm for sandstone topping.
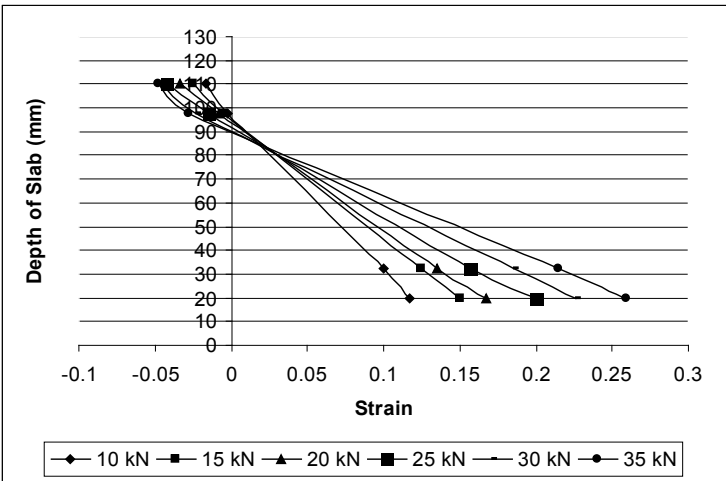
Figure 7. Strain distribution at mid span section for OPS topping slab
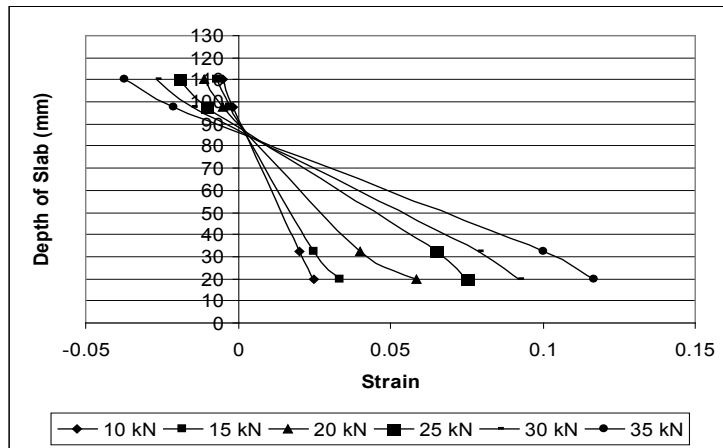
Figure 8. Strain distribution at mid span section for granite topping slab
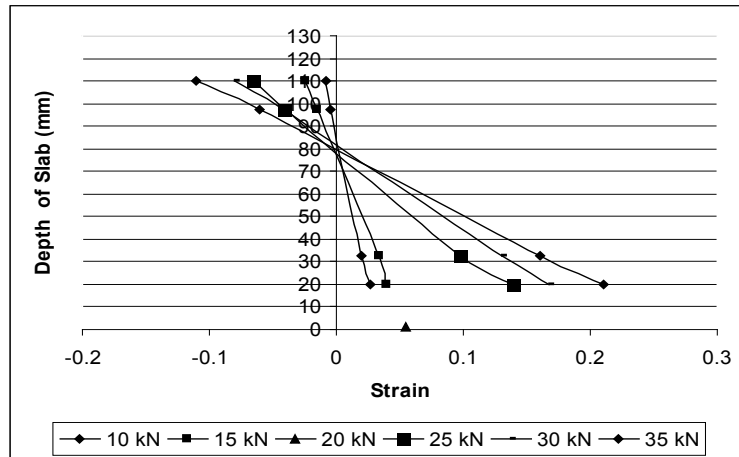
Figure 9. Strain distribution at mid span section for sandstone topping slab

Table 5 compares the theoretical ultimate load with the Experimental Ultimate Loads. It is observed that the experimental ultimate load for semi-precast slabs with sandstone and granite toppings is 7.4% and 5.1% higher than the corresponding theoretical ultimate load. Semi-precast slabs with OPS topping on the other hand, have experimental ultimate load 2% lower than the theoretical ultimate load. From the theoretical analysis, the ultimate load can be calculated as the equation below

$$M = A_s f_y (d - 0.5a)$$

Where A_s = Area of tension reinforcement
        f_y = characteristic tensile strength of reinforcement
        d = effective depth of tension reinforcement
        a = depth of neutral axis

Table 5. Comparison between Theoretical and Experimental Ultimate Load for Semi precast Slabs

(1) Slab	(2) Type of Topping	(3) Theoretical Ultimate Load (kN)	(4) Experimental Ultimate Load (kN)	$(5) = \dfrac{(4)}{(3)}$
S1	OPS	60.18	59.00	0.980
S2	Sandstone	59.13	63.55	1.074
S3	Granite	61.58	64.70	1.051

CONCLUSIONS

From the results discussed, the following conclusions can be made.

a. The use of OPS as coarse aggregates for the topping layer of the semi-precast slab resulted in a reduction of 23% of the weight of slab. However, the reduction of load capacity was only 10% when compared to that with sandstone and granite toppings. Therefore, OPS concrete can be a potential topping as it fulfils the minimum criteria for compressive strength of concrete used in slab which is >25 N/mm².

b. The average crack spacing of the slab with OPS toppings were very close with the spacing of cracks in slabs with sandstone topping.

c. The semi-precast slab with OPS concrete topping had greater deflections compared with the slabs with the other two toppings. However, the deflections were within permissible limit which is < 40 mm at service load.

d. The crack pattern and the strain distribution of the semi-precast slabs tested confirmed a very good composite action between the precast part and the toppings.

e. The experimental ultimate loads are in good agreement with the theoretically predicted loads for all the slabs.

ACKNOWLEDGEMENT

REFERENCES

Alca, N. Alexander, S.D.B & MacGregor, J.G (1997) *Effect of Size on Flexural Behaviour of High Strength Concrete Beam*, ACI Structural Journal 94(1):1-9.

Basri, H. B., Mannan, M.A., Zain, M. F. M. (1999). Concrete using Waste Oil Palm Shells as Aggregate. *Cement and Concrete Research* 29: 619–622.

BS 1881: Part 110:1983. Method of Making Test Cubes from Fresh Concrete, British Standard Institution, London.

BS 812: Part 109:1990. Method for Determination of Aggregate Crushing Value, British Standard Institution, London.

BS 812: Part 110:1990. Method for Determination of Aggregate Impact Value, British Standard Institution, London.

BS 812: Part 110:1990. Method for Determination of Aggregate Impact Value, British Standard Institution, London.

Legg, F.E. (1998) *Aggregate, Concrete Construction Handbook*, Fourth Edition, McGraw-Hill Publication, New Delhi, India.

Mannan, M.A., Ganapathy, C. (2002). Engineering Properties of Concrete with Oil Palm Shell as Coarse Aggregate. *Construction and Building Materials*. 16: 29–34.

Mannan, M.A., Ganapathy, C. (2004). Concrete from an Agriculture Waste-Oil Palm Shell (OPS). *Building and Environment*. 39: 441–448.

Neville, A.M. (2005) *Properties of Concrete*, Fourth Edition and Final Edition, Pearson Education Limited, London.

Teo, D. C. L., Mannan, M. A,, Kurian, V. J., Ganapathy, C. (2007). Lightweight Concrete Made from Oil Palm Shell (OPS): Structural Bond and Durability Properties. *Building and Environment*. 42: 2614–2621.

RESPONSE OF CERAMIC FOAMS CORE SANDWICH COMPOSITES UNDER FLEXURAL LOADING

Mohd Al Amin Muhamad Nor[1], Hazizan Md. Akil[2], Sharul Ami Zainal Abidin[2] and Zainal Arifin Ahmad[2*]

[1]*Department of Chemical Sciences, Faculty of Science and Technology, Universiti Malaysia Terengganu, 21030 Kuala Terengganu, Terengganu, Malaysia*

[2]*School of Materials and Mineral Resources Engineering, Engineering Campus, Universiti Sains Malaysia 14300 Nibong Tebal, Pulau Pinang, Malaysia*
Corresponding author: zainal@eng.usm.my

Abstract

Ceramic foam can be potentially used as a core material in sandwich structure construction. The construction of sandwich structure involves joining two thin and stiff faces with a thick and low density core material by using adhesive. As a result, a structure with superior bending stiffness, lightweight and high specific properties is obtained. In this work, in house produced ceramic foams core with density of $1185 kg/m^3$ was used as core materials in sandwich construction with aluminium plate facing materials by using epoxy adhesive. Our study is focus on the determination of a range of sandwich properties including shear modulus, G and bending stiffness, D by conducting a series of three-point bend tests over the spans of 150, 200, 250, 300 and 350 mm. The load-deflection behavior of a composite sandwich beam in three-point bending was investigated. The load-deflection curves were plotted up to the point of failure initiation. This consisted of an initial linear part followed by a nonlinear portion. A nonlinear mechanics of material analysis that accounts for the combined effect of the nonlinear behavior of the facings and core materials (material nonlinearity) and the large deflections of the beam (geometric nonlinearity) were developed. The shear modulus, G and bending stiffness, D was calculated from the intercept of δ/PL against L^2 and δ/PL^3 against $1/L^2$, respectively. It was found that the shear modulus, G and bending stiffness were 19.68 GPa and 74.41 N, respectively which were comparable to those polymeric foams core materials. As conclusion, ceramic foams core has high potential to be used as core materials for sandwich structure construction.

Keywords: *Sandwich structure, ceramic foams core, three-point bend test, flexural properties*

INTRODUCTION

Sandwich structure is widely used as it is suitable and amenable for the development of lightweight structures with high in plane and flexural stiffness. The concept of sandwich structure involves joining two thin and stiff faces with a thick and low density core material by using adhesive. As a result, a structure with superior bending stiffness, lightweight and high specific properties is obtained.

The properties of primary interest for the core are density, shear modulus, shear strength, stiffness perpendicular to the faces, thermal and acoustical insulation (Zenkert, 1995). The core helps in increasing the moment of inertia in such a way that the structure becomes efficient in resisting bending and buckling loads. This is the way sandwich panels are utilized in applications where weight saving is critical, for instance in aircraft and portable structures. Moreover, sandwich material also exhibits favourable properties. It provides an excellent thermal insulation, has a long life with low maintenance cost, good water and vapour barriers and has excellent acoustic damping properties. It's surface-finished faceplates provide good resistance against aggressive environments (Allen, 1969 and Stuart, 1990).

There are 4 main groups of core materials used: foams, honeycomb, corrugate and wood. Typically, polymeric or metallic foams are most commonly used as core materials in sandwich fabrication. They can be manufactured from a variety of materials, such as synthetic polymers, i.e. polyvinyl chloride, polystyrene, polyurethane, etc. and metal foam such as aluminium. Ceramic foam is a new class of core material that is potentially used in sandwich construction. Ceramic foam poses advantages over other classes of foams because it has good thermal properties, and high strength; and provides better resistance to chemical attacks, etc.

The flexural behavior of sandwich beams has been studied extensively by many investigators. Original works include Hoff and Mautner (1948), Krajeinovic (1971 & 1975), DiTaranto (1973), Rao (1976), Frostig and shenhar (1995) and others. Other studies of sandwich beams using strength of materials analysis were performed by Teti and Caprino (1989) and Johnson and Sims (1986). From the experimental point of view, Lingaiah and Suryanarayana (1991) performed three-point and four-point bending tests on sandwich specimens with fiberglass-reinforced plastics and aluminum for the facings and aluminum honeycomb and polyurethane foam for the core. In this work, a simple three point bend test was used to determine the shear modulus and bending stiffness of ceramic foams core sandwich composites with aluminium facing.

Theoretical background

Sandwich beams are commonly used to determine a range of sandwich properties including shear modulus, G and bending stiffness, D. These properties can be obtained by conducting a series of three-point bend tests at different span. The shear stiffness of the sandwich structure is required in order to model the impact response of sandwich structure. During each test, the load–displacement curve was recorded. Based on sandwich beams theory[4], the deflection under the central point load is:

$$\delta = \delta_b + \delta_s = \frac{PL^3}{48D} + \frac{PL}{4AG} \qquad (1.0)$$

Where;

δ_b = Deflection due to bending (m)
δ_s = Deflection due to shear (m)
P   = Applied load (N)
D   = Flexural stiffness of the sandwich beam (Nm^2)
AG = Shear stiffness of the sandwich beam (N)
A   = bd^2/c (m^2)
d   = $(h - c)/2$ (m)
c   = thickness of the core (m)
L   = Support span (m)

Clearly if deflection is measured on two beams supported over different spans, equation 1.0 can be solved for D and AG. This can only be true if one span is large enough to ensure that the deflection is predominantly due to bending and the other is small enough to ensure that the deflection is due mainly to shear (Volmir, 1967). Therefore the most reliable method is to recast Equation 1.0 as follows:

$$\frac{\delta}{PL} = \frac{L^2}{48D} + \frac{1}{4AG} \tag{1.1}$$

$$\frac{\delta}{PL^3} = \frac{1}{48D} + \left(\frac{1}{4AG}\right)\left(\frac{1}{L^2}\right) \tag{1.2}$$

Equation 1.1 can be represented as a straight line in a plot of δ/PL against L^2 as shown in Figure 1a. Similarly Equation 1.2 can be represented as a straight line in a plot of δ/PL^3 against 1/L^2 as shown in Figure 1b. The values of G and D were then determined from the intercept value on the y-axes in Figures 2a and 2b.
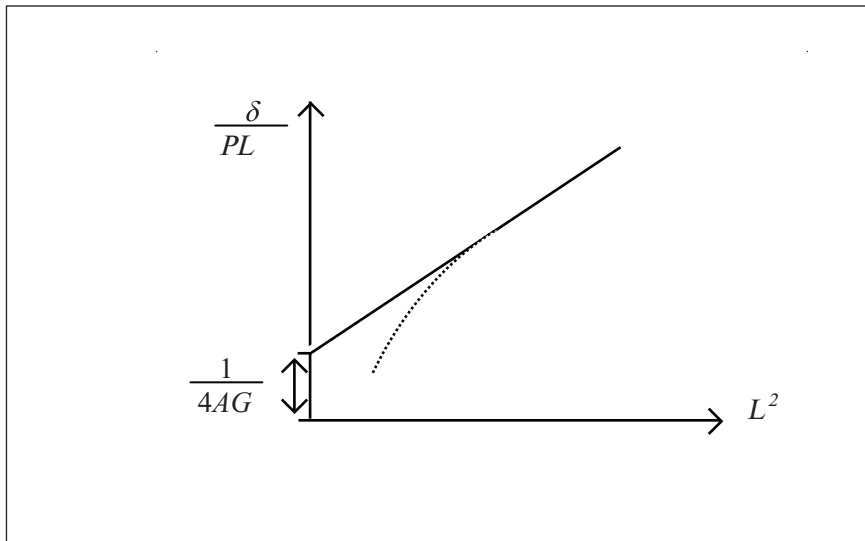
Figure 1.a. Schematic plot of δ/PL against L^2 (Volmir, 1967)
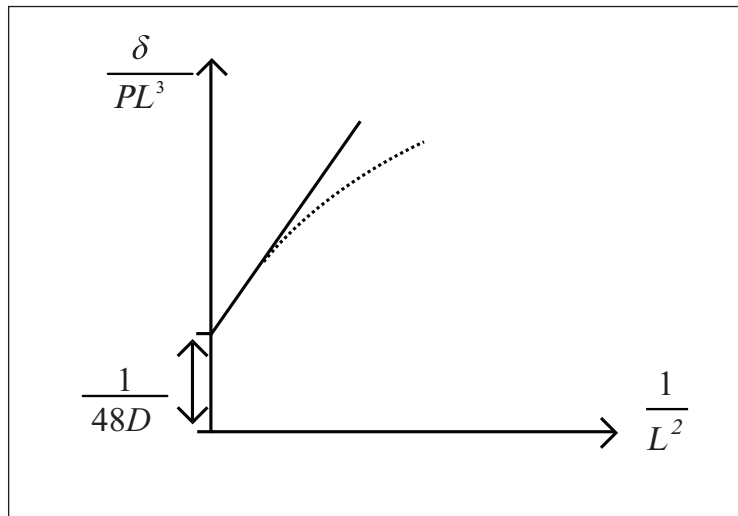
Figure 1.b. Schematic plot of δ/PL^3 against $1/L^2$ following a three-point bend test on a simply supported sandwich beam (Volmir, 1967)

MATERIALS AND METHODOLOGY

Preparation of ceramic foam

Polymeric foam (template material) was obtained from Pexafoam Sdn. Bhd. It was cut into dimension of 400 mm x 300 mm x 16.4 mm for sample preparation. The porcelain powder was produced in-house by mixing ball clay, quartz, kaolin and feldspar in the ratio of 10%, 30%, 40% and 20% by weight respectively. The porcelain slurry was prepared at 1.3653 g/cm^3, in distilled water medium. The mixture was ball-milled for 2 hours in porcelain jar to produce porcelain slurry, using porcelain balls as grinding media. The density of ceramic slurries was measured using Pycnometer. The foam was squeezed manually to remove trapped air prior to dipping process in the slurry. The squeezed foam was kept in the slurry for 5 minutes to ensure an adequate filling time of the template. Any excess slurry was removed. The foam containing the slurry was then dried in an oven at 50-60°C for 72 hours and subsequently at 100°C for 1 hour. The sample was further sintered in a gas furnace at the temperature and heating rate of 1250°C and 5°C/min, respectively with 2 hours of holding time. The resulted ceramic foams then cut to dimension of 22 x 14 x (160, 210, 260, 310 and 360 mm) for three-point bending test at various span.

Preparation of sandwich beam and testing

The sandwich beams were fabricated from aluminium 6063 (0.5 mm thickness) facings and a ceramic foams core (porcelain foams, 1185 kg/m^3) by using epoxy adhesive. Specimens were fabricated at different length for conducting three-point bending test at various spans. Specimens were tested using an Instron machine. A concentrated load was applied at midspan by the movable crosshead of the machine at a speed of 10.0 mm/min. A series of

three-point bend test was carried out on sandwich beams supported over the spans of 150, 200, 250, 300 and 350 mm. The load versus deflection relation was recorded and plotted during the test. Details of the specimens dimension are given in Table 1.

Table 1. Summary of the specimen geometries used to determined the shear modulus of the sandwich beams

Span, L (mm)	Dimension (mm)	Length of overhang (mm)
150	22 x 14 x 160	10
200	22 x 14 x 210	10
250	22 x 14 x 260	10
300	22 x 14 x 310	10
350	22 x 14 x 360	10

The purpose of this study is to determine a range of ceramic foams core sandwich composites properties including the shear modulus, G and bending stiffness, D.

RESULTS AND DISCUSSION

A series of three-point bend tests on specimens with different span lengths were conducted. The specimens were loaded up to failure as shown in Figure 2. Observation on the specimen during testing reveals that failure obtained at the foams was mainly due to shear cracking of core materials. The fractured surface of ceramic foams core observed using SEM is shown in Figure 3. The micrograph reveals that the microstructure of ceramics foams consist of macro and micro open and close cell. The open pores contribute to the weak point for failure during flexural testing.
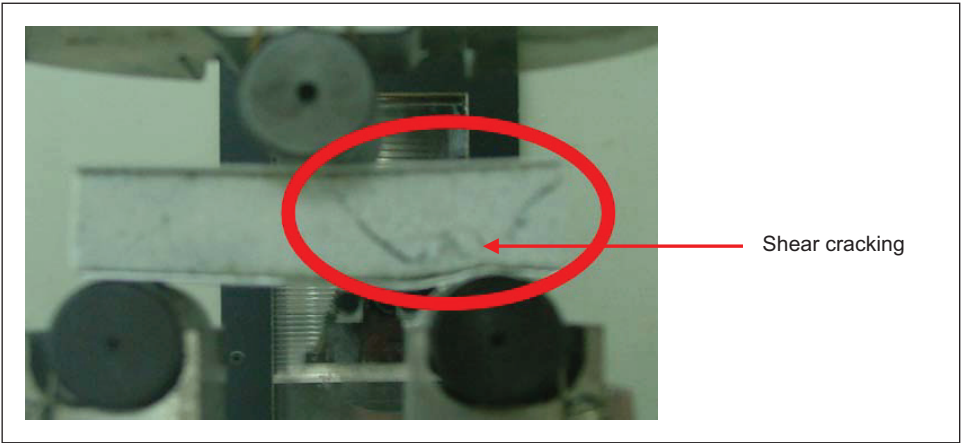
Figure 2. Shear cracking failure of ceramic foams core sandwich structure after three-point bend test
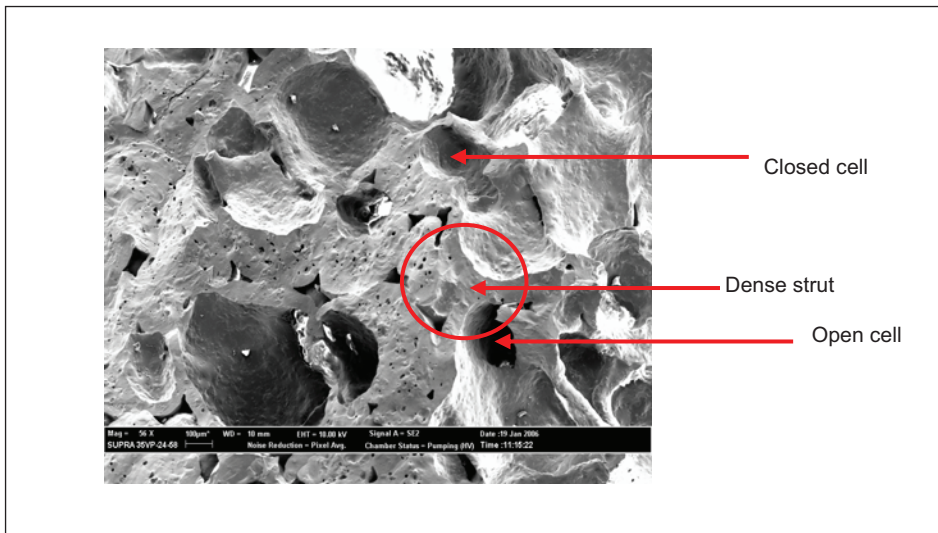
Figure 3: Micrograph of fracture surface of ceramic foams core

The load-displacement and stress-strain curves were plotted for all span length as shown in Figures 4 and 5, respectively. They consist of an initial linear part followed by a nonlinear portion. A nonlinear mechanics of material analysis that accounts for the combined effect of the nonlinear behavior of the facings and core materials (material nonlinearity) and the large deflections of the beam (geometric nonlinearity) were developed.
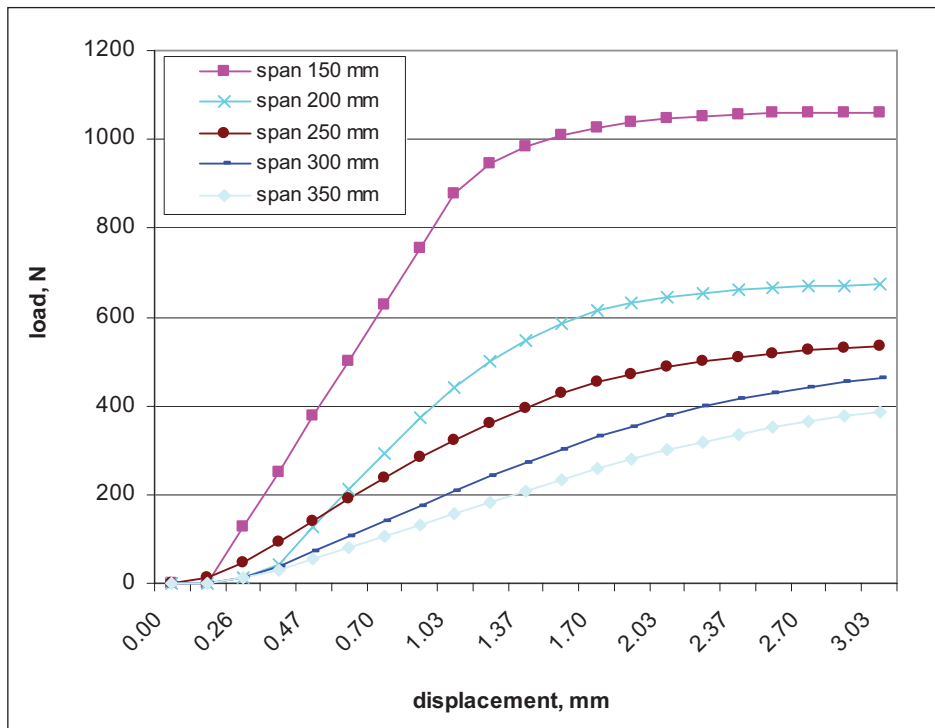
Figure 4. The load-displacement curve for all span length of ceramic foam core sandwich composites tested by three-point bending test
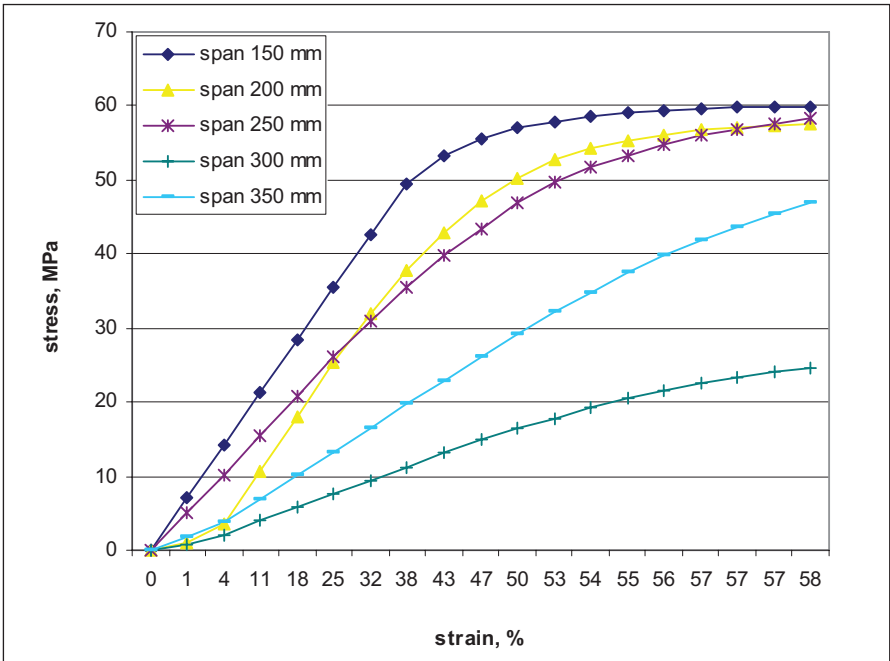
Figure 5. The stress-strain curve all span length of ceramic foam core sandwich composites tested by three-point bending test

As mentioned in the theory, the shear modulus, G and bending stiffness, D were calculated from the intercept of δ/PL against L^2 and δ/PL^3 against $1/L^2$ as shown in Figure 6 and 7, respectively. The shear stiffness of the sandwich beam, AG, shear modulus, G and bending stiffness, D are 6097.6 N, 19.7 GPa and 74.4 N, respectively.
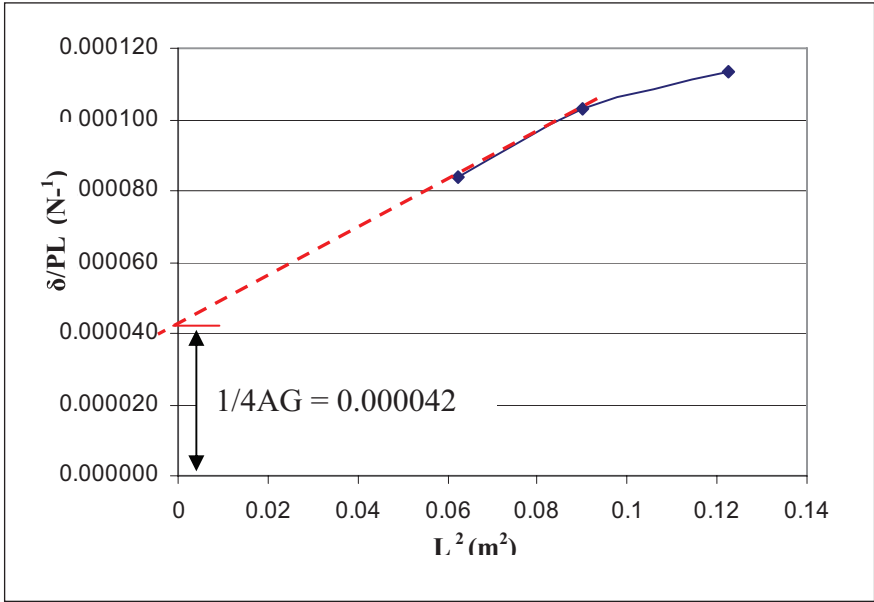
Figure 6. Schematic plot of δ/PL against L^2 for ceramic foams core sandwich composites
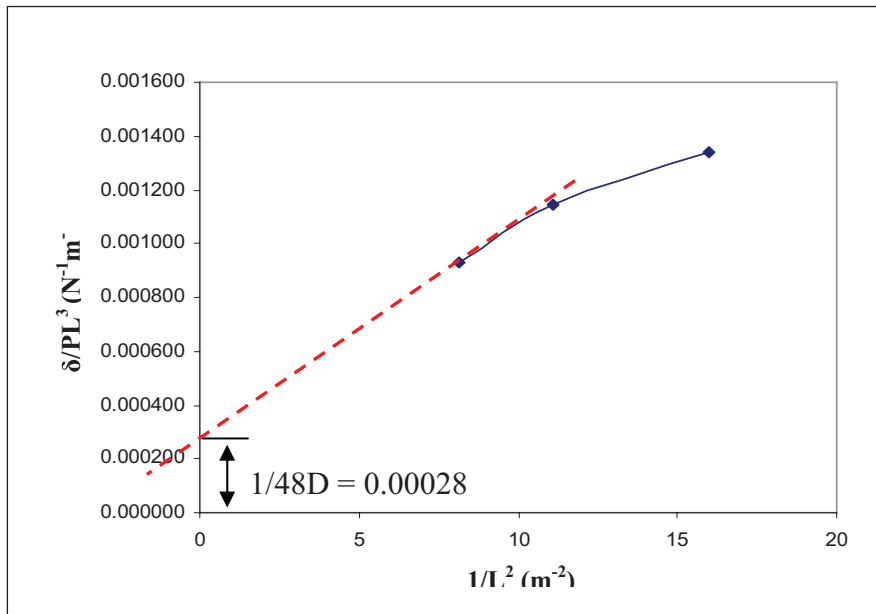
Figure 7. Schematic plot of δ/PL^3 against $1/L^2$ for ceramic foams core sandwich composites

CONCLUSION

The properties of ceramic foam core sandwich composites such as shear modulus, G and bending stiffness, D has been successfully determined by conducting a series of three-point bend tests at different spans. The shear stiffness, AG, shear modulus, G and bending stiffness, D were 6097.6N, 19.7 GPa and 74.4 N respectively which are comparable to those polymeric foams core materials. As conclusion, ceramic foams core has high potential to be used as core materials for sandwich construction.

ACKNOWLEDGEMENT

REFERENCES

Allen, H.G. (1969). *Analysis and design of structural sandwich panels*. London: Pergamon Press.

DiTaranto, R.A. (1973) *Static Analysis of a Laminated Beam*. Journal Eng. Ind. Trans. ASME, 95, Pp. 755-761.

Frostig, Y. and Shenhar, Y. (1995). *High-order Bending of Sandwich Beams with a Transversely Flexible Core and unsymmetrical Laminated Composite Skins*. Composites Eng., 5. 405-414

Hoff, N.J. and Mautner, S.E. (1948) *Bending and Buckling of Sandwich Beams*. Journal Aerospace Sci., 15, 707-720.

Johnson, A.E and Sims, G.D. (1986) *Mechanical Properties and Design of Sandwich Materials*. Composites, 17. Pp. 321-328.

Krajcinovic, D. (1971) Sandwich Beam Analysis. Journal Appl. Mech. Trans. ASME, 38, 773-778

Krajcinovic, D. (1975) *Sandwich Beams with Arbitrary Boundary Conditions*. Journal Appl. Mech. Trans. ASME, 42, 873-880

Lingaiah, K. and Suryanarayana, B. G. (1991) *Strength and Stiffness of Sandwich Beams in Bending.*Experimental Mechanics, 31, Pp. 1-7

Rao, D.K. (1976) *Static Response of Stiff-cored Un-symmetrical Sandwich Beams*. Journal Eng. Ind. Trans. ASME, 98, Pp. 391-396

Stuart M. L. (Ed.). (1990) International Encyclopedia of Composites, Volume 1. New York VCH Publishers Inc.

Teti, R. and Caprino, G. (1989) *Mechanical Behavior of Structural Sandwiches.* Proceedings of the First International Conference on Sandwich Construction. Pp 53-67.

Volmir, A.S. (1967) *A translation of flexible plate and shells*. Affdl-TR-66-216

Zenkert, D. (1995) *An Introduction to sandwich construction.* Engineering Materials Advisory Services LTD. London: Chameleon Pres Ltd.

Guide to Authors

AIMS AND SCOPE:

The Malaysian Construction Research Journal (MCRJ) is the journal dedicated to the documentation of R&D achievements and technological development relevant to the construction industry within Malaysia and elsewhere in the world. It is a collation of research papers and other academic publications produced by researchers, practitioners, industrialists, academicians, and all those involved in the construction industry. The papers cover a wide spectrum encompassing building technology, materials science, information technology, environment, quality, economics and many relevant disciplines that can contribute to the enhancement of knowledge in the construction field. The MCRJ aspire to become the premier communication media amongst knowledge professionals in the construction industry and shall hopefully, breach the knowledge gap currently prevalent between and amongst the knowledge producers and the construction practitioners.

Articles submitted will be reviewed and accepted on the understanding that they have not been published elsewhere. The authors have to fill the Declaration of the Authors form and return the form via fax to the secretariat. The length of articles should be between 3,500 and 8,000 words or approximately 8 – 15 printed pages (final version). The manuscripts should be written in English or Bahasa Melayu an abstract in English must be included. The original manuscript should be typed one sided, single-spacing, single column with font of 11 point (Times New Roman). Paper size should be of Executive (18.42 cm x 26.67 cm) with 2 cm margins on the left, right and bottom and 3 cm for the top. Authors can submit the manuscript:

- By e-mail to maria@cidb.gov.my / hazim@cidb.gov.my
- By hardcopy and softcopy in Microsoft-Word format to MCRJ Secretariat:

Malaysian Construction Research Journal (MCRJ)
Construction Research Institute of Malaysia (CREAM)
Makmal Kerja Raya Malaysia
IBS Centre 1st Floor, Block E,
Lot 8, Jalan Chan Sow Lin,
55200 Kuala Lumpur, Malaysia
Tel : (6) 03-92810800
Fax : (6) 03-92824800

Type of fonts: All text, drawing, graph must be written using Times New Roman
Language: Follow the spelling of the Oxford English Dictionary.
Size/Page Setup: Executive (18.42 cm x 26.67 cm)
Paper title: Arial, 16.

CODIFICATION AND APPLICATION OF SEMI-LOOF ELEMENTS FOR COMPLEX STRUCTURES

Author's name (full name): Arial, 9pt. should follow below the title.

Jamalodin Noorzaei[1], Mohd. Saleh Jaafar, Abdul Waleed Thanoon, Wong Jern Nee

Affiliation (including post codes): Arial, 9pt. Use numbers to indicate affiliations.

[1]*Department of Civil Engineering, Faculty of Engineering, Universiti Putra Malaysia, 43400 UPM, Serdang, Selangor, Malaysia*

Abstract: Arial Bold, 9pt. Left and right indent 0.25 inch.

    Abstract: it should be single paragraph of about 100 – 250 words.

Keywords: Times New Roman Bold, 9pt (Italic). Left and right indent 0.25 inch.

    Keywords: *Cooling tower; Finite element code; Folded plate; Semiloof shell; Semiloof beam*

Body Text: Times New Roman, 11 pt. All paragraph must be differenciate by 0.25 inch tab.

Heading 1: Arial Bold + Upper Case, 11pt.
Heading 2: Arial Bold + Lower Case, 11pt.
Heading 3: Arial Italic + Lower Case, 11pt.

Units: All units and abbreviations of dimensions should conform to SI standards.

Figures: Figures should be in box with line width 0.5pt. All illustrations and photographs must be numbered consecutively as it appears in the text and accompanied with appropriate captions below them.
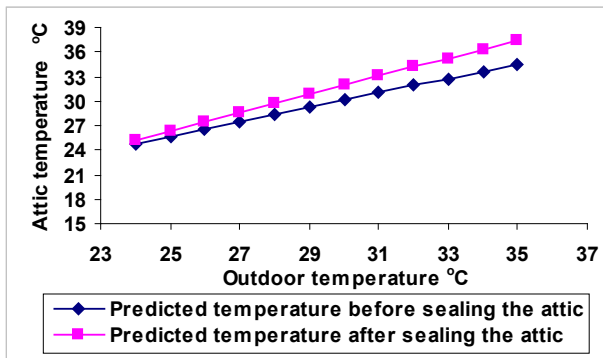
Figures caption: Arial Bold + Arial, 9pt. should be written below the figures.

Figure 8. Computed attic temperature with sealed and ventilated attic

Tables: Arial, 8pt. Table should be incorporated in the text.

Table caption: Arial Bold + Arial, 9pt. Caption should be written above the table.

Table Line: 0.5pt.

Table 1. Recommended/Acceptable Physical water quality criteria

Parameter	Raw Water Quality	Drinking Water Quality
Total coliform (MPN/100ml)	500	0
Turbidity (NTU)	1000	5
Color (Hazen)	300	15
pH	5.5-9.0	6.5-9.0

(Source: Twort et al. 1985; MWA,1994)

Reference: Times New Roman, 11pt. Left indent 0.25inch, first line left indent – 0.25inch. Reference should be cited in the text as follows: "Berdahl and Bretz (1997) found…" or "(Bower et al. 1998)". References should be listed in alphabetical order, on separate sheets from the text. In the list of References, the titles of periodicals should be given in full, while for books should state the title, place of publication, name of publisher, and indication of edition.

Journal
Sze, K. Y. (1994) Simple Semi-Loof Element for Analyzing Folded-Plate Structures. *Journal of Engineering Mechanics*, 120(1):120-134.

Books
Skumatz, L. A. (1993) Variable rate for municipal solid waste: implementation, experience, economics and legislation. Los Angeles: Reason Foundation,157 pp.

Thesis

Wong, A. H. H. (1993) *Susceptibility to soft rot decay in copper-chrome-arsenic treated and untreated Malaysian hardwoods*. Ph.D. Thesis, University of Oxford. 341 pp.

Chapter in book

Johan, R. (1999) Fire management plan for the peat swamp forest reserve of north Selangor and Pahang. In Chin T.Y. and Havmoller, P. (eds) *Sustainable Management of Peat Swamp Forests in Peninsular Malaysia* Vol II: Impacts. Kuala Lumpur: Forestry Department Malaysia, 81-147.

Proceedings

Siti Hawa, H., Yong, C. B. and Wan Hamidon W. B. (2004) Butt joint in dry board as crack arrester. *Proceeding of 22nd Conference of ASEAN Federation of Engineering Organisation* (CAFEO 22). Myanmar, 55-64.

Contents

The contents of the published articles do not represent the views of the Editorial Committee and
Construction Research Institute of Malaysia